Experimental Verifications of Metabolic Potential

In Deeply-Sourced Springs in Western Turkey

BY

ERIN NEVRIYE YARGICOGLU

B.S., University of Illinois at Chicago, 2010

THESIS

Submitted in partial fulfillment of the requirements

for the degree of Master of Science in Earth and Environmental Science

in the Graduate College of the

University of Illinois at Chicago, 2012

Chicago, Illinois

Defense Committee:

D'Arcy Meyer-Dombard, Advisor/Chair

Neil Sturchio

Fabien Kenig

TABLE OF CONTENTS

TABLE OF CONTENTS (continued)

LIST OF TABLES

LIST OF TABLES (continued)

LIST OF FIGURES

SUMMARY

Linking thermodynamic predictions to microbial metabolism *in situ* and genetic capacity will aid in our understanding of both extraterrestrial and ancient life forms. Doing so requires obtaining coupled geochemical and microbiological data sets from analog systems to evaluate the relationship between thermodynamics and observed microbial metabolism. This work describes several new sites in western Turkey that were surveyed in search for serpentinization-associated analog sites. Cultivation from sampled material in targeted growth media in conjunction with taxonomic affiliations with known organisms based on 16SrRNA bacterial phylogeny is used to assess the metabolic diversity in each system. These findings are compared with calculated Gibbs free energies of reaction for several chemosynthetic metabolic pathways to assess whether or not they are consistent with actual metabolic capacity. Nitrogen-cycling functional genes are detected and related to growth in targeted media. Evidence for partial denitrification within an biofilm supported by fluid discharging from an actively burning methane vent (Yanartaş) is substantiated by geochemical and isotopic evidence, as well as observations in culture and the presence of functional nitrogen-cycling genes, substantiating thermodynamic predictions that some exergonic metabolic pathways are utilized *in situ*. Data obtained on taxonomic relationships and observations *in vitro* of heterotrophic, thermophilic enrichment cultures sheds new insight onto the functional diversity of fault-associated hydrothermal and cool spring systems.

1. INTRODUCTION

1.1 A Thermodynamic Framework for Understanding Modern Serpentinization Processes and Astrobiological Targets

The search for life beyond Earth requires both an understanding of biogeochemical processes within potentially habitable systems and the ability to relate quantifiable physico-chemical properties of such systems directly to available metabolic pathways. The same is true for the search for the origins of microbial life on Earth. Without direct access to extraterrestrial and ancient Earth systems, the study of analogous environments on Earth may provide the best window on how microbial life may function or functioned in the past in these geochemical environments. One of the earliest astrobiological targets were submarine hydrothermal vents, first discovered in the 1970's (Weiss et al., 1977; Corliss et al., 1979). Since then, many have suggested the chemical energy obtained from redox gradients produced in these systems played an integral role in the origin of life (e.g. Reysenbach & Shock, 2002; Martin et al., 2008).

While much evidence still supports the importance of hydrothermal activity for energy generation on early Earth (Martin et al., 2008 and references therein), the discovery of an actively serpentinizing hydrothermal system supporting a vast chemolithoautotrophic community (Lost City Hydrothermal Field; Kelley et al., 2005; Brazelton et al., 2009) has prompted many to consider another geologic process – serpentinization – as a possible driver of early microbial metabolism. Serpentinizing systems have garnered recent interest for early Earth and astrobiological targets as they are thought to have been more widespread on early Earth (Nisbet & Sleep, 2001; Sleep et al., 2004; Schulte et al., 2006; Russell, 2007; Martin & Russell, 2010) and may have occurred during the evolution of Mars, or of other rocky, siliceous planets (e.g. Europa and Enceladus) (Ehlmann et al., 2009; Hellevang et al., 2011). Assessing the viability of life supported by serpentinizing systems

requires exploration of biogeochemical processes occurring in similar habitats on the modern Earth.

Much of the research on potential analog systems has targeted subsurface (e.g. Chapelle et al., 2002; Okland et al., 2012) and submarine hydrothermal systems (e.g. Charlou et al., 1998, 2002), given that harsh conditions on the current Martian surface and on early Earth likely restricted life to subsurface or marine environments (Nisbet & Sleep, 2001; Reysenbach & Shock, 2002; Sleep et al., 2004; Van Kranendonk, 2006; Martin et al., 2008). Recent studies have used culture-based methods and genomic analyses to assess the microbial communities in deep oceanic sediments and crust (e.g. Biddle et al.,2006; Parkes et al., 2009; Orcutt et al., 2010a,b), yet terrestrial subsurface studies have thus far been much more limited in number and scope (e.g. Chapelle et al., 2002; Chivian et al., 2008; Lin et al., 2006; Rastogi et al., 2010; Wu & Lai, 2011). Other works have explored Earth's 'cryosphere' (e.g. Skidmore et al., 2011) for microbial life that can survive very cold, and sometimes hypersaline, habitats beneath layers of ice. Microbial life has found a way to survive in almost every type of environmental 'extreme' (acidity, alkalinity, salinity, heat or lack thereof, etc.) As knowledge of subsurface and hydrothermal microbial ecology grows, a working database for a predictive mechanism based on thermodynamic favorability and potential metabolic options for microbial inhabitants may be established for unique geochemical environments.

This work describes several new localities in Turkey in an effort to fill current gaps in knowledge regarding biogeochemistry associated with both terrestrial serpentinization and hydrothermal systems.

1.2 **Research Objectives**

This study identified and sampled several previously undescribed fault-associated springs in western Turkey to characterize the native subsurface microbial communities and possible metabolic pathways using a thermodynamic framework to guide cultivation efforts and genetic

assays. The region was first surveyed in 2010 to locate and sample hydrothermal and cool spring sites along the North Anatolian Fault Zone (NAFZ) where several units (e.g. serpentinite, peridotite, amphibolites) across an ophiolite sequence are known to host numerous springs (Meyer-Dombard et al., 2010). Select sites in northwest Turkey discovered in the initial field survey were chosen for further study and sampled again during a second field survey (Feburary 2012) that included hydrothermal springs and gas vents of the Tekirova ophiolite and nearby units in southwest Turkey. Comparisons are drawn among spring systems based on: 1) host rock lithology; 2) temperature; 3) pH; and 4) relative inputs of meteoric, hydrothermal and serpentinizing fluids to the spring systems. Geochemical, mineralogical and microbiological data obtained during two field surveys of hot and cool springs in northwest and southwest Turkey will tie geochemical datasets with thermodynamic models of metabolic activity in the terrestrial subsurface. By doing so, the following research question will be addressed:

Do thermodynamic calculations of environmental energy availability, based on Gibbs free energies of reactions, predict the genetic and metabolic capacity of the associated microbial community?

By showing accurate predictions of ecosystem function, calculations of energy-yielding reactions can be used as a reliable and practical predictive tool for guiding studies in microbial ecology. Thus far, calculations of Gibbs free energies for potential metabolic pathways has primarily served as a guide for exploratory microbiologists seeking to characterize a novel community and, in most cases (Swingley et al., 2012 recently linked energy predictions to sulfur cycling in Yellowstone National Park), have not been directly correlated with laboratory observations of cultured samples and genetic analyses to confirm the relevance of thermodynamic predictions to *in situ* biogeochemical processes and geochemical conditions (Shock et al., 2010). This project seeks to constrain the relevance of thermodynamic predictions with respect to natural microbial activities and assess the validity of this approach.

This work will add to a growing body of knowledge on microbial and biogeochemical processses in unique chemical environments by presenting microbiological and geochemical data on several hydrothermal and cool springs in western Turkey that have yet to be well-characterized. Sampling springs representative of differing stages of serpentinization and degrees of hydrothermal and meteoric inputs allows comparisons across a spectrum of geochemical alteration and meteoric weathering of the host rocks. Moreover, the recent discovery of CH_4 on Mars (Formisano et al., 2004; Atreya et al., 2007) adds further relevance to our findings at a terrestrial methane seep out of an ophiolite unit in southwestern Turkey. This site, referred to as Yanartaş (YT) throughout this thesis, will be discussed along with the hot and cool spring sites throughout northwest and southwest Turkey, although it is primarily a gas seep (with minor, episodic inputs of meteoric waters) and thus is biogeochemically unique among the sites surveyed.

1.3 **Quantifying Habitability for Astrobiological Targets**

In order to constrain the habitability of a given system independent from direct microbial probing, ties must be made between observed metabolic capability and geochemical and mineralogical proxies. The ability to define habitability in relation to the geochemical environment would allow workers to infer potential metabolic strategies utilized without direct observation, which is not a viable option for extraterrestrial and ancient systems (Shock & Holland, 2007; Hoehler, 2004, 2007). This approach can be further aided by using a thermodynamic framework for energy availability based on calculations of Gibbs free energies for specific metabolic reactions in variable chemical environments (McCollom & Shock, 1997; Amend & Shock, 2001; Hoehler et al., 2007). The Gibbs free energy of a reaction (ΔG_r), is the energy yield provided by that reaction proceeding. Because available energy is immediately useful to microbial inhabitants, it can serve as a rough measure of the energy usable for chemosynthetic and heterotrophic metabolisms, assuming the native organisms possess the genetic capability to perform those specific metabolic functions. **Eq. 1** describes ΔG_r:

$$\Delta G_r = \Delta G_r^\circ + RT(\ln Q) \qquad \textbf{(Eq. 1)}$$

where ΔG_r° is the standard Gibbs free energy of a reaction (at 1 atm and 25°C), ΔG_r is the Gibbs free energy of a reaction at the specified environmental conditions, T is the temperature in degrees Kelvin, R is the universal gas constant and Q is the activity quotient of the reaction. The free energy at system conditions (ΔG_r) – rather than the standard free energy (ΔG_r°) - as determined by the activities of both products and reactants in the system, approximates the energy available to microorganisms (McCollom & Shock, 1997) and is therefore much more relevant in natural geologic environments than calculations of ΔG_r°.

It is important to note that there is a minimum energy flux required for life to construct and maintain its cellular biomass, known as the maintenance energy, or biological energy quantum (Hoehler, 2007), which can be considered as the minimal energy demand to sustain life. As such, reactions that can be thermodynamically exergonic, may not be viable metabolic options despite having negative values of ΔG_r. Furthermore, such limits are specific to the type of organism considered, which will have different minimal levels of complexity - e.g. a human is much more complex than a single-celled organism, and thus will require higher initial amounts of available energy for growth and higher energy influx for maintenance after maturity (a.k.a. the minimum biomass to perform necessary functions to sustain life has been achieved) (Hoehler 2004, 2007). These temporal constraints on habitability must be kept in mind when evaluating metabolic diversity and capacity in real systems in relation to thermodynamic calculations. Estimates have been made for the lower limit of the biological energy quantum at 20 kJ (Hoehler 2004, 2007).

In theory, metabolic options utilized by microbial communities are restricted by the available energy in a system, which can be quantified in terms of Gibbs free energies of reactions if certain geochemical parameters are known (Hoehler, 2004, 2007; Hoehler et al., 2007). In order to constrain the availability of free energy in the system, the activities of major aqueous species must be accurately estimated, giving consideration also to significant mineral phases that may interact

with the system over time. Relevant mineral-alteration process, for example, the aqueous alteration of ultramafic minerals during serpentinization, often produce predictable and measurable byproducts (Seyfried et al., 2007; Oze & Sharma, 2007); in the case of serpentinization, these products are hydrogen, methane, heat, and water. Hydrothermal vents emit a variety of reduced compounds (e.g. H_2S, CH_4) depending on the geochemistry of the magma source. Both processes have garnered the interest of many astrobiologists as a potential source of reducing power and – consequently – available chemical energy for microorganisms able to oxidize the reduced compounds to drive chemosynthetic metabolic pathways. The following sections will describe serpentinization and hydrothermal processes and implications for subsurface biogeochemistry in related systems.

1.4 **Scientific Rationale: Modern Serpentinization & Subsurface Biogeochemistry**

Serpentinization occurs within oceanic crustal units in a number of tectonic settings, including seafloor spreading centers (e.g. the Mid-Atlantic Ridge), ridge flanks, and destructive margins (e.g. Mével, 2003), as well as along subduction zones between continental and marine plate boundaries (Iyer et al., 2008; Dilek & Furnes, 2011). Consequently, a diverse suite of geochemical environments can arise from serpentinization of assorted mineral assemblages in different settings and with varying degrees of hydrothermal and meteoric fluid inputs. This diversity is associated with a variety of chemical processes observed in previously described terrestrial and marine systems thought to be associated with active serpentinization and weathering of serpentinites on land.

I will first review the serpentinization process and its effects on chemistry of discharging fluids (e.g. in cool or hydrothermal springs) and the surrounding geochemical environment. Next I will provide an overview of the distribution and biogeochemical data obtained from known terrestrial serpentinizing systems on the modern Earth and implications for using these systems as analog sites for astrobiological targets.

1.4.1 **Serpentinization: Effects on Fluid Chemistry & Host Rock Mineralogy**

During serpentinization, water inclusions from hydrated minerals or circulating groundwater (e.g. in marine and terrestrial hydrothermal systems) cause weathering of ultramafic silicate minerals (primarily olivine [$(Mg,Fe)_2SiO_4$] and pyroxene [$(Mg,Fe)\text{-}SiO_3$]) and rock alteration to produce H_2 gas and altered metamorphic mineral assemblages (e.g. serpentine, brucite) (refer to **Eqs. 2** & **3**). The first step of serpentinization (**Eq. 2**) involves the hydration of olivine (both Fe and Mg endmembers of olivine are shown). The production of $H_{2(g)}$ results from the formation of magnetite by ferrous iron-rich minerals; partial oxidation of Fe(II) in $Fe(OH)_2$ coupled with the reduction of H_2O liberates $H_{2(g)}$ (**Eq. 3**).

$$Fe_2SiO_4 + 5Mg_2SiO_4 + 9H_2O \rightarrow 3Mg_3Si_2O5(OH)_4 + Mg(OH)_2 + 2Fe(OH)_2 \quad \textbf{(Eq. 2)}$$
fayalite + forsterite + water → serpentine + brucite + iron hydroxide

$$3Fe(OH)_2 \rightarrow Fe_3O_4 + 2H_2O + H_2 \quad \textbf{(Eq. 3)}$$
iron hydroxide → magnetite + water + hydrogen

The overall reaction is exothermic (heat-producing) and the hydration of ultramafic minerals also results in a volume expansion of the altered rock by as much as 60% (Hostetler et al., 1966; Shervais et al., 2005a). Volume expansion causes secondary fracturing, exposing new surfaces to fluid alteration, prolonging active serpentinization within the host rock and allowing long-lived hydrothermal circulation of the reduced fluids produced (Früh-Green et al., 2003; Blank et al., 2008). The production of $H_{2(g)}$ and reducing conditions generates alkalinity, with fluids reaching pH values as high as 12 in some cases (e.g. Barnes et al., 1982; Abrajano et al., 1988, 1990). As serpentinized fluids ascend to the surface and interact with different rock units, various elements (e.g. Mg, Cr, Ni) can become mobilized and enriched in the upwelling spring fluids. Interaction with the more oxic surface environment, or near-surface meteoric waters, often leads to precipitation of some of these mobilized elements (especially Ca^{2+} and Mg^{2+}) in oxidized mineral phases, e.g. hydromagnesite [$Mg_5(CO_3)_4(OH)_2 \bullet 4(H_2O)$] and travertine [$CaCO_3$] (Barnes et al., 1982; Tiago et al., 2004; Blank et al., 2009). Serpentinization-derived fluids tend to be depleted in iron and sulfate (in

contrast to some hydrothermal fluids), but enriched with simple hydrocarbons (CH_4, H_2) (e.g. Früh-Green et al., 2004; Kelley et al., 2005; Proskurowski et al., 2008). As such, these spring fluids represent chemical environments distinct from typical surface waters and it is thought that they may harbor distinct microbial communities as well.

1.5 Present-day Serpentinization: Occurrence of Known Serpentine and Ophiolite-hosted Systems

On the modern Earth, liquid water interacting with mafic and ultramafic rocks constitutes extensive environments of chemical disequilibrium (Schulte et al., 2006) and thus may host substantial chemolithoautotrophic communities (McCollom & Shock, 1997; Takai et al., 2004; Brazelton et al., 2009, 2010a,b, 2011a,b). Fluids enriched in H_2 and CH_4 have been frequently observed discharging from serpentine-hosted marine systems (e.g. Kelley et al., 2001, 2005; Charlou et al., 1998, 2002; Proskurowski et al., 2008) as well as from terrestrial systems (e.g. Barnes et al., 1967, 1972, 1982; Barnes & O'Neill, 1971, 1978,; Sturchio et al., 1989; Cardace et al., 2012; Okland et al., 2012) supporting the growth of heterotrophic and autotrophic microorganisms.

Ophiolites – sections of oceanic crust and parts of the upper mantle that have been tectonically emplaced on land – are often host to serpentine minerals and as such have been targeted for evidence of terrestrial serpentinization (e.g. Szponar et al., 2010; Cardace et al., 2012). Ophiolites can become incorporated with continental crust via a variety of tectonic settings, including continental collision, at accretionary margins and subduction zones, and due to ridge-trench interactions (Dilek & Furnes, 2011). Today, ophiolites are exposed throughout Turkey and the Mediterranean in the suture zones formed by the closure of the Tethys ocean in the Late Tertiary (Okay, 2008; Meyer-Dombard et al., 2010).

Ophiolite-hosted fluid and gas systems have been associated with active terrestrial serpentinization at depth and are likely reflective of prior serpentinization of ultramafic rocks in oceanic crust (e.g. basalt, gabbros) that continue to undergo water-rock interactions after

emplacement onto land. Evidence of continual hydrogen generation in partially-serpentinized ophiolite units (primarily dunites) has been observed by Okland et al. (2012) and others, suggesting that this process may continue to provide chemical energy long after its initiation in the subsurface. Their accessibility relative to the seafloor has made them ideal candidates for the study of low-temperature terrestrial serpentinization processes and to explore the extent of subsurface microbial communities in similar lithologies (Okland et al., 2012).

1.5.1 **Terrestrial Systems**

Suitable host rocks for modern-day serpentinization in terrestrial environments (i.e. ophiolites, peridotites) are exposed at the surface in California (Cedars ultramafic complex, Wood, 1970; Blank et al., 2009; Cardace et al., 2012), New Zealand (Milford Sound, Cardace & Hoehler, 2009b), the Phillipines (Abrajano et al., 1988, 1990; Sturchio et al., 1989), Oman and Yugoslavia (Barnes & O'Neill, 1978; Neal & Stanger, 1983), Portugal (Cabeço de Vide groundwater, Tiago et al., 2004), Newfoundland (Tablelands ophiolite, Schrenk et al., 2010; Szponar et al., 2010), Italy (Boschetti & Toscani, 2008; Tassi et al., 2012) and in parts of Turkey (e.g. along the North Anatolian Fault Zone, Meyer-Dombard et al., 2010) and in the southwest near Antalya (Tekirova ophiolite; Etiope et al., 2011). These uplifted sections of upper mantle/lower oceanic crusts contain numerous hot and cool geothermal springs emanating highly reduced, alkaline fluids reflective of the release and subsequent interaction of entrapped ancient ocean waters or modern meteoric waters with surrounding mafic minerals (e.g. olivines, pyroxenes). As such, geochemical and biological analysis of fluids emanating from these units can provide a window into subsurface geochemical, and potentially microbiological, processes.

In some locations (e.g. the Zambales ophiolite in the Philippines), the unit is dominated by highly reduced gas seeps (versus reduced fluids) produced by active serpentinization at depth (Abrajano et al., 1988, 1990; Sturchio et al., 1989). In that case, fluids at the surface may interact with these reduced gases, potentially accelerating weathering alteration processes of ultramafic

mineral assemblages that will impact chemistry of associated surface waters. A similar situation was observed at Yanartaş (YT) during our 2012 field survey of the Tekirova ophiolite (SW Turkey), from which methane-dominated natural gas and minor amounts of fluid discharge along fault lines producing alkaline (up to pH~12) fluids that likely support ephemeral biofilm communities. Low-temperature (30-70°C) generation of methane by olivine hydrolysis has recently been demonstrated experimentally (Neubeck et al., 2011), indicating that some of the methane emitted at Yanartaş may be related to surface weathering of ultramafic minerals. This is especially relevant as the Tekirova Ophiolite is enriched in chromium-bearing minerals, which have proven efficient catalysts for Fischer-Tropsch Type (FTT) synthesis of CH_4 (Etiope et al., 2011; Foustoukos & Seyfried, 2004; Neubeck et al., 2011). As such, methane generated may be derived from multiple sources, including serpentinization at depth and lower-temperature olivine hydrolysis in ultramafic assemblages closer to the surface, as well as a minor thermogenic component sourced from a coal-bearing limestone unit ~ 6km at depth (Hosgörmez et al., 2008; Etiope et al., 2011). Results from cultivation experiments, genetic assays for nitrogen-cycling functional genes, and fluid chemistry from this site will be discussed in Chapter 5.

Differences in water:rock ratios in subsurface serpentinizing system can greatly impact the degree of alkalinity generated, with higher water:rock ratios generally leading to dilution of hydroxide alkalinity and lower pH values (Okland et al., 2012). As such, these systems can create a variety of geochemical habitats for the subsurface microbiome over the life of the serpentinization process. The study of weathering serpentinites on land versus those freshly exposed at the seafloor will shed light on how microbial communities respond to differences in fluid and rock chemistry over long time scales.

1.5.2 **Submarine Systems**

Compared to terrestrial serpentinizing systems, the geomicrobiology of submarine hydrothermal systems associated with serpentinization has received much more detailed study,

and as such, much more is known about the chemolithoautotrophic communities supported by submarine serpentinization processes. Fluids enriched in $H_{2(g)}$ derived from serpentinization of the oceanic crust below have been observed emanating out of the seafloor from hydrothermal fields along the Central Indian Ridge (Takai et al., 2004), the mid-Atlantic ridge (MAR), (Charlou et al., 1998, 2002) and at lower temperature vents off-axis from the MAR (Kelley et al., 2001, 2005). Several of these sites (e.g the Lost City Hydrothermal field (LCHF); Kelly et al., 2001; Brazelton et al., 2009, 2010a-d, 2011), host vast microbial communities subsisting nearly entirely of chemical energy (with little or no inputs of carbon or energy from photosynthesis) obtained from sharp redox gradients produced by the mixing of reduced hydrothermal fluids discharging into oxygenated seawater.

Recent work by Brazelton et al. (2009) suggest that systems at LCHF may have been hydrothermally active for over ~30,000 years based on evidence of prior microbial communities within older, now dormant chimneys consistent with communities still living in younger chimneys nearby. These chimney structures – composed primarily of calcium carbonate and magnesium hydroxides – were precipitated as a result of excess serpentinization-derived Ca^{2+} and Mg^{2+} in solution (Kelley et al., 2001). Further evidence for the longevity of serpentinization-derived energy is the existence of ophiolite-hosted springs with detectable levels of reduced gases (H_2, CH_4) produced as fluids interact with newly exposed ultramafic mineral surfaces created by faulting or secondary fracturing of the host rock (Lowell & Rona, 2002; Okland et al., 2012). As such, serpentinization may generate chemical energy over timescales long enough to provide many opportunities for microbial life to harvest it and establish chemosynthetic communities.

1.6 **Serpentinization and Astrobiological Targets**

Several workers have proposed that serpentinization may have provided one of the earliest abiotic sources of energy in the form of H_2 (Sleep et al., 2004; Schulte et. al., 2006; Martin & Russell,

2007; Russell et al., 2010), a strong reductant that can drive several unique microbial metabolisms (e.g. methanogenesis, Fe(III) reduction). Some of these metabolisms – methanogenesis, for example - are among the most ancient and deeply-rooted metabolic pathways based on 16SrRNA phylogenetic reconstructions (Pace, 1991; Sleep et al., 2004). Recent studies utilizing spectral imagery of the Martian surface and atmosphere have indicated the likely presence of both methane gas (Formisano et al., 2004; Atreya et al., 2007) and altered silicate minerals (Ehlmann et al., 2009) – two lines of evidence indicative of prior or ongoing serpentinization processes. As such, subsurface serpentinizing systems are of particular interest to astrobiology and early Earth paleobiology because the geochemical conditions associated with serpentinization may be analogous to those on early Earth (Nisbet & Sleep, 2001; Sleep et al., 2004; Schulte et al., 2006) and during the evolution of Mars (Ehlmann et al., 2009).

Frequently, serpentinization produces fluids containing both H_2 and CH_4, allowing the development of both hydrogen and methane-based metabolisms (e.g. methanotrophs)(Kelley et al., 2005; Schulte et al., 2006). These highly reduced gases and fluids produced from serpentinization processes at depth are out of equilibrium with conditions at the surface (Cardace & Hoehler, 2009), providing ample chemical energy for microorganisms able to utilize electron donors (e.g. H_2, CH_4) to drive exergonic redox reactions for cellular synthesis and to reduce $CO_{2(g)}$ (carbon fixation) into biomass . Both hydrogen and methane are strong reductants, and thus can drive exergonic redox reactions if an appropriate electron acceptor (e.g. nitrate [NO_3^-]; sulfate [SO_4^{2-}]; permanganate [MnO_4^-]) is available in sufficient quantities and rates) (McCollom & Shock, 1997; Amend & Shock, 2001; Shock et al., 2010). It has been postulated that hydrogenotrophic methanogenesis may have originated within serpentinizing fluids, given that methanogens can flourish at $H_{2(g)}$ concentrations ($\sim$13 nM) well below those attained when $CO_{2(g)}$-rich fluids are in equilibrium with serpentinization-derived waters, which may reach as high as $\sim$75 mM, based on experimental studies and theoretical yields (Sleep et al., 2004; Cardace & Hoehler, 2009). Estimates of $H_{2(g)}$

concentrations for related, terrestrial seeps are on the order of ~300 μM (Cardace & Hoehler, 2009) although actual observed $H_{2(g)}$ concentrations in studied alkaline seeps have generally been lower. This may be due to rapid consumption of H_2 by microorganisms or gaseous diffusion out of the fluid at the surface.

Abiotic $CO_{2(g)}$ reduction to $CH_{4(g)}$ (as in **Eq. 4**) and other light hydrocarbons has been observed experimentally from the mixing of serpentinized-derived waters with $CO_{2(g)}$-rich fluids in hydrothermal conditions (Berndt et al., 1996; Horita & Berndt, 1999; McCollom & Seewald, 2003, 2007; Foustoukos & Seyfried, 2004; Seewald et al., 2006; Seyfried et al., 2007; Fu et al., 2007; Lazar et al., 2012), potentially limiting the amount of $H_{2(g)}$ available for hydrogenotrophic methanogens existing on early Earth (Sleep et al., 2004).

$$CO_2 + H_2 \rightarrow CH_4 + H_2O \qquad \textbf{Eq. 4}$$

The impact of competing abiotic consumption of $H_{2(g)}$ via such processes (e.g. Fischer-Tropsch type synthesis of hydrocarbons) is not known . As such, the amounts and rates of $H_{2(g)}$ production during serpentinization and the degree of abiotic $CO_{2(g)}$ reduction to $CH_{4(g)}$ are currently active topics of research using both geochemical modeling (e.g. McCollom & Bach, 2009; Cardace & Hoehler, 2009; Hellevang et al., 2011) and laboratory studies (e.g. Allen & Seyfried, 2003; McCollom & Seewald, 2003a,b, 2007; Oze & Sharma, 2007).

Several workers have also suggested that the reduction of CO_2 or CO by $H_{2(g)}$ produced from serpentinization may have catalyzed the abiotic formation of organic hydrocarbons, providing a possible source for the precursors to modern biomolecules necessary for the evolution of life (e.g. Berndt et al., 1996; Shock & Schulte, 1998; Sleep et al., 2004; Martin & Russell, 2007). This type of reaction is referred to as Fischer-Tropsch type synthesis, and can be generally written as:

$$(n + 0.5m)H_{2(g)} + nCO_{(g)} \rightarrow C_nH_{m(s)} + nH_2O_{(g)} \qquad \textbf{Eq. 5}$$

Field observations of abundant light hydrocarbons in vent fluids at the Lost City Hydrothermal Field ~15km away from the Mid-Atlantic Ridge have indicated that this process may be actively

occurring (Proskurowski et al., 2008; Charlou et al., 2010). If so, it is reasonable to assume this process may have operated in hydrothermal systems on early Earth as well, providing the necessary organic molecules for life to abound. In order to deduce whether this was a viable possibility for the abiotic synthesis of key organic precursor molecules, the amount of energy actually available in these systems must be constrained.

Relating thermodynamic calculations to predict microbial community function in unique geochemical settings may provide insight on potential Martian and early Earth analogs for microbial life. Calculations of Gibb's free energies of reactions for several potential metabolic options (methanogenesis, methanotrophy, ferric iron reduction, nitrate reduction, and sulfate reduction) indicate that these reactions are exergonic over a wide range of temperatures and H_2 activities representative of known serpentinizing environments, and thus may support microbial metabolisms (Cardace & Hoehler, 2009a). Gibbs free energies of reaction for several metabolic pathways based on high and low estimates of key geochemical parameters expected at field sites along the NAFZ in June 2010 were calculated assuming some input from serpentinization-derived fluids. These calculations indicate that most chemosynthetic metabolisms (e.g. Fe(III), nitrate or sulfate reduction) are exergonic in these systems. It is fair to assume that if these systems are truly representative of early Earth or extraterrestrial habitats, then the same metabolisms exergonic in analog sites should be favorable at astrobiological targets as well. This work tests metabolic options utilized in culture in the context of these predictions. The results and their correspondence with these calculations are discussed in Chapter 5.

1.7 **Hydrothermal Systems & Serpentinization on the Early Earth**

Although active, terrestrial serpentinizing systems are uncommon on Earth today (Tiago et al., 2004), they may have been much more widespread on the early Earth (Blank et al., 2009), leading many to speculate whether early microbial life utilized the $H_{2(g)}$ produced as a reductant to drive chemosynthetic metabolic pathways (Russell et al., 2010), possibly within an alkaline

hydrothermal vent system (Früh-Green et al., 2004; Schulte et al., 2006; Martin & Russell, 2007). Several workers have proposed a hydrothermal origin for microbial life based on phylogenetic reconstructions of the tree of life using 16S rRNA gene sequences (e.g. Russell and Hall, 1997; Reysenbach and Shock, 2002; Pace, 1997, 2001). These reconstructions are founded on the assumption that all organisms once derived from one cell or community of cells - the Last Universal Common Ancestor, or LUCA (Boussau and Gouy, 2012). According to nucleic acid-based phylogeny, the most deeply-rooted (and thus presumably the most ancient) organisms are thermophilic Archaea and Bacteria. This is consistent with current thinking that the Archaean Earth was a much warmer world (estimated surface temperatures of 40-85°C) due to recent impacts and residual heat energy in the mantle associated with the newly accreting planet following the Big Bang (Hazen et al., 2008).

Immediately following the formation of Earth circa 4.5 bya, the distribution of crustal minerals was much more homogenous than at present (Van Kranendonk, 2006). The Earth's core had yet to differentiate from the mantle; consequently, the distribution of ultramafic minerals (e.g. olivine and pyroxene, which are only stable at the elevated temperatures and pressures found within the mantle) at the surface was much more widespread than at present (Nisbet & Sleep, 2001; Sleep et al., 2004). Higher heat flow following Earth's formation increased the degree of water-rock interaction in the Earth's crust (Schulte et al., 2006) and in the absence of widespread continental crust formation, hydrothermal fluid alteration of ultramafic minerals was inevitable. As such, both serpentinization and hydrothermal activity were prevalent on early Earth.

The modern atmosphere had yet to develop and was virtually devoid of free O_2, with higher levels of CO_2 and CH_4 due to volcanism and mantle degassing (Hazen et al., 2008). The lack of both O_2 and O_3 in the atmosphere allowed intense UV radiation from the Sun to reach the surface, making terrestrial habitats fairly inhospitable to incipient life forms. The Achaean oceans, although thought to be much warmer than today's oceans, would have provided shelter from ionizing

radiation and, near hydrothermal vents, may have provided sufficient chemical disequilibrium to fuel chemosynthetic metabolisms (Martin et al., 2008). This view is in light of recent knowledge of entirely chemoautotrophic communities observed fueled by the oxidation of reduced species (e.g. H_2S, CH_4) within venting hydrothermal fluids near oceanic spreading centers and submarine volcanoes (Martin et al., 2008; Russell and Hall, 1997). Fossil evidence strongly suggests that the earliest life forms date prior to the origin of photosynthesis (Nisbet & Sleep, 2001; Van Kranendonk, 2006), further implicating that chemosynthetic metabolisms were among the first to emerge on early Earth.

Finding conclusive answers to these questions remains difficult without knowledge of biogeochemistry in comparable systems. In order to address habitability in extreme environments that may have fostered the earliest forms of life, comprehensive geochemical and microbiological characterization of analog sites must be undertaken. This study highlights the need for a reliable predictive mechanism based on quantifiable physico-chemical parameters of a system and presents data on a newly described analog site in western Turkey to contribute to ongoing research efforts. The following chapters will describe field localities surveyed in 2010 and 2012, methodology used to characterize metabolic options used by resident microorganisms, and ties to genetic functioning and 16SrRNA taxonomy of microbial communities cultured from these hydrothermal and serpentine-associated systems.

CITED LITERATURE:

Abrajano, T. A., Sturchio, N. C., Bohlke, J. K., Lyon, G. L., Poreda, R. J., & Stevens, C. M. (1988) Methane-hydrogen gas seeps, Zambales Ophiolite, Philippines: Deep or shallow origin? *Chem Geol* **71**: 211-222.

Abrajano et al. (1990) Geochemistry of reduced gas related to serpentinization of the Zambales ophiolite, Philippines. *Applied Geochemistry* **5**:625-630.

Allen, D. E. & Seyfried, W. E. (2003) Alteration and mass transfer in the $MgO–CaO–FeO–Fe_2O_3–SiO_2–Na_2O–H_2O–HCl$ system at 400 °C and 500 bars: implications for pH and compositional controls on vent fluids from ultramafic-hosted hydrothermal systems at mid-ocean ridges. *Geochim. Cosmochim. Acta*, **67**:1531–1542

Amend, JP and Shock, E. L. (2001) Energetics of overall metabolic reactions of thermophilic and hyperthermophilic Archaea and Bacteria. *FEMS Microbiology Reviews* **25**:175-243.

Atreya, S. K., Mahaffy, P. R., & Wong, A. (2007) Methane and related trace species on Mars: Origin, loss, implications for life, and habitability. *Planetary and Space Science* **55**:358–369.

Barnes, I., Lamarche, V. C., & Himmelberg, G. R. (1967) Geochemical evidence of present-day serpentinization. *Science* **56**:830-832.

Barnes, I. & O'Neil, J. R. (1971) The relationship between fluids in some fresh Alpine-type ultramafics and possible modern serpentinization, Western United States. *Bull. Geol.* Soc. *Am.* **80:**1947-1960.

Barnes, I., Rapp, J. B., & O'Neil, J. R. (1972) Metamorphic Assemblages and the Direction of Flow of Metamorphic Fluids in Four Instances of Serpentinization. *Contr. Mineral. and Petrol*. **35**:263—276.

Barnes, I. & O'Neil, J.R. (1978) Present-day serpentinization in New Calcedonia, Oman and Yugoslavia. *Geochimica et Cosmochimica Acta* **42**:144-145.

Barnes, I., Presser, T. S., Saines, M., Dickson, P., & Van Groos, A. F. K. (1982) Geochemistry of highly basic calcium hydroxide groundwater in Jordan. *Chemical Geology* **35**:147-154.

Berndt, M. E., Allen, D. E., and Seyfried, W. E. (1996) Reduction of CO_2 during serpentinization of olivine at 300C and 500 bar. *Geology* **24**(4):351-354.

Biddle J.F., Lipp, J.S., Lever, M.A., Lloyd, K.G., Sørensen, K.B., et al. (2006) Heterotrophic Archaea dominate sedimentary subsurface ecosystems off Peru. *Proc Natl Acad Sci USA* **103**: 3846–51.

Blank, J. G., Green, S., Blake, D., Valley, J., Kita, N., Treiman, A. et al. (2009) An alkaline spring system within the Del Puerto ophiolite (California USA): A Mars analog site. *Planet Space Sci* **57**:533-540.

Boschetti, T., & Toscani, L. (2008) Springs and streams of the Taro–Ceno Valleys (Northern Apennine, Italy): reaction path modeling of waters interacting with serpentinized ultramafic rocks. *Chemical Geology* **257**: 76–91.

Boussau, B. & M. Gouy, M. (2012) What genomes have to say about the evolution of the Earth. *Gondwana Research* **21**:483-494.

Brazelton, W. J., Ludwig, K. A., Sogin, M. L., Andreishcheva, E. N., Kelley, D. S., Shen, C., Edwards, R. L., & Baross, J. A. (2009) Archaea and bacteria with surprising microdiversity show shifts in dominance over 1,000-year time scales in hydrothermal chimneys. *PNAS* **107**(4):1612-1617.

Brazelton, W.J. & Baross, J.A. (2010a). Metagenomic comparison of two Thiomicrospira lineages inhabiting contrasting deep-sea hydrothermal environments. *PLoS One*, 5(10): 1-8.

Brazelton, W.J., Sogin, M.L. & Baross, J.A. (2010b). Multiple scales of diversification within natural populations of archaea in hydrothermal chimney biofilms. *Environmental Microbiology Reports*, **2**: 236-242.

Brazelton, W. J., Mehta, M. P., Kelley, D. S., & Baross, J. A. (2011a) Physiological Differentiation within a Single-Species Biofilm Fueled by Serpentinization. mBio **2**(4):e00127-11.

Brazelton, W.J., Nelson, B. & Schrenk, M.O. (2011b). Investigating the Potential for Subsurface Primary Production Fueled by Serpentinization. American Geophysical Union Meeting. San Francisco, CA.

Cardace, D. & Hoehler, T. M. (2009a) Serpentinizing fluids craft microbial habitat. *Northeastern Naturalist* **16**(5): 272-284.

Cardace, D. & Hoehler, T. M. (2009b) Fluid Chemistry and Associated Biological Potential in Diverse Serpentinizing Systems of New Zealand's South Island. American Geophysical Union, Fall Meeting 2009, Abstract #B23C-0393.

Cardace, D., Carnevale, D., Hoehler, T., McCollom, T., & Schrenk, M. (2012) Active Serpentinization in the Coast Range Ophiolite: Intersections of Petrography, Geochemistry, and Bioenergetics. AbSciCon 2012 Meeting, Abstract #4491.

Chapelle, F. H., O'Neil K., Bradley, P.M., Methé, B.A., Ciufo, S.A., et al. (2002) A hydrogen-based subsurface microbial community dominated by methanogens. *Nature* **415**: 312–315.

Charlou, J. L., Fouquet, Y., Bougault, H., Donval, J. P., Etoubleau, J., Jean-Baptiste, P. et al. (1998) Intense CH_4 plumes generated by serpentinization of ultramafic rocks at the intersection of the 15°20′ N fracture zone and the Mid-Atlantic Ridge. *Geochim Cosmochim Acta* **62**: 2323-2333.

Charlou, J.L., Donval, J.P., Fouquet, Y., Jean-Baptiste, P., Holm, N., 2002. Geochemistry of high H_2 and CH_4 vent fluids issuing from ultramafic rocks at the Rainbow hydrothermal field (36°14_ N, MAR). *Chem*. *Geol*. **191**: 345– 359.

Charlou, J. L., J. P. Donval, C. Konn, H. Ondréas, Y. Fouquet, P. Jean-Baptiste, & E. Fourré (2010), High production and fluxes of H_2 and CH_4 and evidence of abiotic hydrocarbon synthesis by serpentinization in ultramafic-hosted hydrothermal systems on the Mid-Atlantic Ridge. *Diversity of Hydrothermal Systems on Slow Spreading Ocean Ridges*, *Geophys. Monogr. Ser.* **188**:265-296.

Chivian, D. et al. (2008) Environmental genomics reveals a single-species ecosystem deep within Earth. *Science* **332**: 275.

Corliss, J. B. Dymond, J., Gordon, L.I., Edmond, J.M., Herzen, R.P.V., Ballard, R.D., Green, K., Williams, D., Bainbridge, A., Crane, K., & Vanandel, T.H.(1979) Submarine thermal springs on the Galapagos Rift. *Science* **203**:1073–1083.

Dilek, Y. & Furnes, H. (2011) Ophiolite genesis and global tectonics: Geochemical and tectonic fingerprinting of ancient oceanic lithosphere. *Geological Socieity of America Bulletin* **123**:387-411.

Ehlmann, B.L., Mustard, J.F., Swayze, G.A., Clark, R.N., Bishop, J.L., Poulet, F., Des Marais, D.J., Roach, L.H., Milliken, R.E., Wray, J.J., Barnouin-Jha, O., & Murchie, S.L. (2009) Identification of hydrated silicate minerals on Mars using MRO-CRISM: geologic context near Nili Fossae and implications for aqueous alteration. *J Geophys Res-Planet* **114**: E00D08.

Etiope, G., Schoell, M., & Hosgörmez, H. (2011) Abiotic methane flux from the Chimaera seep and Tekirova ophiolites (Turkey): Understanding gas exhalation from low temperature serpentinization and implications for Mars. *Earth and Planetary Science Letters* **310**:96–104.

Formisano, V., Atreya, S., Encrenaz, T., Ignatiev, N., and Giuranna, M. (2004) Detection of methane in the atmosphere of Mars. *Science* **306**:1758–1761.

Foustouskos, D.I. & Seyfried, W.E. (2004) Hydrocarbons in hydrothermal vent fluids: The role of chromium-bearing catalysts. *Science* **304**:1002–1005.

Früh-Green, G. L., Kelley, D. S., Bernasconi, S. M., Karson, J. A., Ludwig, K. A., Butterfield, D. A., Boschi, C., & Proskurowski, G. (2003)30,000 Years of Hydrothermal Activity at the Lost City Vent Field *Science* **301**:495-498.

Früh-Green, G.L., Connolly, J.A.D., Plas, A., Kelley, D.S., Grobety, B., 2004. Serpentinization of oceanic peridotites: implications for geochemical cycles and biological activity. The subseafloor biosphere at mid-ocean ridges E. F. D. W. S. D. Wilcock, D. S. Kelley, J. A. Baross, and S. C. Cary. American Geophysical Union **144**: 119–136.

Fu, Q., Sherwood Lollar, B., Horita, J., Lacrampe-Couloume, G., & Seyfried, J. W. E. (2007) Abiotic formation of hydrocarbons under hydrothermal conditions: constraints from chemical and isotopic data. *Geochimica et Cosmochimica Acta*, **71**:1982–1998.

Hazen, R. M., Papineau, D., Leeker, W. B., Downs, R. T., Ferry, J. M., McCoy, T. J., Sverjensky, D. A., & Yang, H. X. (2008) Mineral evolution. *American Mineralogist*, **93**(11-12):1693-1720.

Hellevang, H., Huang, S., & Thorseth, I. H. (2011) The potential for low-temperature abiotic hydrogen generation and a hydrogen-driven deep biosphere. *Astrobiology* **11**(7):711-724.

Hoehler, T. M. (2004) Biological energy requirements as quantitative boundary conditions for life in the subsurface. *Geobiology* **2**:205-215.

Hoehler, T. M. (2007) An energy balance concept for habitability. *Astrobiology* **7**(6):824-838.

Hoehler, T. M., Amend, J. P., & Schock, E. L. (2007) A "Follow the Energy" Approach for Astrobiology. *Astrobiology* **7**(6):819-823.

Horita, J. & Berndt, M. E. (1999). Abiogenic Methane Formation and Isotopic Fractionation Under Hydrothermal Conditions. *Science* **285(**5430):1055-1057.

Hosgörmez, H., Etiope, G., & Yalcin, M. N. (2008) New evidence for a mixed inorganic and organic origin of the Olympic Chimaera fire (Turkey): a large onshore seepage of abiogenic gas. *Geofluids* **8**:263–273.

Hostetler, P. B., Coleman, R. G., & Mumpton, E. A. (1966) Brucite in alpine serpentinites. *Am. Mineral*. **51**:75–98.

Iyer, K., Austrheim, H., John, T., & Jamtveit, B. (2008) Serpentinization of the oceanic lithosphere and some geochemical consequences: Constraints from the Leka Ophiolite Complex, Norway. *Chemical Geology***249**:66-90.

Kelley, D. S., Karson, J. A., Blackman, D. K., Früh-Green, G. L., Butterfield, D. A., Lilley, M. D., Olson, E. J., Schrenk, M. O., Roe, K. K., Lebon, G. T., Rivizzigno P., and the AT3-60 Shipboard Party. (2001) An off-axis hydrothermal vent field near the Mid-Atlantic Ridge at 30°N. *Nature* **412**:145–149.

Kelley, D. S. et al. (2005) A serpentinite-hosted ecosystem: the Lost City hydrothermal field. *Science* **307**: 1428–1434.

Lazar, C., McCollom, T. M., & Manning, C. E. (2012) Abiogenic methanogenesis during experimental komatiite serpentinization: Implications for the evolution of the early Precambrian atmosphere. *Chem Geol* **326–327:** 102-112.

Lin, L.H., Wang, P.L., Rumble, D., Lippmann-Pipke, J., Boice, E., Pratt, L.M., Lollar B., Brodie, E.L., Hazen, T.C., Andersen, G.L., DeSantis, T.Z., Moser, D.P., Kershaw, D., & Onstott, T.C. (2006) Long-term sustainability of a high-energy, low-diversity crustal biome. *Science* **314**: 479

Lowell R. P. and Rona P. A. (2002) Seafloor hydrothermal systems driven by the serpentinization of peridotite. *Geophys. Res. Let* **29**(26):1–5.
Martin, W., Baross, J., Kelley, D., & Russell, M. J. (2008) Hydrothermal vents and the origin of life. *Nature Reviews* **6**:805-814.
McCollom, T. M., Bach, W., and Hoehler, T. (2010) Hydrogen generation for microbial activity in ultramafic-hosted hydrothermal systems. *Geochimica et Cosmochimica Acta*. **74**:A686-A686.
McCollom, T. M., & Shock, E. L. (1997) Geochemical constraints on chemolithoautotrophic metabolism by microorganisms in seafloor hydrothermal systems. *Geochimica et Cosmochimica Acta*. **61**:4375-4391.
McCollom, T. M., & Seewald, J. S. (2003a) Experimental constraints on the hydrothermal reactivity of organic acids and acid anions: I Formic acid and formate. *Geochimica et Cosmochimica Acta* **67**:3625-3644.
McCollom, T. M., & Seewald, J. S. (2003b) Experimental study of the hydrothermal reactivity of organic acids and acid anions: II Acetic acid, acetate, and valeric acid. *Geochimica et Cosmochimica Acta* **67**:3645-3664.
McCollom, T. M., & Seewald, J. S. (2007) Abiotic synthesis of organic compounds in deep-sea hydrothermal environments. *Chem. Rev.* **107**:382–401.
Mével, C. (2003) Serpentinization of abyssal peridotites at mid-ocean ridges. *CR Geosci*., **335**:825–852.
Meyer-Dombard, D. R., Cardace, D., Uzunlar, N., Güleçal, Y., Yargıçoğlu, E., Carbone, J. N. (2010) Microbial Community Diversity in Fault-Associated and Ophiolite-Hosted Springs. American Geophysical Union, Fall Meeting 2010, Abstract #B51A-0334.
Neal, C., & Stanger, G. (1983) Hydrogen generation from mantle source rocks in Oman. *Earth Planet Sci Lett* **66**: 315-320.
Neubeck, A., Duc, N.T., Bastviken, D., Crill, P., & Holm, N.G. (2011) Formation of H_2 and CH_4 by weathering of olivine at temperatures between 30 and 70 °C. *Geochemical Transactions* **12**.
Nisbet, E. G. & Sleep, N. H. (2001) The habitat and nature of early life. *Nature* **409**(22):1083-1091.
Okay, A.I. (2008) Geology of Turkey: A synopsis. *Anschnitt* **21**:19-42.
Okland, I.,Huang, S., Dahle, H., Thorseth, I.H., & Pedersen, R.B. (2012) Low temperature alteration of serpentinized ultramafic rock and implications for microbial life. *Chemical Geology* **318-319**:75-87.
Orcutt, B., Wheat, C. G., & Edwards, K. J. (2010) Subseafloor Ocean Crust Microbial Observatories: Development of FLOCS (FLow-through Osmo Colonization System) and Evaluation of Borehole Construction Materials. *Geomicrobiology Journal* **27**:143-157.
Oze, C. & Sharma, M. (2007) Serpentinization and the inorganic synthesis of H_2 in planetary surfaces. *Icarus* **186**:557-561.
Pace, N. R. (1991) Origin of life – facing up to the physical setting. *Cell* **65**:531-533.
Pace, N. R. (1999). Microbial Ecology and Diversity. *Am. Soc. Microbiology News* **65**:328-333
Pace, N. R. (2001) The universal nature of biochemistry. *PNAS* **98**(3):805-808.
Pace, N. R. (2009) Mapping the Tree of Life: Progress and Prospects. *Microbiol. Mol. Biol. Rev.* **73**(4):565-576**.**
Parkes, R. J., Sellek, G., Webster, G., Martin, D., Anders, E., Weightman, A. J., & Sass, H. (2009) Culturable prokaryotic diversity of deep, gas hydrate sediments: first use of a continuous high-pressure, anaerobic, enrichment and isolation system for subseafloor sediments (DeepIsoBUG). *Environ Microbiol* **11**: 3140-3153.
Proskurowski, G., Lilley, M.D., Seewald, J.S., Früh-Green, G.L., Olson, E.J., Lupton, J.E., Sylva, S.P., and Kelley, D.S. (2008) Abiogenic hydrocarbon production at Lost City hydrothermal field. *Science* **319**:604–607.
Rastogi, G., Osman, S., Kukkadapu, R., Engelhard, M., Vaishampayan, P. A., Andersen, G. L., & Sani, R. K. (2010) Microbial and Mineralogical Characterizations of Soils Collected from the Deep Biosphere of the Former Homestake Gold Mine, South Dakota. *Microb Ecol* **60**: 539-550.
Reysenbach, A. & Shock, E. L. (2002) Merging Genomes with Geochemistry in Hydrothermal Ecosystems *Science* **296**:1077-1082.
Russell, M. J. & Hall, A. J. (1997) The emergence of life from iron monosulfide bubbles at a submarine hydrothermal redox front. *Journal of the Geological Society (London)* **54**:377-402.
Russell, M.J. (2007) The alkaline solution to the emergence of life: energy, entropy, and early evolution. Acta *Biotheoret*. **55**:133-179.
Russell, M. J., Hall, A. J., & Martin, W. (2010) Serpentinization as a source of energy at the origin of life. *Geobiology* **8**: 355-371.Schulte, M., Blake, D., Hoehler, T. M., & McCollom, T. (2006) Serpentinization and its implications for life on the early Earth and Mars. *Astrobiology* **6**:364 –376.
Seewald, J. S., Zolotov, M. Y. & McCollom, T. M. (2006) Experimental investigation of single carbon compounds under hydrothermal conditions. *Geochim. Cosmochim. Acta* **70**:446–460.

Seyfried, W.E., Jr., Foustoukos, D.I., & Fu, Q. (2007) Redox evolution and mass transfer during serpentinization: an experimental and theoretical study at 200°C and 500 bar with implications for ultramafic-hosted hydrothermal systems. *Geochim. Cosmochim. Acta* **71**:3872–3886.

Shervais, J. W., Kolesar, P. & Andreasenm K. (2005a) A Field and Chemical Study of Serpentinization—Stonyford, California: Chemical Flux and Mass Balance. *International Geology Review*, **47**:1–23.

Shervais, J. W., Kimbough, D. L., Renne, P. R., Murchey, B., & Hanan, B. B. (2005b) Radioisotopic and biostratigraphic age relations in the Coast Range Ophiolite, northern California: implications for the tectonic evolution of the Western Cordillera. *Geol. Soc. Am. Bull.* **117**:633-653.

Shock, E. L. & Holland, M. E. (2007) Quantitative Habitability. *Astrobiology* **7(6)**:839-851.

Shock, E. L. & Schulte, M. D. (1998) Organic synthesis during fluid mixing in hydrothermal systems. *J. Geophys. Res*. **103**:28513-28517.

Shock, E.L., Holland, M., Meyer-Dombard, D., Amend, J.P., Osburn, G.R., Fischer, T.P., (2010), Quantifying Inorganic Sources of Geochemical Energy in Hydrothermal Ecosystems, Yellowstone National Park, USA, *Geochimica et Cosmochimica Acta*, **74**:4005-4043.

Skidmore, M. L., Boyd, E. S., Lange, R. K., Mitchell, A. C., Havig, J. R>, Hamilton, T. L., Lafreniere, M. J., Shock, E. & Peters, J. (2011). Diversity, Abundance, and Potential Activity of Nitrifying and Nitrate-Reducing Microbial Assemblages in a Subglacial Ecosystem. AGU Fall Meeting 2011, Abstract#B22A-02.

Sleep, N. H., A. Meibom, Th. Fridriksson, R. G. Coleman, & D. K. Bird. (2004) H_2-rich fluids from serpentinization: Geochemical and biotic implications. *PNAS* **101**(35):12818-12823.

Sturchio, N. C., Abrajano, T. A., Murowchick, J. B., & Muehlenbachs, K. (1989) Serpentinization of the Acoje massif, Zambales ophiolite, Philippines: hydrogen and oxygen isotope geochemistry. *Tectonophysics*, **168**(1–3):101–107.

Szponar, N., Morrill, P.L., Brazelton, W.J., Schrenk, M.O., Bower, D.M. & Steele, A. (2010). Present-day serpentinization in the Tablelands, Gros Morne National Park, Newfoundland: a Mars Analogue Site. American Geophysical Union Meeting. San Francisco, CA.

Takai, K., Toshitaka, G., Urumu, T., Noriko, N., Hisako, H., Nealson, K. H. & Koki, H. (2004) Geochemical and microbiological evidence for a hydrogen-based, hyperthermophilic subsurface lithoautotrophic microbial ecosystem (HyperSLiME) beneath an active deep-sea hydrothermal field. *Extremophiles* **8**:269-282.

Tassi, F., Fiebig, J., Vaselli, O., & Nocentini, M. (2012) Origins of methane discharging from volcanic-hydrothermal, geothermal and cold emissions in Italy. *Chemical Geology* **310–311**:36–48.

Tiago, I., Chung, A. P., and Veríssimo, A. (2004) Bacterial Diversity in a Nonsaline Alkaline Environment: Heterotrophic Aerobic Populations. *Applied and Environmental Microbiology* **70**(12): 7378–7387.

Van Kranendonk, M. J. (2006) Volcanic degassing, hydrothermal circulation and the flourishing of early life on Earth: A review of the evidence from c. 3490-3240 Ma rocks of the Pilbara Supergroup, Pilbara Craton, Western Australia. *Earth-Sci Rev* **74:** 197-240.

Wood, B. L. (1970) Metamorphosed ultramafites and associated formations near Milford Sound, New Zealand. *N.Z. J. Geol. Geophys.* **15**:88-128.

Wu, S.Y. & Lai, M.C. (2011) Methanogenic archaea isolated from Taiwan's Chelungpu Fault. *Applied and Environmental Microbiolgy* **77**: 830-838

2. STUDY SITE SELECTION AND GEOLOGIC CONTEXT

2.1 Introduction

As described in Ch. 1, the use of analog sites is a developing concept in astrobiology that requires comprehensive environmental datasets in order to define meaningful constraints on modeled biogeochemical processes. The exploration of previously undescribed sites that hold promise as potential analogs remains an important aspect of our research in this regard. Recent studies in terrestrial ophiolite complexes in other parts of the world (e.g. the Cedars Ophiolite mélange at McLaughlin Reserve, Northern CA; Cardace et al., 2012; Cabeço de Vide groundwater, Tiago et al., 2004) suggest that a diverse suite of metabolic options may be associated with subsurface fluids with varying degrees of input from weathering serpentines and, in some cases, active serpentinization occurring within these units (Cardace et al., 2012). While active serpentinization is known to occur in marine settings along ocean-spreading centers accompanying the production of new oceanic crust (Dilek & Furnes, 2011), the extent to which serpentinization continues at depth within oceanic crust after tectonic emplacement onto land is unconstrained. As such, the study of ophiolite-hosted systems may shed light on fluid and gas geochemistry during the latter stages of serpentinization and address whether this process continues to hold energetic potential for chemosynthetic subsurface microbial communities.

The complex geological evolution of Turkey has allowed the formation of a number of deeply-sourced, fault-associated spring systems and gas seeps across the highly dissected and variably altered terrain, with approximately 1,000 springs identified by the MTA as of 1980 (MTA, 1980; Simsek, 1988). The few studies that have been conducted on geothermal areas in western Turkey (e.g. Mutlu & Gulec, 1998; Vengosh et al., 2002; Süer et al., 2008; Magri et al., 2010; Sanliyuksel, 2011; Pavsanoğlu, 2011; Sanliyuksel & Baba, 2011) have focused on geothermometry and geothermal energy potential, and have not addressed the microbial ecology or functioning of

these systems. Based on field observations of alkaline springs emanating from various units (including serpentines, peridotites, and amphibolites)(N. Uzunlar, Pers. Comm.) throughout the North Anatolian Fault Zone (NAFZ), Turkey, initial field surveys were undertaken to assess the metabolic potential associated with these fluids. In June of 2010, we pioneered new research into several deeply-sourced hot and cool springs associated with the NAFZ in northwest Turkey. A second field survey of springs along the NAFZ as well as springs and gas seeps in southwest Turkey was conducted in February of 2012. These sites – described in the following sections – afford a unique opportunity to observe subsurface biogeochemistry without drilling directly into the rock, which can prove both expensive and technically challenging.

2.2 Geologic Evolution of Western Turkey

Over the past several hundred million years, tectonic stresses have created the landmass presently known as Turkey from the accretion of continental and oceanic crustal fragments (a.k.a. terranes). The creation and eventual amalgamation of these micro-continents was a result of continental collision between the rifted portions of the African and Eurasian plates (the Anatolide-Tauride block (ATB) and the Sakarya block, respectively) and resultant subduction re-initiation and slab break-off (van Hinsbergen et al., 2010; Okay, 2008). The collision between the two supercontinents (Laurasia to the north and Gondwana to the south) lead to the closure of several intracontinental oceans once separating them, the most recent being the Tethys Ocean, that existed since the Carboniferous until its closure in the Late Tertiary (Okay & Tüyüz, 1999; Okay, 2008). The Tethyan ocean was unique in that it consisted of several narrow seaways rather than one larger body, leading to the development of several sutures (Okay, 2008). These forces continue to place pressure on Anatolia, primarily from the African plate to the south, the Arabian platform to the east, and the Eurasian terranes to the north and west (see Fig. 1 for regional tectonics and the major tectonic units in Turkey).

FIGURE 1: TECTONIC MAP OF TURKEY.

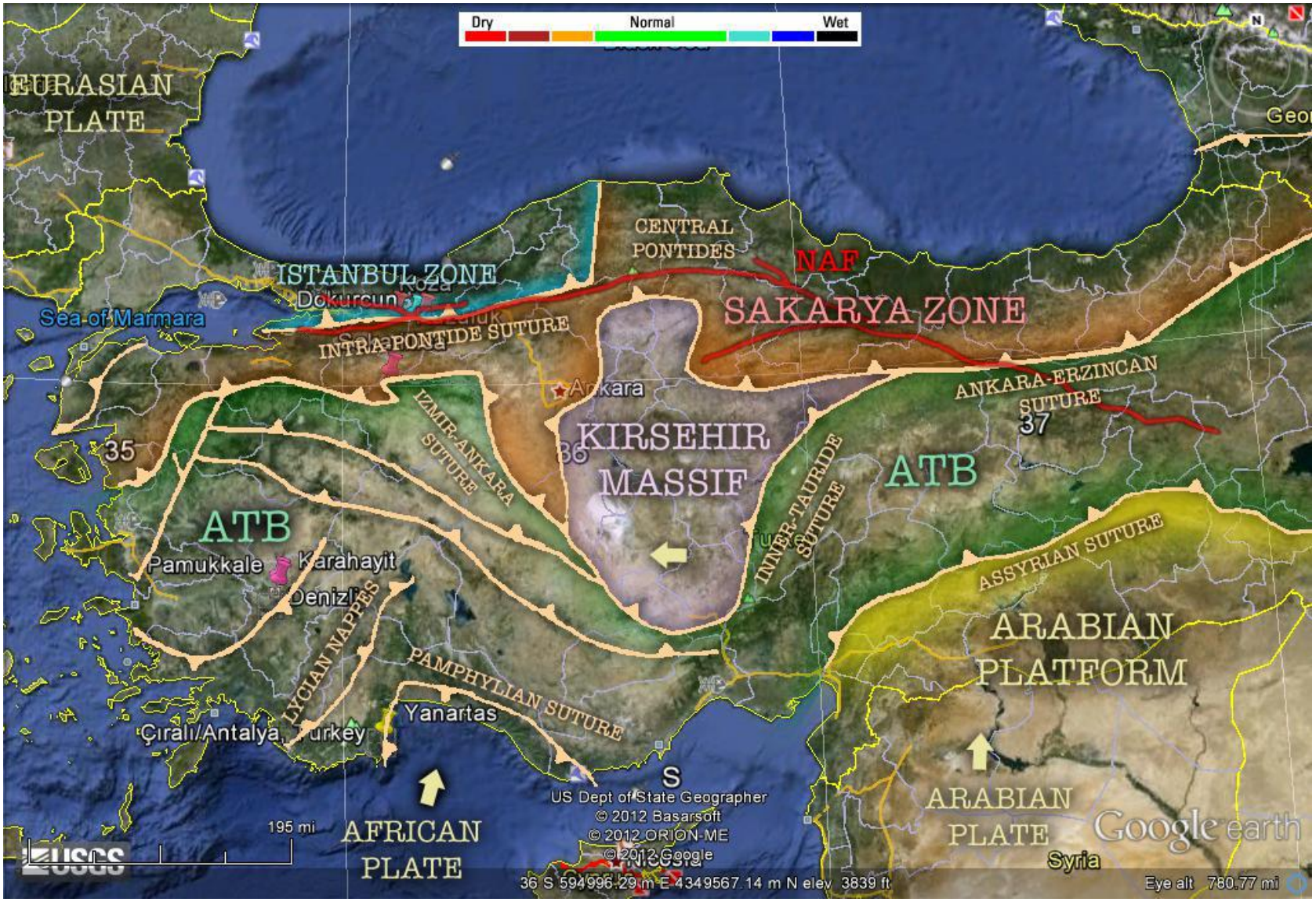

Today, the country can be divided into three major tectonic units: the Pontides, the Anatolide-Tauride Block (ATB), and the Arabian Platform (Okay, 2008). The Pontides are often further subdivided into three main terranes with Laurasian affinities - the Istanbul terrane, the Strandja terrane, and the Sakarya terrane - though each evolved independently of each other prior to the Early Cretaceous (Okay, 2008, 2011; see Fig. 1 for a simplified tectonic map). The North Anatolian Fault (NAF) represents both sutures of major terranes within the Pontides (i.e. the Intra-Pontide Suture) and segments of the northern boundary of the ATB – primarily composed of oceanic crust and overlying marine sedimentary sequences - that is being pushed westwards as the Arabian and Eurasian plates collide (Neugebauer, 1995; Okay, 2008). The result of these tectonics is the development of convergent margins and an extensive strike-slip fault (the NAF), with numerous extensional oversteps and bends and normal faults parallel to the principal fault.

During the closure of the Tethyan Ocean, crustal materials broke off from both the northern and southern boundaries of the former ocean basin, eventually drifting towards the opposite continental margins, resulting in the accretion of continental and oceanic fragments separated by numerous suture zones, which today define the major fault lines in the area (Okay & Tüyüz, 1999). In the northwest, the Intra-Pontide Suture separates the Istanbul zone from the Sakarya Zone (Okay, 2008). The northern boundary of the ATB with the Sakarya Zone is separated into two segments to the west (the Izmir-Ankara Suture) and east (the Ankara-Erzincan Suture) of the Kirşehir Massif, a crystalline complex in central Anatolia that intrudes/interrupts the E-W trending suture between the Pontides and the ATB (Okay, 2003, 2008). As these crustal fragments rifted apart from either Laurasia or Gondwana, they underwent low-temperature, high pressure metamorphism and major contractional event of the oceanic lithosphere, followed by accretion of the Karakaya Complex to Eurasia (Okay, 2011). By the late Tertiary, the terranes had united as a single landmass during the Alpide orogeny (Okay, 2008).

During the Late Miocene to Pliocene eras, the North Anatolian Fault (NAF) formed from the collision of the Arabian and Eurasian plates in present-day eastern Turkey and the closure of the ancient Tethys ocean (Neugebauer, 1995; Okay, 2008). With the closure of the Tethys Ocean, it is likely that some of the ancient ocean waters and water incorporated in hydrated minerals (i.e. serpentinite) were captured in the suture zone defined by the NAF. Metamorphism from tectonic stresses would release water from hydrated minerals at depth; numerous artesian springs in this suture zone allow the escape of these deeply sourced waters. As the Anatolian block is pushed westward, fragmented mantle rock previously uplifted from the compressional stresses associated with the closure of the Tethyan ocean are exposed in the suture zone (Andrieux et. al., 1995). These rocks - mostly periodotites (i.e. dunite, harzburgite), serpentinites, and amphibolites - contain high amounts of magnesium, iron, and other trace metals (e.g. copper, chromium). Fluid interaction with these ultramafic minerals produces hydrogen gas and serpentine minerals and a concomitant increase in the hydroxide alkalinity of the subsurface waters (see Chapter 1, Section 1.4.1 for an explanation of geochemical changes associated with serpentinization).

Exposed throughout the region at topographic highs are Miocene age volcaniclastic layers, deposited during a period of widespread volcanism brought on by the collision of the African plate with Anatolia during the late Tertiary (Pavsanoğlu & Chandrasekharam, 2011). Numerous thermal springs were created as a result of the high heat flow and volcanic activity associated with the African-Anatolian convergent system (Pavsanoğlu, 2011). Because of the great amount of pressure and elevated regional heat flow from tectonic stresses, surface upwellings from deeply-sourced hot springs are common throughout the region, providing many windows into deep subsurface aqueous geochemistry and microbiology.

Erosion following the closure of the Tethyan Ocean deposited layers of lake sediments and intercontinental red beds, observed as iron oxide-rich conglomerate layers within the sedimentary sequence. Sedimentary basins were filled with evaporites at various stages of rifting and ocean

closure throughout the Tertiary (Gündoğan et al., 2008; Okay, 2008). Peridotite, serpentinite, pyroxenite and amphibolite host rocks were all observed in close proximity due to the complexity of the fault zone and the presence of olivine-rich mantle rock wedged in the suture zone. As such a diverse suite of lithologies (e.g. amphibolites, serpentinites, volcanclastics, sedimentary sequences) host both hot and cool springs throughout the NAFZ, allowing for study of both meteoric water-derived and deeply sourced fluids, with varying degrees of fluid interaction with weathering serpentines.

Given the complexity of the landscape and possibility for a diverse set of subsurface habitats, the sites presented in this work merely scratch the surface in terms of understanding broader trends within these systems. Nevertheless, I will draw general comparisons observed from the data gathered thus far, with recommendations for continued studies in these unique systems.

2.3 **Regional Distribution of Hydrothermal Systems**

In Turkey, there are currently few magmatic intrusions and no "hot spot" related volcanism that would create hydrothermal springs. As such, the majority of the hydrothermal systems in the western region are fault-associated and their distribution reflects this: hot springs are predictably located along the suture zone of the major tectonic units, and often exist along splay faults normal to the NAF in the northwest and along the Pamphylian Suture in the southwest (refer to Fig. 1 for a tectonic map). Springs in western Turkey tend to be hosted by volcanic units (e.g. Tuzla geothermal field; Baba et al., 2008); the only slightly alkaline springs are hosted by ultramafic minerals found in both the Lower Cretaceous Almacik Ophiolite Mélange (NW Turkey) and the Tekirova Ophiolite (near the Lycian Nappes, SW Turkey).

Frequent seismic events occasionally result in the formation of new springs. The appearance of several warm geothermal springs observed along the Duzce Fault (an E-W trending normal segment on the northern branch of the North Anatolian Fault (NAF) following a 7.2 magnitude earthquake on November, 12th 1999 (Karakus & Simsek, 2008) is evidence of an ever-

changing tectonic landscape. These seismic events rupture the bedrock, allowing deeply sourced fluids and gases to ascend through faults and secondary fractures. Methane emission and combustion was noted along the shores of Efteni Lake, located along the rupture zone of the northern branch of NAF in Duzce Province (Karakus & Simsek, 2008) immediately following the 1999 earthquake, suggesting subsurface generation of hydrocarbons.

2.4 **Previous Work**

Prior studies of geothermal springs throughout the region (e.g. Süer et al., 2008; Karakus & Simsek, 2008; Davraz, 2008; Sanliyuksel & Baba, 2011) have primarily focused on the geochemistry of the waters, with microbiological studies focusing on lower temperature (<60°C) organisms (e.g. Cadirci et al., 2007; Gul-Guven et al., 2008; Inan et al., 2011) with rare exceptions (e.g. Adiguzel et al., 2009; Canakci et al., 2007; Cihan et al., 2011a,b). Most of these works focused on anthropocentric concerns, e.g. geothermal energy generation and pollution in hot spring systems (e.g. Baba, 2003; Pasvanoğlu et al., 2012). Currently, little is known about the microbial ecology of spring systems in Turkey with relation to geochemical parameters. Of the limited studies on thermophilic microorganisms from Turkish hot springs no attempts are made to explain observed metabolic functions with geochemical proxies. Nevertheless, results from these studies (i.e. the types of thermophilic strains that have been isolated from Turkish hot springs) will provide a useful comparison between my cultured samples and strains obtained by using standard cultivation techniques (without incorporation of site-specific geochemistry in growth media). This work will help to bridge site-specific datasets regarding geochemistry and microbial functional diversity of deeply-sourced springs in the area, providing a baseline for further studies.

2.5. **June 2010 Field Survey**

Several artesian wells were located along main roadways (i.e. Mihalgazi/Eskeşhir Rd.) that followed a southward transect through a peridotite complex, variably altered to serpentinite, with a number of cisterns. Many of these springs have been tapped for drinking water, with pumping

stations already constructed at Kuzuluk and Sakarıılıca, and in construction at Koza. Consequently, these systems are not as pristine as those found at Yellowstone National Park, for example, where restrictions prevent human alteration of the natural hydrothermal system. The effect of anthropogenic influence on the biogeochemistry is not known, though it is important to keep in mind when comparing the data presented with other systems.

The regional basement rock is the Precambrian Yedigoller formation (primarily metagranite, amphibolite, and gneiss), overlain by Paleozoic sedimentary sequences (Karakus & Simsek, 2008). The ridge of the Almacik Block outcrops in highlands south of the Duzce Plain, where it overthrusts Eocene volcanic deposits (andesite, basalt, agglomerate) with serpentinite exposed along secondary faults within this block (Karakus & Simsek, 2008). Four springs in particular were chosen for further study (Sakarıılıca, Kuzuluk, Dokurcun, and Koza) and are described in Table I. This area in northwest Turkey, which had numerous tapped wells, is known as the Kupülüce complex, primarily composed of altered ultramafic mantle rock. Volcaniclastic layers overlying the local bedrock are exposed throughout the region and host some of the hot springs with circumneutral pH values.

The chemical and biological signatures at the surface of these deeply-sourced springs are likely diluted by meteoric waters. However, if recharge to the hydrothermal reservoirs feeding these springs is sourced at depth, the fluids will contain biomass and reduced minerals also sourced at depth. As such, we can infer the metabolic capacities of subsurface communities from analysis of emanating fluids at the surface.

TABLE I: SPRINGS IN NORTHWEST TURKEY SAMPLED DURING THE 2010 SURVEY.

Site Name	Geologic Setting & Description	pH	Temperature (°C)	GPS coordinates (UTM)
Sakarıılıca (STTM)	Amphibolite host rock, adjacent Peridotite; fluids sourced ~150 m depth	6.65	49.4	36S0293908 East 4429270 North
Kuzuluk (KK)	Miocene volcanic; near amphibolites; fluids sourced ~ 190 m depth	6.66	82 (73.6)	36T0301738 East 4500101 North
Koza (KZA)	Amphibolite host rock, close to serpentinite unit	8.63	62.3	36T0331460 East 4496308 North
Dokurcun (DK)	Serpentinite-hosted cool seep	8.22	21.6	36T0321808 East 4494958 North

FIGURE 2: MAP OF SAMPLE LOCATIONS (2010 SURVEY) IN NORTHWEST TURKEY.

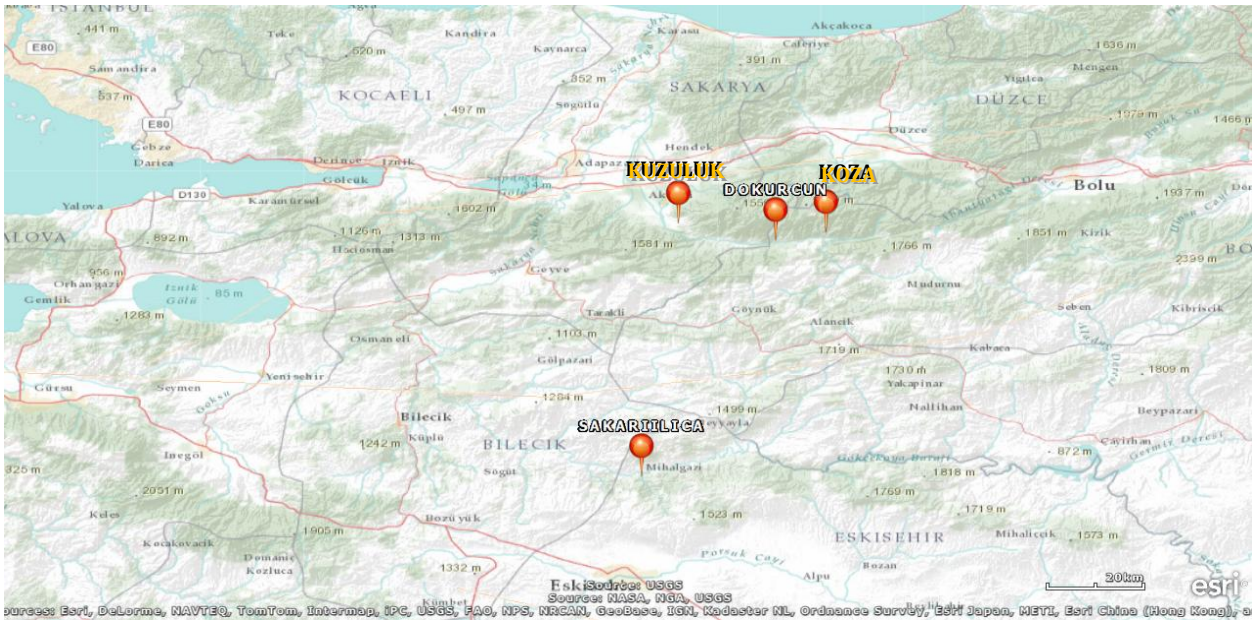

2.6 **February 2012 Field Survey**

A second field survey was undertaken from Feb. 25th-Mar. 2nd, 2012 to resample sites from northwest Turkey and to survey the Tekirova ophiolite and Denizli geothermal areas for surface expressions of subsurface hydrothermal and serpentinization processes. Relevant study sites visited during this survey are described in the following sections.

2.6.1. **Northwest Turkey**

During the second field survey, three of the four sites described in the June 2010 survey along the NAFZ were revisited for additional sampling (Koza, Kuzuluk and Dokurcun) (Table II). The cold seep (Dokurcun [DK]) was not observable in February 2012 and thus was not sampled a second time. Snow in the vicinity of Dokurcun seep was sampled for fluid analyses (i.e. major cations and anions, trace elements, carbon and oxygen isotopes) and is representative of local meteoric water.

TABLE II: SPRINGS IN WESTERN TURKEY SAMPLED DURING THE 2012 SURVEY.

Site	Location[a]/Geologic Setting	pH	Temperature (°C)
Dokurcun_Snow	NW Turkey; serpentine exposure, no fluid seep observed in 2012	6.753	11.1[a]
Koza	NW Turkey; amphibolites, adjacent serpentinite unit; well-house constructed by 2012	8.613-8.7	49.3
Kuzuluk	NW Turkey; Miocene volcanic; sampled from well	6.653-6.88	66.5
Pamukkale	SW Turkey; Travertine & carbonate sediments	6.815	24.6
Babacik	SW Turkey; Denizli area, near Tekke & Inaltı, but higher sulfide content	5.925	56.4
Karahayit	SW Turkey; Carbonate sediments	6.22	49.4
Tekke	SW Turkey, Denizli area	7.54	69.2
Inaltı	SW Turkey; Denizli area; construction of nearby geothermal springs	7.156	83.7
Yanartaş	Actively burning CH_4 seep on ophiolite exposure (partially serpentinized harzburgite)	9.402 at Site C; 11.948 at source (Site E)	Fluids: 18.5-19.1 Sediments: ~60

[a]Temperature of sediments recorded rather than temperature of the snow (~0°C)

2.6.2 **Southwest Turkey: Denizli Region**

In southwestern Turkey, hydrothermal springs are distributed throughout the landscape along fault lines and secondary fractures, and are often utilized for geothermal energy production by the local population. Table II lists all sites sampled during the 2012 survey, indicating temperature, pH and geologic setting of the spring fluids; sites without cultivation results are shown to provide regional context of fault-associated spring chemistry. Pamukkale – located near the town of Denizli and among the world's most famous hot springs - is unique due to the large travertine deposits that have accumulated as a result of precipitation of Ca^{2+} and Mg^{2+} ions upon reaching CO_2-laden air at the surface (Blank et al., 2009; Surour and Arafa 1997). This 'alkaline volcanism' is thought to be a result of extensional rifting in the Quaternary (Ozler, 1996), allowing magmatic intrusions to ascend to shallower depths as the upper crust became thinner in the areas under the greatest tension (Ozler, 2000). This region – known as the Curuksu hydrothermal system – is tectonically influenced by the E-W trending Buyuk Menderes Graben (Ozler, 2000). This graben system (similar to the Basin and Range in the Western USA) is related to extensional forces acting on western Anatolia and believed to be primarily controlled by the northern movement of the Arabian plate to the east, which is steadily pushing the Anatolian block westwards (Simsek, 1985; Ozler, 2000). Tectonic fracturing of the host rocks has created a high degree of secondary permeability in the region, allowing meteoric waters to circulate through the reservoir rocks, producing karstic structures and travertine deposition, such as are observed at Pamukkale (Ozler, 2000).

Due to the variety of host rock lithologies and complex network of joints and fractures through which water can circulate, the fluid chemistry among these springs can vary widely. Pamukkale and Karahayit are hosted by Paleozoic marbles and Mesosoic limestones (Simsek, 2003). Both sulphidic (e.g. Babacik) and non-sulphidic hot springs were observed with temperatures as high as 90°C (e.g. Inaltı).

2.6.3. **Southwest Turkey: Yanartaş (Çıralı)**

Near the southern coast of Turkey, a large ophiolite exposure hosts one of the few known terrestrial methane seeps in the world, which is thought to have been continuously burning for ~2,000 years (Hosgörmez et al., 2008; Etiope et al., 2011). The only other known occurrences of similar large methane seeps on land are located in Oman (Barnes et al., 1978), New Zealand (Lyon et al., 1990), and the Philippines (Abrajano et al., 1988). Located near the city of Antalya, the Pamphylian suture represents the boundary between the southern portion of the Anatolide-Tauride Block and accreted oceanic crustal material and parallels the location of diffuse methane seepage. Though prior work on the gas geochemistry has been conducted at the Çıralı gas seeps in southwest Turkey (e.g. Hosgörmez et al., 2008; Etiope et al., 2011), no microbiological data has been obtained. Our work will provide the first reported geomicrobiological dataset for this site

An alkaline, cold fluid seep was observed trickling out of the mouth of one of several burning gas vents observed in an outcrop of the Tekirova ophiolite near the town of Çıralı. In this area, serpentinized harzburgite is exposed at the surface (Bağci et al., 2006) and serpentinite of the same complex (Antalya Complex) is exposed nearby. This site is likely the best example of active serpentinization in the area, and it is thought that some of the methane is derived from serpentinization processes at depth (Etiope et al., 2011). This site – known to the locals as Yanartaş (YT) (meaning "flaming rock') – consists of several small gas seeps occurring along fault lines and secondary fractures in the rock, with significant diffuse seepage of hydrocarbons noted in the vicinity of the larger, actively burning vents (Hosgörmez et al., 2008; Etiope et al., 2011). Biomass from the microbial mat observed was sampled for cultivation and genetic analyses; fluids were sampled for partial chemical analyses (spring discharge was very low so obtaining sufficient fluid samples for complete chemical analyses was not possible).

2.7 **Summary**

Collectively, these sites will allow characterization of microbiological habitats fluids emanating from fault-associated, deeply-sourced ecosystems in western Turkey, along a gradient of exposure to ophiolite terranes. The Yanartaş site is unique among those surveyed and will represent a serpentinized-system endmember (without hydrothermal inputs), in contrast with the other sites, all of which have some degree of hydrothermal interaction. The cool seep at Dokurcun will represent meteoric waters weathering through serpentinite; Koza, Kuzuluk, and Sakarıılıca represent varying degrees of hydrothermal fluid interaction with serpentines and other ultramafic minerals (peridotite, amphibolites) and are treated as intermediate systems along a gradient of serpentinized and hydrothermal-derived fluids. These are the first studies of microbial ecosystems in Turkish springs and seeps employing nested observations of microbiology and geochemistry.

CITED LITERATURE:

Adiguzel, A., Ozkan, H., Baris, O., Inan, K., Gulluce, M., & Sahin, F. (2009) Identification and characterization of thermophilic bacteria isolated from hot springs in Turkey. *Journal of Microbiological Methods* **79**:321-328.

Andrieux, J., Över, S., Poisson, A., and Bellier, O. (1995) The North Anatolian Fault Zone: distributed Neogene deformation in its northward convex part. *Tectonophysics* **243**: 135-154.

Baba, A. (2003) Geothermal environmental impact assessment with special reference to the Tuzla, Geothermal Area, Canakkale Turkey. Geothermal Training Programme, Iceland, pp. 75-114.

Baba, A., Deniz, O., Ozcan, H., Erees, S. F., & Cetiner, Z. (2008) Geochemical and radionuclide profile of Tuzla geothermal field, Turkey. *Environ. Monit. Assess.* **145**:361–374.

Bağci, U., Parlak, O., and Höck, V. (2006) Geochemical character and tectonic environment of ultramafic to mafic cumulate rocks from the Tekirova (Antalya) ophiolite (southern Turkey). *Geol. J.* **41**: 193–219.

Barnes, I., O'Neil, J.R., Trescases, J.J. (1978) Present day serpentinization in New Caledonia, Oman, and Yugoslavia. *Geochim. Cosmochim. Acta* **42**:144–145.

Blank, J. G., Green, S., Blake, D., Valley, J., Kita, N., Treiman, A. et al. (2009) An alkaline spring system within the Del Puerto ophiolite (California USA): A Mars analog site. *Planet Space Sci* **57**:533-540.

Cadirci, B. H., Tuney, I., Yasa, I., Sukatar, A., & Gokcen, G. (2007) Isolation and Identification of a Thermophilic Cyanobacterium from Balcova, Izmir, Turkey. *Rapp. Comm. Int. Mer Medit.,* **38**:353.

Cardace, D., Carnevale, D., Hoehler, T., McCollom, T., & Schrenk, M. (2012) Active Serpentinization in the Coast Range Ophiolite: Intersections of Petrography, Geochemistry, and Bioenergetics. *AbSciCon 2012 Meeting*, Abstract #4491.

Canacki, S., Inan, K., Kacagan, M., & Belduz, A. O. (2007) Evaluation of Arabinofuranosidase and Xylanase Activities of Geobacillus spp. Isolated from Some Hot Springs in Turkey. *J. Microbiol. Biotechnol*. **17**(8):1262–1270.

Cihan, A. C., Ozcan, B., Tekin, N., & Cokmus, C. (2011a) Phylogenetic diversity of isolates belonging to genera Geobacillus and Aeribacillus isolated from different geothermal regions of Turkey. *World J. Microbiol. Biotechnol.* **27**:2683–2696.

Cihan, A. C., Ozcan, B., Tekin, N., & Cokmus, C. (2011b) Geobacillus thermodenitrificans subsp. calidus, subsp. nov., a thermophilic and α-glucosidase producing bacterium isolated from Kizilcahamam, Turkey. *Gen Appl Microbiol* **57**(2):83-92.

Davraz, A. (2008) Hydrogeochemical and hydrogeological investigations of thermal waters in the Usak Area (Turkey) *Environmental Geology***54**:615-628.

Dilek, Y. & Furnes, H. (2011) Ophiolite genesis and global tectonics: Geochemical and tectonic fingerprinting of ancient oceanic lithosphere. *Geological Socieity of America Bulletin* **123**:387-411.

Ehlmann, B. L., Mustard, J. F. and Murchie, S. L. (2010) Geologic setting of serpentinite deposits on Mars. *Geophysical Research Letters*, **37**: L06201.

Etiope, G., Schoell, M., & Hosgörmez, H. (2011) Abiotic methane flux from the Chimaera seep and Tekirova ophiolites (Turkey): Understanding gas exhalation from low temperature serpentinization and implications for Mars. *Earth and Planetary Science Letters* **310**:96–104.

Gul-Guven, R., Guven, K., Poli, A. & Nicolaus, B. (2008) *Anoxybacillus kamchatkensis* subsp. *asaccharedens* subsp. nov., a thermophilic bacterium isolated from a hot spring in Batman. *J. Gen. appl. Microbiol.* **54**:327-334.

Gündoğan, I., Helvacı, C., & Sözbilir, H. (2008) Gypsiferous carbonates at Honaz Dagi (Denizli): First documentation of Triassic gypsum in western Turkey and its tectonic significance. *Journal of Asian Earth Sciences* **32**:49-65.

Hosgörmez, H., Etiope, G., & Yalcin, M. N. (2008) New evidence for a mixed inorganic and organic origin of the Olympic Chimaera fire (Turkey): a large onshore seepage of abiogenic gas. *Geofluids* **8**:263–273.

Inan, K., Çanakçı, S., & Beldüz, A. O. (2011) Isolation and characterization of xylanolytic new strains of Anoxybacillus from some hot springs in Turkey. *Turk. J. Biol.***35**:529-542.

Karakus, H. & Simsek, S. (2008) Hydrogeological and geochemical studies of Efteni and Derdin geothermal areas, Turkey *Geothermics* **37**:510-524.

Lyon, G., Giggenbach, W.F., Lupton, J.F. (1990) Composition and origin of the hydrogen-rich gas seep, Fiordland, New Zealand. *EOS Trans*. V51D–10:1717.

Magri, F., Akar, T., Gemici, U. & Pekdeger, A. (2010) Deep geothermal groundwater flow in the Seferihisar-Balçova area, Turkey: results from transient numerical simulations of coupled fluid flow and heat transport processes. *Geofluids* **10**:388-405.

Mutlu, H. & Gulec, N. (1998) Hydrogeochemical outline of thermal waters and geothermometry applications in Anatolia (Turkey). *Journal of Volcanology and Geothermal Research* **85**:495-515.

MTA, (1980) Hot and mineral water inventory. General Directorate of Mineral Research and Exploration (MTA), MTA Report, Ankara.

Neugebauer, J. (1995) Structures and kinematics of the North Anatolian Fault zone, Adapazari-Bolu region, northwest Turkey. *Tectonophysics* **243**: 119-134.

Okay, A.I. (2008) Geology of Turkey: A synopsis. *Anschnitt*, **21**:19-42.

Okay, A.I. & Göncüoğlu, M.C. (2004) Karakaya Complex: a review of data and concepts. *Turkish Journal of Earth Sciences*, **13**:77-95.

Okay, A.I., Monod, O. & Monié, P. (2002) Triassic blueschists and eclogites from northwest Turkey: vestiges of the Paleo-Tethyan subduction. *Lithos*, **64**:155-178.

Okay, A. I., & Tüyüz, O. (1999) Tethyan Sutures of northern Turkey. In: Durand, B. L., Jolivet, F., Horvath, Séranne, M. (Eds.), The Mediterranean Basin: Tertiary Extension within the Alpine Orogen. *Geological Society, London, Special Publications*, **156**:475-515.

Ozler, H. M. (2000) Hydrogeology and geochemistry in the Curuksu (Denizli) hydrothermal field, western Turkey. *Environmental Geology* **39(10)**:1169-1180.

Pavsanoğlu, S. (2011) Hydrogeochemical and isotopic investigation of the Bursa-Oylat thermal waters, Turkey. *Environmental Earth Science* **64**:1157-1167.

Pavsanoğlu, S. & Chandrasekharam, D. (2011) Hydrogeochemical and isotopic study of thermal and mineralized waters from the Nevşehir (Kozakli) area, Central Turkey. *Journal of Volcanology and Geothermal Research* **202**:241–250.

Pavsanoğlu, S., Güner, A., & Gültekin, F. (2012) Environmental problems at the Nevşehir (Kozakli) geothermal field, central Turkey. *Environmental Earth Science* **66**:549-560.

Sanliyuksel, D. & Baba, A. (2011) Hydrogeochemical and isotopic composition of a low-temperature geothermal source in northwest Turkey: case study of Kirkgecit geothermal area. *Environmental Earth Science* **62**:529-540.

Simsek, S. (1985) Geothermal model of Denizli, Sarayköy-Buldan area. *Geothermics* **14(2/3)**:393–417.

Simsek, S. (2003) Hydrogeological and isotopic survey of geothermal fields in the Buyuk Menderes graben, Turkey. *Geothermics* **32**:669-678.

Süer, S., Güleç, N., Mutlu, H., Hilton, D. R., Çifter, C., & Sayin, M. (2008) Geochemical Monitoring of Geothermal Waters (2002–2004) along the North Anatolian Fault Zone, Turkey: Spatial and Temporal Variations and Relationship to Seismic Activity. *Pure and Applied Geophysics* **165**:17–43.

Surour, A. A. & Arafa, E. H. (1997) Ophicarbonates: calichified serpentinites from Gebel Mohagara, Wadi Ghadir area, Eastern Desert, Egypt. *Journal of African Earth Science* **24**(3):315-324.

Tiago, I., Chung, A. P., and Veríssimo, A. (2004) Bacterial Diversity in a Nonsaline Alkaline Environment: Heterotrophic Aerobic Populations. *Applied and Environmental Microbiology* **70**(12): 7378–7387.

van Hinsbergen, D.J.J., Kaymakci, N., Spakman, W. and Torsvik, T. H. (2010) Reconciling the geological history of western Turkey with plate circuits and mantle tomography. *Earth and Planetary Science Letters* **297**:674–686.

Vengosh, A., Helvac, I. C., & Karamanderesi, I. H., (2002) Geochemical constraints for the origin of thermal waters from western Turkey. *Applied Geochemistry* **17**:163–83.

3. **METHODOLOGY**

3.1 **Field methods and *in situ* analyses**

In field measurements included: temperature (ThermoScientific™ temperature probe), pH (Accumet™ AB15 pH meter), and conductivity (YSI Model 30 SCT™ handheld conductivity meter), GPS coordinates, and on-site determination of redox-sensitive chemical species. Vials containing liquid media for microbial growth were inoculated on site and transferred into artificial media for cultivation experiments upon return to the USA.

3.1.1. **Sample Collection**

Samples collected for future analysis included dissolved gases, fluid samples (for cation, anion, trace elements), and solid phase samples (for mineralogy, and ^{15}N isotopic analysis). Table III below lists what types of materials were collected during each field survey (June 2010 and February 2012). Site-specific restrictions (i.e. the absence of sufficient quantities of fluid for complete chemical analyses in seeps with very low flow rates, as in Dokurcun [DK] and some locations (Sites A,B and D) at Yanartaş [YT]) that affected what types of materials could be sampled are noted where appropriate. GPS coordinates (UTM) for sample locations were recorded for sites surveyed in 2010 using a portable GPS unit; exact GPS coordinates are not recorded for sample locations during 2012 survey due to technical issues with the GPS unit.

TABLE III: TYPES OF SAMPLES TAKEN AT EACH SITE DURING THE JUNE 2010 SURVEY AND FEBRUARY 2012 SURVEY.

Site	Fluids		Sediment		Biomass		Rock		DNA		Dissolved Gases
	2010	2012	2010	2012	2010	2012	2010	2012	2010	2012	2012
Dokurcun	Y[a]	Snow[c]	Y	Y	Y	N[b]	Y	Y	Y	N	N
Sakarıılıca	Y	N	N	N	N	N	N	N	Y	N	N
Koza	Y	Y	Y	N	N	N	Y	N	Y	N	Y
Kuzuluk	Y	Y	N	N	N	N	N	N	Y	N	Y
Yanartaş	N	Y	N	Y	N	Y	N	Y	N	Y	N

[a] Y = Yes, sample obtained.

[b] N = No, no sample obtained.

[c] Snow = no fluid seep observed in 2012 survey so nearby snow sampled.

Aseptic techniques were used in the sampling of all material utilized in cultivation experiments and genetic work. All spatulas, tweezers and containers were sterilized via autoclaving (prior to use in the field). Flame sterilization with ethanol immediately prior to sampling sediments and biofilms was performed to ensure that no contamination of any tools had occurred during transport to the field from the laboratory at the University of Illinois at Chicago (UIC). Fluids for subsequent culturing were collected in sterile 50-ml Falcon tubes. Rock samples and loose sediment were collected in sterile whirlpacks. Sediments and biomass collected for genetic assays were kept cold and frozen as soon as possible (within 8-10 hours) following collection to minimize degradation of organic matter and nucleic acids.

3.1.2 **Inoculation of Prepared Artificial Media with Spring Fluids**

Empty serum vials (10-ml) and six serum vials filled with targeted carbon and energy amendments (listed in Table VI, Section 3.3.4) were prepared at UIC and brought into the field for inoculation with sampled spring fluids. All vials were stoppered with butyl rubber stoppers, crimped with aluminum seals, and sterilized via autoclaving at 121 °C for 30 min at UIC. The growth amendments were kept in separate vials until inoculation, and were always added via a 0.2µm Whatman filter before the addition of spring fluids (~5ml) to prevent contamination of the stock solutions. Amendments were concentrated and added in the same volumetric proportions each time (0.25 ml growth amendment per 4.75 ml fluid).

3.1.3 ***In Situ* Spectrophotometry of Redox-Sensitive Aqueous Species**

A portable Hach 2400 Spectrophotometer was used to measure the concentrations of redox-sensitive aqueous species (NO_3^-, SO_4^{2-}, Fe(II), Total Fe, S^{2-}, dissolved O_2,) in spring fluids while on-site to prevent loss of these species through atmospheric oxidation. Sample blanks using either deionized water or sample fluid (dependent on the protocol for each aqueous species) were run prior to each analysis and each measurement was taken in triplicate. Standard protocols for each analyte were used according to manufacturer's instructions for Hach D2400 spectrophotometers.

3.2 **Post-field Geochemical Analyses**

Fluids from each spring site were collected and subjected to more detailed chemical analyses, summarized in Table IV.

TABLE IV: TYPES OF ANALYSES PERFORMED ON SAMPLES COLLECTED AT FIVE STUDY SITES IN 2010 AND 2012 FIELD SURVEYS.

Analysis	Dokurcun		Koza		Kuzuluk		Sakarıılıca	Yanartaş
	2010	2012	2010	2012	2010	2012	2010	2012
Cations	No	*Snow	Spectro.	Yes	Spectro.	Yes	Spectro.	C, E only
Anions	No	*Snow	Spectro.	Yes	Spectro.	Yes	Spectro.	C, E only
Trace Elements	Yes	*Snow	Yes	Yes	Yes	Yes	Yes	C, E only
H/O isotopes	Yes	*Snow	Yes	No	Yes	Yes	Yes	C only
DIC	No	*Snow	Yes	Yes	Yes	Yes	Yes	C only
DOC	No	*Snow	Yes	Yes	Yes	Yes	Yes	C only
Organic Acids	No	*Snow	No	Yes	No	Yes	No	C, E only

3.2.1 **Ion Chromatography: Major Cations and Anions**

Ion chromatography (IC) was performed by Dr. Everett Shock's laboratory at Arizona State University. All fluid samples were filtered (0.2 μm Whatman filter) into 60ml Nalgene bottles the same day as sample collection, and then kept frozen until analysis. No IC was performed on fluids from Sakarıılıca because the site was not sampled in 2012. For Dokurcun, no fluid seep was observed in 2012 so snow was sampled instead, providing an estimate of background levels for the measured analytes.

3.2.2 **Inductively-Coupled Plasma Mass Spectrometry (ICP-MS): Trace Elements**

Trace elemental concentrations of fluids collected during the 2012 survey were determined by inductively coupled plasma mass spectrometry (ICP-MS), performed by Dr. Everett Shock at Arizona State University (ASU). Samples were filtered as described above, and collected in 60ml Nalgene bottles spiked with concentrated nitric acid (pre-soaked in 10 % OmniTrace nitric acid). Samples were then transported back to the USA and shipped to ASU for analysis. Refer to Table III for a record of samples collected at each site.

3.2.3 **Gas Chromatography: Dissolved Gases**

Dissolved gas chemistry was determined via gas chromatography (GC), performed at University of Chicago with Bo He in collaboration with Dr. Albert Coleman. To ensure a pure sample was obtained, several measures were undertaken to prevent microbial alteration of the dissolved gases in the vials during storage and transport: the serum vials (10-ml) were pre-cleaned and sterilized (by autoclaving at 250°F for 30 min); each vial was flushed with Argon gas (~45 sec), which provided background control and a scaling (dilution) factor for final calculations. Additionally, 100 µl of 0.1 M $Hg^*(NO_3)_2$ was added to each vial prior to sample collection to prevent microbial growth and associated gas production or consumption. Spring fluids were sampled in triplicate in the field with a sterile syringe (withdrawn without a needle). Once the sample was obtained, a needle was placed onto the syringe and the fluid was injected into prepared vials and analyzed upon return. The GC used (Shimadzu 2014 model) is configured with: 1) thermal conductivity detector (TCD) for detecting H_2, O_2, and Ar; 2) a flame ionization detector (FID) for detecting C1 gases (CO, CH_4, CO_2) and 3) a Carboxen 100, 60/80, 1/8"x15' column for methanization of C1 gases prior to detection on the FID.

The GC was calibrated with a standard mix of CO, CH_4, and CO_2 to construct a calibration curve for interpretation of the results output by the GC (integrated areas beneath each peak in the chromatograph) into concentrations of dissolved gases. At least three injections of standard gas (of known concentrations) were run prior to sample injection; re-calibration was performed as needed after 3-5 samples were run to ensure accurate detection. The same syringe was used to withdraw all samples and was flushed several times with ambient air between each measurement.

3.2.4 **Fluid Isotopic Analyses**

Sampled fluids were collected as in sterile falcon tubes and transported to the USA for isotopic analysis. ^{18}O and ^{2}H isotopes were determined using a laser water isotope analyzer (LWIA) by the Stable Isotope Facility at UC-Davis. Standard procedures were utilized, with each sample

injected 8 times, with the average of injections 5-8 used in isotope ratio calculations. Isotopic ratios of samples are standardized against several IAEA standard reference materials (VSMOW, GISP, and SLAP); final values are reported relative to VSMOW.

3.2.5 **Solid Phase Chemistry**

Samples of biofilm and portions of the sediment surrounding it were obtained aseptically from sites along the outflow channel at Yanartaş (Sites A, B, D, and E; refer to Fig. 2, in Ch. 4, for map of study site locations). Total weight percent of organic and inorganic carbon and nitrogen was determined by weighing samples before and after desiccation (at 90°C for 3 days) followed by elemental analyzer-isotope ratio mass spectrometer (EA-IRMS) analysis to determine the total weight percent (wt%) of C and N remaining in the solids, as well as C^{13} and N^{15} contents as described in Loiacono et al. (2012). From that, ΔC^{13} and ΔN^{15} values for the biomass and associated carbonate precipitates observed at Yanartaş were determined. Total weight % of organic C in solids was also determined via EA-IRMS.

3.3 **Laboratory Cultivation of Sampled Biomass**

Once viable samples were obtained and returned to UIC, cultivation efforts of native microbial communities were undertaken using artificial growth media designed to mimic the natural geochemistry of the spring waters. Specific metabolic functions were targeted via the careful design of growth media, and, if initial growth experiments were successful, were followed by a genetic assay for diagnostic genes for relevant metabolic functions to tie observed metabolic activities to the genetic potential of the sampled community.

After the initial June 2010 survey, several strains were isolated using the dilution to extinction technique. Mixed cultures from the February 2012 survey were cultivated in media targeted for different metabolic options, as amendments listed in Table VI. Initial growth media for cultures sampled in 2010 was based on prior literature and further refined based on the results of chemical fluid analyses in 2010 and 2012. Cultures were grown in test tubes and serum vials (10-

ml and 60-ml) and were incubated at steady temperatures in water baths. Growth was monitored visually and microscopically to assess whether or not cultures were utilizing the targeted metabolic option imposed.

3.3.1 **Design of Site-Specific Growth Medium**

Cultivation efforts utilized growth media designed to mimic site-specific chemistry. Prior to the 2010 field campaign, previously reported data were used to estimate local geochemical compositions of the anticipated sample locations. Following collection of fluid samples in 2010, major ions and trace elements were analyzed in the hydrothermal fluids for each sampled site (see Section 3.2.1 and 3.2.2 for analytical techniques). The results of these analyses were then used to design site-specific artificial growth medium intended to mimic the *in situ* fluid chemistry and presumably target native populations with minimal bias (Meyer-Dombard et al., 2012).

Targeted growth media were designed such that only certain electron donors and acceptors were available, necessitating the use of the targeted metabolic option to survive. Site-specific chemical data was used to determine the appropriate amounts of each element in the overall media; charge-balance was calculated based on the number of moles of each major cation and anion, and NaCl was added to maintain charge neutrality. Media recipes for each site are given in Appendix A.

Growth media for both aerobic and anaerobic cultures with the following energy sources were designed and applied to environmental samples: organic carbon (sugars; yeast extract & peptone; organic acids); Fe(III) as Fe_2Cl_6 (Fe reduction); SO_4^{2-} as Na_2SO_4 (sulfate reduction) and NO_3^- as $NaNO_3$ (nitrate reduction). If applicable to the site conditions, both anaerobic and aerobic cultures were tested with each targeted media.

Growth media for each site consisted of 1 L base solution, amended with 10 ml of N/P solution, 10 ml of trace element solution, 5 ml of $CaCl_2$ solution, and 2 ml of Fe(II)-EDTA solutions with concentrations of each solution component varying depending on the site fluid chemistry (see

Appendix A for detailed compositions of each site's growth media and associated solutions used). Modifications were made to some of initial artificial growth media (e.g. dilution of trace elements; removal of stronger oxidants to subculture redox-sensitive metabolisms) to target certain subpopulations or to enhance growth in the months following sample collection; these changes will be noted where appropriate and all recipes used are listed in detail in Appendix A.

Because it was suspected that vitamin content in these subsurface environments is fairly low, initially cultivation was attempted without additional growth factors. In some cases however (especially at higher temperature sites, e.g. Kuzuluk and Koza), cultures were resistant to growth in artificial media and cell density was somewhat enhanced by the addition of vitamins. If growth was weaker than expected, approximately 5 ml of Vitamin Solution were added to 1 L of base solution (after the base media and amendments were sterilized by autoclaving) via 0.2μm Whatman filter (see Tables XXVI-XXX, Appendix A for solution components).

3.3.2. **pH Determination & Buffering in Growth Media**

The pH of the growth media was measured using an Accumet AB15 pH meter and adjusted to the desired value using 1 N NaOH just prior to autoclaving the base solution (and N/P amendments). A variety of organic buffers (i.e. HEPES, PIPES, CAPS) and inorganic buffers (e.g. HCO_3^-/CO_3^{2-}) were employed at a concentration of 3 g per L of base media to maintain the solution pH throughout each cultivation experiment. The type of buffer used was dependent on the target pH of the media and whether or not organic buffers would interfere with subculturing of target populations (e.g. organic buffers were omitted when preparing growth media for strict chemoautotrophs because they are a potential source of organic carbon). Table V (below) indicates which pH buffers were employed for each pH range examined and the range of pH obtained.

Once the media were properly buffered, the pH was measured before and after autoclaving to ensure that heating the solution did not alter the pH significantly. Additionally, several prepared vials and test tubes were randomly chosen for additional pH measurements to confirm the pH of

the solution has remained stable prior to inoculation (in the event that the solutions were not immediately utilized). Additionally, an indicator dye (2ml of 0.2% resazurin salt solution added per L of media) was employed to assist in the detection of shifts in solution pH, redox and oxygen content. This dye shifts from a blue color at alkaline, reducing conditions to a pink hue in circumneutral and reducing solutions, and nearly colorless in acidic or oxidizing conditions. As such, changes in pH during incubation were easily detected while avoiding likely contamination of the culture from the insertion of a pH probe.

TABLE V: PH BUFFERS EMPLOYED IN THIS STUDY AND APPLICABLE BUFFER RANGES.

pH Buffer	Buffering Range	pKa		Target pH of Media
		25°C	37°C	
PIPES	6.1-7.5	6.76	6.66	6.5-6.8
HEPES	6.8-8.2	7.48	7.31	8.0-8.3
CAPS	9.7-11.1	10.40	10.02	9.5-10.5
$NaHCO_3/Na_2CO_3$	9.2-10.8	N/A [a]	N/A [a]	9 – 10.5

[a] Dependent on relative amounts of carbonate and bicarbonate in solution; the amount added varied depending on the target pH of the media. The Henderson-Hasselbach equation was used to calculate the relative molar ratios of HCO_3^- and CO_3^{2-} required in solution to maintain a specified pH (Dawson et al., 1986).

3.3.3 **Preparation of Anaerobic Media**

Anaerobic conditions are achieved through the use of a heated glass tube filled with copper fillings, which act as a reducing agent to remove the oxygen from air as a mixture of H_2 and CO_2 or N_2 is passed through and pumped into test tubes, leaving the remaining headspace largely devoid of O_2. The tube is heated for 10-15 minutes under 100% $H_{2(g)}$ before media preparation (under 80% N_2 and 20% H_2 in most cases). The O_2-stripped gas then used to transfer growth media (when boiling) anaerobically to test tubes under flowing N_2/H_2 gas.

3.3.4 **Targeted Carbon & Energy Sources as Amendments**

Carbon and energy sources were added as concentrated amendments allowing for flexibility in media design and preparation. Table VI describes the components of the carbon and energy

amendments used to target specific metabolic options. Each amendment is designed so that 0.5ml of stock solution are added to ~9.5 ml of growth media; volumes were scaled up proportionally for culturing larger volumes (i.e. for cultures grown for DNA extractions).

3.4. **Microscopy**

Microscopic imaging of samples at different stages of the growth cycle was used to constrain growth rates and total cell numbers and densities. In some cultures, cell enumeration was difficult due to the tendency for the cells to clump together; as such, all numbers presented are the best estimates of cell numbers based on turbidity and microscopic cell enumeration. Increases in cell numbers over time support qualitative observations of cell growth. For basic observations, phase contrast or brightfield microscopy was routinely employed. For cell enumeration, epifluorescence microscopy was utilized.

3.4.1 **Epifluorescence Microscopy**

To aid in visualization of microorganisms, a fluorescent dye (DAPI, 4',6'-diamidino-2-phenylindole) that binds to nucleic acids was applied to the cultures before imaging using a fluorescent bulb. A small volume (~0.1 ml, using less for more turbid cultures) of fluid was taken from cultures via a sterile syringe and applied to a sterile Whatman filter. An equal amount of 10 ppm DAPI was applied to the sample and allowed to stain it for 10-15 minutes in the dark before a vacuum was applied to the filter. At this point, the cells are bound to the filter and if stained properly will fluoresce under an ultraviolet light (UV) source.

TABLE VI: COMPOSITION OF TARGETED CARBON/ENERGY AMENDMENTS USED IN CULTIVATION EXPERIMENTS.

NAF YP[d] A/N[f]	**For 8 mL:**	**For 60 mL:**	**NAF Sugars A/N[f]**	**For 8 mL:**	**For 48 mL:**
Yeast Extract	480 mg	3,600 mg	Sucrose	800 mg	4800 mg
Peptone	480 mg	3,600 mg	Lactose	800 mg	4800 mg
NH_4Cl [b]	1,600 uL	12,000 uL	Glucose	800 mg	4800 mg
$NaNO_3$ [a]	160 uL	1,200 uL	NH_4Cl [b]	1600 ul	9600 ul
K_2HPO_4 [c]	160 uL	1,200 uL	$NaNO_3$ [a]	160 ul	960 ul
TE Solution	1,600 uL	12,000 uL	K_2HPO_4 [c]	160 ul	960 ul
D.I. Water	4,680 uL	35,100 uL	TE Solution	1600 ul	9600 ul
			Water	4400 ul	26400 ul
NAF OA[e] A/N[f]			**NAF CH4gens**		
Formate	224 mg	1344	Acetate	224 mg	1344 mg
Acetate	224 mg	1344	$NaHCO_3$	22 mg	132 mg
Propionate	224 mg	1344	NH_4Cl [b]	1600 ul	9600 ul
NH_4Cl [b]	1600 ul	9600	$NaNO_3$ [a]	160 ul	960 ul
$NaNO_3$ [a]	160 ul	960	K_2HPO_4 [c]	160 ul	960 ul
K_2HPO_4 [c]	160 ul	960	TE Solution	1600 ul	9600 ul
TE Solution	1600 ul	9600	Vitamin Sol.	80 ul	480 ul
Vitamin Sol.	80 ul	480			
Water	4400 ul	26400			
NAF SN A/N[f]			**NAF FeRed**		
Na_2SO_4	32 mg	192 mg	$FeCl_3$	4.8 mg	28.8 mg
$NaHCO_3$	22 mg	132 mg	$NaHCO_3$	22 mg	132 mg
$NaNO_3$[a]	1600 uL	9,600 uL	NH_4Cl[b]	1600 ul	9600
K_2HPO_4[c]	160 uL	9,600 ul	K_2HPO_4 [c]	160 ul	960
TE Solution	1,600 uL	9,600 ul	TE Solution	1600 ul	9600
Vitamin Sol.	80 uL	480 uL	Vitamin Sol.	80 ul	480
D.I. Water	4,560 uL	27,360 uL	Water	4560 ul	26400

[a] $NaNO_3$ as 15mg/5ml stock solution

[b] NH_4Cl as 25mg/5ml stock solution

[c] K_2HPO_4 as 1.5 mg/5ml stock solution

[d] YP = Yeast extract + Peptone

[e] OA = Organic Acids

[f] A/N = Aerobic or anaerobic media.

3.5 **Genetic Assays: 16SrRNA and Functional Genes**

The genetic assay serves to confirm thermodynamic predictions and any observed metabolic functions *in vitro*. DNA extracted from selected cultures and environmental samples were subjected to the Polymerase Chain Reaction (PCR) to excise and amplify specific functional genes. PCR was performed on several diagnostic genes for specific metabolisms as well as the 16SrRNA gene, a highly conserved genetic region often used to establish phylogenetic relationships among uncultured and known microorganisms (Pace, 1991, 2009; DeLong & Pace, 2001). A PCR targeting the bacterial 16SrRNA gene was run before any functional genes to determine if the DNA extraction was successful (the absence of this gene is unlikely in any sample containing one or more bacterial cells). If so, further genetic characterization was undertaken, including 16SrRNA taxonomy for all amplifiable DNA extracts. Cloning of select PCR products was performed to obtain the exact genetic sequences of gene fragments detected in samples via gel electrophoresis to 1) verify that the gene amplified was consistent with targeted gene sequences and 2) describe taxonomic relationships comparing environmental gene sequences detected in my samples with those from known organisms.

3.5.1 **DNA Extraction for Downstream Genetic Assays**

Cultures that grew well in artificial media (i.e. to a sufficient cell density, verified by microscopic inspection of increased cell numbers) were selected for downstream genetic assays for functional genes and 16SrRNA taxonomy to establish relationships with known species. Select cultures were centrifuged at 13,000 rcf for 5-10 minutes in a Sorvall Legend RT+ centrifuge (Thermo-Scientific) to remove excess liquid and pellet the cells. Genomic DNA was extracted from the pelleted cells using commercial DNA extraction kits from Mobio (Power Biofilm Extraction Kit) and from Qiagen (Fast DNA Spin Kit for Soils) according to the manufacturer's instructions. Extracted DNA was stored in a -20°C freezer to minimize DNA degradation.

3.5.2 **Polymerase Chain Reaction (PCR) for Functional Genes**

DNA extracted from cultured samples was screened for selected functional genes using the polymerase chain reaction (PCR). A number of nitrogen-cycling functional genes were targeted by utilizing different gene-specific primers and PCR conditions. Table VII lists the reactants added in a 20 µl PCR reaction; minor modifications were made to improve reaction efficiency as needed (i.e. some primers amplified DNA better with the addition of 0.5 µl BSA [Bovine Serum Albumin, 1:50 dilution]with an equal reduction in water volume to maintain a total reaction volume of 20 µl). Table VIII lists nitrogen-cycling processes and functional genes for those processes targeted via PCR. Table IX summarizes the primers used for each gene targeted, PCR conditions employed, and relevant references. Refer to the listed references for detailed explanations of PCR protocols employed (i.e. number of cycles, length of extension and annealing steps, etc.).

TABLE VII: COMPONENTS IN A 20 µL POLYMERASE CHAIN REACTION (PCR).

Component Name	Amount Added per PCR (µl)
Water, sterile	13.75
$MgCl_2$	1.8
10X TAE Buffer	2.0
Forward Primer[a]	0.5
Reverse Primer[a]	0.5
dNTPs[b]	0.2
Taq Polymerase	0.25

[a]Primers used dependent on the targeted gene fragment;

[b] dNTPs = deoxynucleoside triphosphates

TABLE VIII: NITROGEN-CYLING PROCESSES TARGETED VIA PCR.

Process[a]	Reaction	Diagnostic Gene	Enzyme Encoded by Gene	Approx. Gene Fragment Length[b]
Nitrate reduction	$NO_3^- \rightarrow NO_2^-$	NarG	Nitrate reducatse	650 bp
Nitrite reduction	$NO_2^- \rightarrow NO$	NirS/NirK	Nitrite reductase	NirS: 425 bp NirK: 470 bp
Nitric oxide reduction	$NO \rightarrow N_2O$	NorB	Nitric oxide reductase	cnorB: 390 bp qnorB2F-7R: 637 bp qnorB2F-5R: 262 bp
Nitrous oxide reduction	$N_2O \rightarrow N_2$	NosZ	Nitrous oxide reductase	415-453 bp
N_2 fixation	$N_2 + 8H^+ + 8e^- \rightarrow 2NH_3 + H_2$	nifH	Nitrogenase	350 bp
Nitrification	$NH_4^+ + O_2 \rightarrow NO_2^- + O_2 \rightarrow NO_3^-$	amoA	Ammonia monoxygenase	675 bp

[a]The first four rows are consecutive steps in the denitrification process and proceed in the order listed.

[b]If more than one primer is used to target a diagnostic gene, the approximate gene fragment length targeted for each primer used is listed.

Agarose gel electrophoresis was used to image amplified gene fragments following PCR. Agarose gel (1.5%) was prepared by heating a mix of 4.5 grams of agarose gel with 300 ml of TAE buffer. Ethidium bromide is added (0.5 µl ethidium bromide per 1 ml of agarose gel) to allow visualization of dyed nucleic acids under UV light. The gel is set in a rig with a positive and negative terminal with a comb positioned to create wells in the gel as it cools and solidifies. Then, 5 µl of PCR product and 1 µl of loading dye are added to the wells via pipette tip. A current of constant voltage is then applied to the gel, causing the negatively-charged nucleic acids to migrate towards the positive terminal. Gene fragments are separated based on mass, so that larger gene fragments do not migrate as quickly as shorter fragments. A 100bp or 1kbp ladder (New England BioLabs™) containing gene fragments of a known size is run alongside the samples to estimate the length of gene fragments detected in the gel.

TABLE IX: PRIMERS UTILIZED IN THIS STUDY AND THE GENE OR GENE FRAGMENT TARGETED AND PCR CONDITIONS EMPLOYED.

Target Gene	Primers Used[a]	Primer Sequences[b] (5'-3')	Primer Conc. (pmol/ µl)	PCR Conditions[c,d]	References
16S Bac	27F-1492R	F: AGAGTTTGATCCTGGCTCAG R: GGTTACCTTGTTACGACTT	100	Ta= 52°C	Lane, 1991
nifH	nifH1F-R	F: GGHAARGGHGGHATHGGNAARTC R: GGCATNGCRAANCCVCCRCANAC	100	Ta = 55°C	Mehta et al., 2003; Mehta & Baross, 2006
norB	qnorB2F-5R	F: GGN CAY CAR GGN TAY GA R: ACC CAN AGR TGN ACN ACC CAC CA	50	Ta = 57°C	Braker & Tiedje, 2003
	qnorB2F-7R	F: GGN CAY CAR GGN TAY GA R: GGN GGR TTD ATC ADG AAN CC	50	Ta = 57°C	
	cnorB2F-6R	F: GAC AAG NNN TAC TGG TGG T R: GAA NCC CCA NAC NCC NGC	50	Ta = 57°C	
narG	narG1960F-2650R	F: TAY GTS GGS CAR GAR AA R: TTY TCR TAC CAB GTB GC	100	Touchdown Ta=60-55°C	Philippot et al., 2002
nirS	nirSFcd3aF-R3cd	F: GTSAACGTSAAGGARACSGG R: GASTTCGGRTGSGTCTTGA	50	Ta = 55.5-57°C	Throbäck et al., 2004
nirK	F1aCu R3Cu	F: ATCATGGTSCTGCCGCG R: GCCTCGATCAGRTTGTGGTT	50	Ta = 55 °C	Hallin & Lindgren, 1999
nosZ	nosZF-1622R	F: CGYTGTTCMTCGACAGCCAG R: CGSACCTTSTTGCCSTYGCG	100	Ta = 53°C	Throbäck et al., 2004
amoA AOA	Arch-amoAF Arch-amoAR	F: STAATGGTCTGGCTTAGACG R: GCGGCCATCCATCTGTATGT	10	Ta = 56°C	Francis *et al.*, 2005
amoA β-AOB	amoA-1F amoA-2R	F: GGGGTTTCTACTGGTGGT R: CCCCTCKGSAAAGCCTTCTTC	50	Ta = 55°C	Rotthauwe *et al.*, 1997

[a] Forward and reverse primers are indicated by F and R as the last letter, respectively. Each primer set is shown as a pair.

[b] N = A, C, G, or T; Y = C or T; R = A or G; D = G, A, or T.

[c] T_a = annealing temperature.

[d] Touchdown = indicates T_a was incrementally decreased by 1 degree Celsius with each successive cycle during the annealing step.

3.5.3 **Cloning and Sequencing of 16S DNA Sequences**

Successfully amplified 16SrRNA and nitrogen-cycling functional genes (see Table VIII for description of N-cycling genes targeted) were chosen for cloning and sequencing using the TA TOPO Cloning Kit (Qiagen™). The amplified gene fragments (PCR products) from each culture were introduced in a vector and inserted into the genome of E. coli according to the manufacturer's instructions from Qiagen's TA Topo Cloning Kit™; the *E. coli* was incubated at 37°C. *E.coli* cells that successfully incorporated the PCR products were chosen and whole cell DNA was amplified via PCR (using M13 primers designed to excise gene fragments incorporated into the genome using Qiagen's TA Topo Cloning Kit™). Success fully inserted gene fragments (verified by gel electrophoresis) were identified and chosen for full sequencing. The amplified M13 PCR products were sequenced at Univ. of Illinois at Chicago by the DNA Sequencing Facility.

3.5.4 **Taxonomic Inferences of Sequenced Gene Fragments**

Once the sequences for the 16SrRNA genes in the cultured samples were obtained, taxonomic relationships could be established utilizing the Basic Local Alignment Search Tool (BLAST) (Altschul et al., 1990). The sequences were first trimmed using CodonCode™ and then aligned using BLAST to identify nearest known taxonomic relatives based on genetic sequence similarities. Results are discussed in the following chapter.

CITED LITERATURE:

Altschul, S. F., Gish, W., Miller, W., Myers, E. W. & Lipman, D. J. **(**1990) Basic local alignment search tool. *J. Mol. Biol.* **215:**403–410.

Braker, G. & Tiedje, J. M. (2003) Nitric oxide reductase (norB) genes from pure cultures and environmental samples. *Appl Environ Microbiol.* **69**:3476–3483.

Dawson, R. M. C.; Elliot, D. C.; Elliot, W. H.; Jones, K. M. Data for Biochemical Research; 3rd ed., Oxford Science Publ., 1986.

Francis, C.A., Roberts, K.J., Beman, J.M., Santoro, A.E., Oakley, B.B. (2005). Ubiquity and diversity of ammonia-oxidizing archaea in water columns and sediments of the ocean. *Proc Natl Acad Sci USA* **102**: 14683–14688.

Hallin, S. & Lindgren, P. (1999) PCR Detection of Genes Encoding Nitrite Reductase in Denitrifying Bacteria. *Appl. Environ. Microbiol.* **65**(4):1652-1657.

Lane, D. J. (1991) 16S/23S rRNA sequencing. In: Stackebrandt, E. Goodfellow, M. (eds) Nucleic acid techniques in bacterial systematics. Wiley, Chichester, pp. 115-175.

Loiacono, S. T., Meyer-Dombard, D. R., Havig, J. R., Poret-Peterson, A. T., Hartnett, H. E., & Shock, E. L. (2012) Evidence for high-temperature *in situ nifH* transcription in an alkaline hot spring of Lower Geyser Basin, Yellowstone National Park. *Environmental Microbiology* **14**(5):1272–1283.

Mehta, M. P., Butterfield, D. A., & Baross, J. A. (2003) Phylogenetic Diversity of Nitrogenase (*nifH*) Genes in Deep-Sea and Hydrothermal Vent Environments of the Juan de Fuca Ridge. *Appl. Environ. Microbiol* **69**(2):960-970..

Mehta, M. P. & Baross, J. A. (2006) Nitrogen Fixation at 92°C by a Hydrothermal Vent Archaeon. *Science* **314**:1783-1786.

Meyer-Dombard, D. R., Shock, E. L., & Amend, J. P. (2012) Effects of trace element concentrations on culturing thermophiles. *Extremophiles* **16**:317-331.

Pace, N. R. (2001) The universal nature of biochemistry. *PNAS* **98**(3):805-808.

Pace, N. R. (2009) Mapping the Tree of Life: Progress and Prospects. *Microbiol. Mol. Biol. Rev.* **73**(4):565-576**.**

Philippot, L. et al. (2002) Denitrifying genes in bacterial and archaeal genomes. *Biochim Biophys Acta Gene Struct Expr.* **1577**:355–376.

Rotthauwe, J., Witzel, K. & Liesack, W. (1997) The Ammonia Monooxygenase Structural Gene *amoA* as a Functional Marker: Molecular Fine-Scale Analysis of Natural Ammonia-Oxidizing Populations. *Applied and Environmental Microbiology* **63**(12):4704–4712.

Throbäck, I. N., Enwall, K., Jarvis, A., & Hallin, S. (2004) Reassessing PCR primers targeting *nirS*, *nirK* and *nosZ* genes for community surveys of denitrifying bacteria with DGGE. *FEMS Microbiol Ecol*. **49**:401–417.

4. **RESULTS**

4.1 **Spring Fluid Chemistry**

Several springs were observed and sampled throughout western Turkey; of those, only four (Kuzuluk [KK], Koza [KZA], Sakarıılıca [STTM] and Dokurcun [DK]) were chosen for detailed study and cultivation experiments. Data for other hot springs observed (Babacik [BC]; Tekke [TK]; Inaltı [IN]; Karahayit [KH]; and Pamukkale [PM]) are shown as points of reference for local hydrothermal fluids, without serpentinization-derived fluid inputs (discussed in Chapter 5).

The following analyses were performed on sampled fluids: trace element and major cation and anion concentrations; on site spectrophotometric analysis of redox-sensitive species; gas chromatography of relevant dissolved gases (CO_2, CH_4, H_2); ^{18}O and deuterium isotopes (for 2010 spring fluids only); and dissolved organic and inorganic carbon (DOC and DIC, respectively) in sampled spring fluids. DOC and DIC measurements are shown for 2012 fluids with other biologically-relevant ions and trace elements in Table X, found in Section 4.1.1.

4.1.1 **Redox-Sensitive Aqueous Species**

Spectrophotometry was used in the field to determine concentrations of redox sensitive aqueous species (e.g. dissolved $O_{2(g)}$) that vary rapidly when fluids are exposed to the atmosphere. Table XI shows the results of these analyses. Kuzuluk, Koza, and Sakarıılıca are among the five primary study sites; all other sampled sites are shown to provide typical values observed in local hydrothermal systems with no known inputs from subsurface serpentinization. Concentrations of redox-sensitive ions and aqueous species were determined on-site for all sites visited except Dokurcun and Yanartaş due to insufficient fluid flow.

Ion Chromatography (IC) data was also obtained, providing further detail on concentrations of major ions in solution. Data obtained from IC analyses for relevant ions is also shown in Table X, along with DOC and DIC measurements for fluids sampled during the 2012 survey. For a complete

record of chemical parameters measured in spring fluids from both surveys, refer to Appendix A and B.

TABLE X: BIOLOGICALLY-RELEVANT IONS AND DOC/DIC IN SPRING FLUIDS, 2012 SURVEY

Units: ppm	Na^+	K^+	Mg^{2+}	Ca^{2+}	NO_3^-	NH_4^+	SO_4^{2-}	DIC[a]	DOC[a]
Dokurcun_snow (DK)	0.36	15.09	0.00	3.00	0.39	0.33	0.87	*2.1*	1.9
Kuzuluk (KK)	1551.42	92.50	36.21	126.69	0.29	12.44	135.6	*330*	3.6
Koza (KZA)	204.3	4.88	0.00	136.30	0.07	0.61	689.4	*1.5*	1.7
Babacik (BC)	988.53	92.01	175.91	389.91	0.121	15.06	2598	191	2.0
Inaltı (IN)	1890.94	178.66	19.57	79.87	1.042	20.41	2978.3	127	*5.4*
Pamukkale (PM)	43.50	5.94	95.49	203.18	1.34	0	601.2	*220*	0.7
Karahayit (KH)	118.18	23.75	124.50	294.37	0.27	1.42	810.2	*236*	0.6

[a]Italicized values fall outside the calibration range of the instrument used (Range for DIC: 10-200ppm; Range for DOC: 0.2 - 5 ppm C)

4.1.2 **Trace Elements and Artificial Media**

Elemental concentrations of trace metals and rare earth elements, major cations and anions, and other chemical parameters (alkalinity, pH, temperature) were determined via methods described in Ch. 3. The resulting chemical profiles allowed for the design of site-specific artificial growth media that attempted to recreate *in situ* chemical conditions to improve culturing success. Table XII lists concentrations of biologically-relevant trace elements used in growth media for each site, as determined by inductively coupled plasma-mass spectrometry (ICP-MS). Full media recipes are listed in Tables XXVII – XXX, Appendix A.

TABLE XI: FLUID CHEMISTRY DETERMINED VIA SPECTROPHOTOMETRY IN THE FIELD. ALL UNITS ARE IN MG/L, UNLESS OTHERWISE NOTED.

Site	Year	Temp. (°C)	pH	Cond. (µS)	D. O.[a]	NO_3^-	NH_4^+	Fe^{+2}	Total Fe	S^{-2} (µg/)	SiO_2	$CaCO_3$[d]	PO_3^{4-}
KK	2010	73.6 [c]	6.67	n.d.[b]	0.7	2.8	7.47	0	n.d.[b]	294	126	n.d.[b]	n.d.[b]
	2012	66.5	6.65	6740	0.7	2.77	12.44	n.d.[b]	0.19	20	138	1142	1.78
KZA	2010	62.3	8.63	n.d.[b]	2.7	0.73	n.d.[b]	0.62	0.042	47	44.8	n.d.[b]	0.37
	2012	49.3	8.61	1581-2086	1.5	1.5	0.11	0.01	0.14	60	43.2	16.5	0.41
STTM	2010	49.4	6.65	n.d.[b]	0.2	0.6	~ 1.0	n.d.[b]	0.33	n.d.[b]	94.4	n.d.[b]	0.84
BC	2012	55	6.12	6000	<0.1	12.2	5.73	0	0.01	19700	377	576	0.66
IN	2012	80-85	7.15	10420	n.d.[b]	2.27	6.2	n.d.[b]	0.01	297	1.55	536	n.d.[b]
PM	2012	25-30	6.81	1131	5.1	1.93	0	0	0	0	26.5	690	0.1
KH	2012	50	6.17	4030	0.22	1.8	0.24	1.01	0.79	0	3	1380	0.61

[a] D.O. = Dissolved $O_{2(g)}$.

[b] n.d. = not determined.

[c] Fluid cooled to 73.6°C before safe measurement could be obtained but workers confirmed the outflow temperature was at least 82°C upon reaching the surface.

[d] Alkalinity was determined by titration and is given in terms of $CaCO_3$.

TABLE XII: BIOLOGICALLY-RELEVANT TRACE ELEMENT CHEMISTRY AS DETERMINED BY ICP-MS FOR 2012 SPRING FLUIDS AND DK-SNOW.

(ppb)	DK-snow	KK	KZA	BC	IN	PM	KH
Mg	235	14400	172	71200	4900	85000	105000
Ca	1360	79800	96000	184000	15800	380000	320000
Mn	4	25.2	1.94	5.52	*0.19*	17.8	34.3
Fe	54	176	51	44.2	12.2	*44.9*	*400*
P	15	*450*	700	*2000*	19	*1340000*	*1280000*
Ni	*0.72*	5.9	1.55	*0.39*	*0.19*	9.86	7.6
Co	*0.124*	*0.06*	*0.034*	*0.04*	*0.02*	0.057	2.3
Zn	0.2	0.6	0.3	0.4	0.5	0.5	0.4
Cu	*0.92*	*0.28*	*0.33*	*0.4*	*0.42*	0.725	*0.63*
Rb	0.44	181	24.8	213	*372*	21	81
Sr	*4.6*	980	581	9400	3360	*5500*	*8540*

4.1.3 **Dissolved Gas Chemistry**

Dissolved gases also affect microbial metabolism and can be produced biologically or abiologically (e.g. generation of reduced gases via serpentinization). As such, dissolved gas concentrations were determined for species relevant to serpentinization (e.g. H_2) as well as methane uptake and production (CO_2, CO, CH_4) that can occur as a result of either abiotic or biotic methane generation. Table XIII shows the concentrations of CO_2, CO, CH_4 and H_2 in sampled spring fluids, averaged among triplicate samples from each site (February 2012 survey only). At Yanartaş, we were unable to sample dissolved gases as the seep was very low flow (<1cm depth); however, concentrations of $H_{2(g)}$ in serpentinizing fluids in equilibrium with the atmosphere , as in terrestrial seeps, are predicted to be on the order of ~300 micromolar (Sleep et al., 2004). At depth, these concentrations can be several orders of magnitude greater (Cardace & Hoehler, 2009a).

TABLE XIII: CONCENTRATIONS OF DISSOLVED GASES AS DETERMINED BY GAS CHROMATOGRAPHY.

Site	**$CO_{(aq)}$** (μM)	**$CH_{4(aq)}$** (μM)	**$CO_{2(aq)}$** (μM)	**$H_{2(aq)}$** (μM)
Koza	0.278	6.095	86.94	bdl[a]
Kuzuluk	0.222	1.267	6604.0	bdl[a]
Pamukkale	0.281	0.104	3881.0	4.043
Karahayit	0.479	0.564	11216.0	0.365
Inaltı	0.415	0.267	2663.0	0.964
Babacik	1.041	2.508	6889.0	bdl[a]
Babacik, 45ft from source	0.539	3.29	6171.0	bdl[a]

[a] bdl = Below detection limit; indicates that no gas peak was observed for that species.

4.1.4 **Isotopic Data**

During the 2010 survey, stable isotope ($\delta^{18}O$, $\delta^{2}H$) measurements were undertaken for all hot and cool springs sampled (KK, KZA, STTM and DK). These results will be discussed in relation to known values for these isotopes at nearby hot and cool spring localities as well as both the global and Mediterranean meteoric water lines in Section 5.1.2. These data allow inference of relative inputs of meteoric and hydrothermal waters and the degree of water-rock interaction at depth.

4.2 **Yanartaş Gas Seep**

This site represents the surface expression of serpentinization-derived waters discharging and interacting with meteoric waters. Because this study is the first to note the occurrence of this seep and the biofilm it supports, no thermodynamic predictions of exergonic metabolic pathways were made prior to sampling this site. However, theoretical calculations of serpentine-associated systems can be applied and chemical data from these fluids will be compared with the other sites when inferring differences in observed metabolic capacities.

FIGURE 3: OVER-HEAD PHOTOGRAPH OF SAMPLE SITES AT YANARTAŞ.

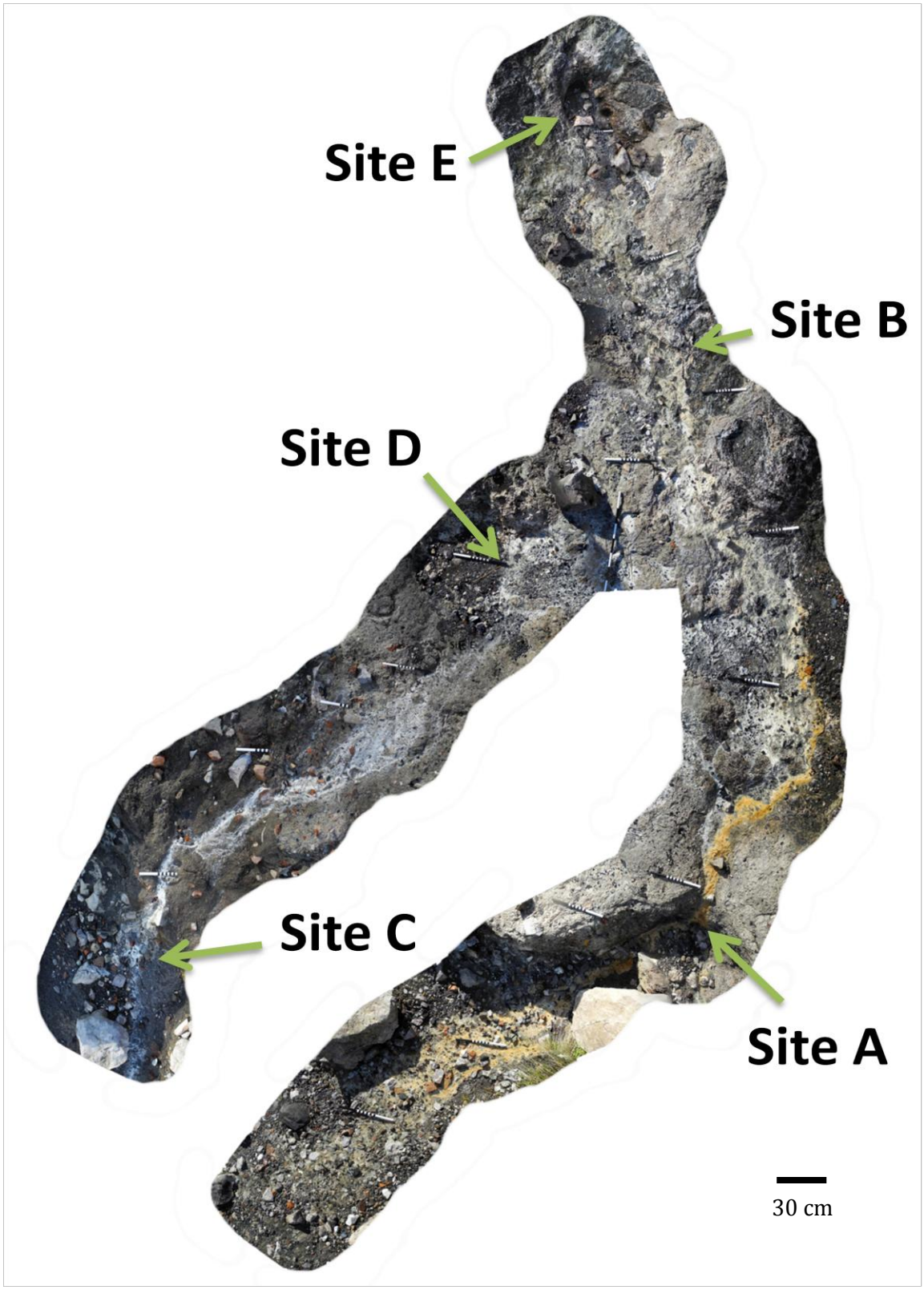

4.2.1 **Fluid Chemistry**

Fluids were sampled at two locations (Sites E and C, near the top and bottom of the outflow channel, respectively) for chemical analyses, although analysis of the detail reported above in section 4.1 is lacking due to low fluid volume. Refer to Fig. 3 for sample site locations . Site E was located just beneath an actively burning methane seep, with sediment temperatures of ~60°C measured as directly beneath the flame as practical; temperatures of the fluid discharging were lower (~18.5°C) but had a very alkaline pH of 11.9, that dropped along the outflow channel to pH ~9.4 at Site C (~7.3 m from Site E). Ion chromatography (IC) was used to measure concentrations of major ions in these fluids, shown in Table XIV, below. No spectrophotometric analyses were obtained at this site due to insufficient fluid flow.

TABLE XIV: MAJOR IONS DETERMINED BY ION CHROMATOGRAPHY IN FLUIDS AT YANARTAŞ.

Concentration (ppm)	Cl^-	SO_4^{-2}	NO_3^-	Na^+	NH_4^+	K^+	Mg^{+2}	Ca^{+2}
Site E (top)	18.3	8	0.054	11.48	0.57	2.82	0.69	138.82
Site C (bottom)	24.31	29.1	0.0852	12.25	0	6.90	68.56	10.98

4.2.2 **Nitrogen Isotopic Data**

At Yanartaş [YT], solid phases of biofilm and associated mineral precipitates were sampled and analyzed for total nitrogen content (wt.%) and ^{15}N isotopes. This solid-phase chemical data is discussed in Chapter 5 in support of observed genetic capacity for nitrogen-cycling processes detected in enrichment cultures from YT. Measurements were taken at four points along the outflow channel, with Site E being closest to the actively burning methane vent, and sites A and D being farthest away from the same source, along two divergent channels. Total wt. % and δN^{15} values for Sites A, B, D and E are shown in Table XV, below.

TABLE XV: TOTAL NITROGEN CONTENT (WT.%) AND $\delta^{15}N$ VALUES OF SOLIDS SAMPLED ALONG AN OUTFLOW CHANNEL AT YANARTAŞ.

Site	Distance from source (m)	Total N of solids[a] (wt.%)	Std. Dev. (%)	$\delta^{15}N$ vs air (‰)	Std. Dev. (‰)
E	0	0.03	0.001	2.27	0.86
B	1.5	0.03	0.002	3.38	0.22
D	2.5	0.04	0.002	2.99	0.43
A	5.5	0.05	0.004	3.23	0.84

[a] Both biofilm and solid precipitates sampled; no separation attempted.

4.3 **Observed Growth in Enrichment Cultures**

The success of cultivation experiments varies widely depending on the site's natural geochemistry and biodiversity, the chemical conditions imposed in culture, and the viability of the microorganisms under study (Zengler et al., 2002; Stewart, 2012; Meyer-Dombard et al., 2012). Growth generally occurred more readily when organic carbon was abundant (i.e. in a nutrient-rich medium; yeast-extract and peptone). As a result, the degree of success and extent of tests performed was not uniform across all of the sampled sites due to differences in how well microorganisms from environmental samples adapted to artificial media. The influence of such factors (i.e. incubation temperature and headspace, growth in isolation or in a steady-state environment) on cultured microorganisms will be discussed in Chapter 5.

The success of growth was determined either by visual turbidity or by microscopic cell enumeration. Table XVI is the legend for Tables XVII-XXI, below and on the following pages, which describe the results of cultivation experiments for each culture grown in targeted media. Results for growth in methanogen-targeted media are not shown because none of the initial enrichment cultures showed any growth at any of the sites, so no positive results were obtained.

TABLE XVI: LEGEND FOR CULTURE GROWTH, TABLES XVI-XIX.

+++	Positive growth, optimal
++	Positive growth, slightly suboptimal
+	Positive growth, suboptimal
-	No growth
ND	Test not conducted (due to lack of culture growth)
N/A	Test not conducted because not applicable to site conditions

TABLE XVII: RESULTS AND OBSERVATIONS OF GROWTH EXPERIMENTS FOR CULTURES FROM YANARTAŞ.

Site: Yanartaş, site C		**Growth Conditions**				**Observations**
Metabolic Option		Temp. (°C)			pH	Morphology: Rods forming filaments; consistent throughout; motile
		30	40	50		
Yeast + Peptone	Aerobic	**+++**	**+++**	**+++**	8.3-8.5	Fastest growth at pH 8.3; reached cell densities of ~ $1.7*10^7$ cells/ml within 4 hrs (at pH 8.3-9.5)
		++	**++**	**++**	9.5	
		+	**+**	**+**	10.5	
Organic Acids	Aerobic	**++**	**++**	**++**	8.3-8.5	Lower cell density reached than with YP as a C source; cells appear shriveled in pH10.4 media
		+	**+**	**+**	9.5	
		+	**+**	**+**	10.5	
NO_3^- Reduction		**++**	**++**	**++**	8.3-8.5	Growth aided by addition of C_{org}
		+	**+**	**+**	9.5	
		-	**-**	**-**	10.5	
SO_4^{2-} Reduction	Aerobic	**+**	**+**	**+**	8.3 -8.5	Growth aided by addition of C_{org}
		+	**+**	**+**	9.5	
		-	**-**	**-**	10.5	
Sugars	Aerobic	**+**	**+**	**N/A***	8.3-8.5	*Sugars began to caramelize at 50°C so growth was inhibited
		+	**+**	**N/A***	9.5	
		+	**+**	**N/A***	10.5	
Fe(III) Red.	Aerobic	+	+	+	8.3-8.5	Growth aided by addition of C_{org}
		+	+	+	9.5	
		-	-	-	10.5	

TABLE XVIII: RESULTS AND OBSERVATIONS OF GROWTH EXPERIMENTS OF CULTURES FROM FLUIDS AND SEDIMENTS SAMPLED FROM KOZA HOT SPRING.

Site: Koza		Growth Conditions						Observations
Metabolic Options		Temp. (°C)					pH	Morphology: Coccoid; some rods also observed
		50	55	60	65	70		
Yeast + Peptone	aerobic	++	++	++	++	-	8.6	Non-motile cocci; cells tend to form flocs; some motile rods
	anaerobic	+	+	+	-	-		
Org. Acids	aerobic	+	+	+	-	-	8.6	Growth slower than with YP
	anaerobic	-	-	-	-	-		
Sugars	aerobic	-	-	-	-	-	8.6	No observed growth
	anaerobic	-	-	-	-	-		
NO_3^- Red.	aerobic	-	-	+	-	-	8.6	Limited growth
	anaerobic	-	-	-	-	-		
SO_4^{2-} Red	aerobic	-	-	+	-	-	8.6	Limited growth
	anaerobic	-	-	-	-	-		
Fe(III) Red.	aerobic	+*	+*	+*	+*	-	8.6	Growth aided by addition of C_{org}; limited growth without C_{org} (+*)
	anaerobic	+*	+*	+*	+*	-		

TABLE XIX: RESULTS AND OBSERVATIONS OF GROWTH EXPERIMENTS OF CULTURES FROM FLUIDS SAMPLED FROM KUZULUK HOT SPRING.

Site: Kuzuluk		Growth Conditions					Observations
Metabolic Options		Temp. (°C)				pH	Generally low cell densities in culture
		50	60	70	80		
Yeast + Peptone	aerobic	+	++	++	+	6.65	Cocci form clumps readily; non-motile
	anaerobic	-	+	+	-		
Org. Acids	aerobic	-	+	+	+	6.65	Slower growth than YP; cocci
	anaerobic	-	-	-	-		
Sugars	aerobic	-	-	-	-	6.65	No observable growth
	anaerobic	-	-	-	-		
NO_3^- Red.	aerobic	-	+	+	+	6.65	Limited growth; low cell density
	anaerobic	-	-	-	-		
SO_4^{2-} Red	aerobic	-	+	+	+	6.65	Limited growth; low cell densitiy
	anaerobic	-	-	-	-		
Fe(III) Red.	aerobic	-	-	+	+	6.65	Limited growth; low cell density
	anaerobic	-	-	-	-		

TABLE XX: RESULTS AND OBSERVATIONS OF GROWTH EXPERIMENTS OF CULTURES FROM FLUIDS AND SEDIMENTS SAMPLED FROM SAKARIILICA HOT SPRING.

Site: Sakarıılıca		Growth Conditions						Observations
Metabolic Options		Temp. (°C)					pH	Generally low cell densities in autotrophic media; filamentous morphologies and cocci observed
		50	55	60	65	75		
Yeast + Peptone	aerobic	**++**	**+++**	**+++**	**++**	**-**	6.65	Initial enrichment cultures showed high cell densities; Cocci form clumps readily; non-motile; rods numerous
	anaerobic	**-**	**-**	**-**	**-**	**-**		
Org. Acids	aerobic	**-**	**+**	**+**	**+**	**-**	6.65	Limited growth in early dilutions
	anaerobic	**-**	**-**	**-**	**-**	**-**		
Sugars	aerobic	**-**	**-**	**-**	**-**	**-**	6.65	No observed growth
	anaerobic	**-**	**-**	**-**	**-**	**-**		
NO_3^- Red.	aerobic	ND	ND	ND	ND	ND	6.65	Growth in initial enrichment culture; no longer viable
	anaerobic	ND	ND	ND	ND	ND		
SO_4^{2-} Red	aerobic	+	ND	ND	ND	ND	6.65	Growth in initial enrichment culture; no longer viable
	anaerobic	ND	ND	ND	ND	ND		
Fe(III) Red.	aerobic	ND	ND	ND	ND	ND	6.65	Growth in initial enrichment culture; no longer viable
	anaerobic	ND	ND	ND	ND	ND		

TABLE XXI: RESULTS AND OBSERVATIONS OF GROWTH EXPERIMENTS OF CULTURES FROM FLUIDS AND SEDIMENTS SAMPLED FROM DOKURCUN COOL SEEP.

Site: Dokurcun		Growth Conditions				Observations:
Metabolic Options		Temp. (°C)			pH	Rapid growth to high cell densities; motile
		20	25	30		
Yeast + Peptone	aerobic	**+++**	**+++**	**+++**	8.2-8.3	Motile rods; Grew to high cell densities within 4-8 hrs if aerobic
	anaerobic	N/A	N/A	N/A		
Org. Acids	aerobic	+	+	+	8.2-8.3	Growth rates slower than with YP
	anaerobic	N/A	N/A	N/A		
Sugars	aerobic	**-**	**-**	**-**	8.2-8.3	No observed growth in either aerobic or anaerobic media[a]
	anaerobic	**-**	**-**	**-**		
NO_3^- Red.	aerobic	**+**	**+**	**+**	8.2-8.3	Limited Growth
	anaerobic	N/A	N/A	N/A		
SO_4^{2-} Red	aerobic	**+**	**+**	**+**	8.2-8.3	Limited Growth
	anaerobic	N/A	N/A	N/A		
Fe(III) Red.	aerobic	**+**	**+**	**+**	8.2-8.3	Some growth; low cell density
	anaerobic	**+**	**+**	**+**		Similar to aerobic cultures

[a] Though anaerobic metabolism was not expected at DK, anaerobic conditions were employed with sugars to determine if fermentative growth was utilized. No growth was observed.

4.4 **Genetic Surveys**

Cultures that yielded amplifiable DNA were subject to 16S rRNA taxonomic analyses as well as assays for functional genes used in the nitrogen-cycle. Several cultures that showed visible cell growth were selected for DNA extraction and are listed in Table XXIII. Also listed in Table XXIII is whether or not the DNA extraction was successful, as several extractions were not successful despite visible cell growth. Some of these difficulties are attributed to carbonate inhibition of the DNA extraction, as a carbonate-bicarbonate buffer was used for pH 10.4 media and none of those cultures yielded amplifiable DNA. Several nitrogen cycling genes in cultures from Yanartaş and Dokurcun were successfully cloned and sequenced, and the presence of other genes is inferred by gel electrophoresis. Nitrogen-cycling genes that are likely present in cultures are listed in Table XXIV.

4.4.1 **16S rRNA Taxonomy of Cultured Samples**

The nearest known relatives of several isolates and mixed cultures were obtained from sequences of successfully amplified and cloned bacterial 16S rRNA genes. The closest sequenced relatives to cultured samples were identified by homologous BLAST against a known database of organisms available via the NCBI. Nearest taxonomic relatives are shown for all sites except Kuzuluk (which could not be determined) are shown in Table XXII, below.

TABLE XXII: NEAREST TAXONOMIC RELATIVES OF ENRICHMENT CULTURES.

Site	Growth Conditions		Closest Known Relatives*
	Temp. (°C)	pH	(Max % Similarity/Query Coverage)
Dokurcun	20-30	8.2-8.3	*Aeromonas salmonicida* subsp. (100/95); *Aeromonas caviae* (99/95)
Yanartaş	40-50	9.5-10.5	*Bacillus licheniformis* strain (99/95);
Koza	50-65	8.6-8.7	*Meiothermus ruber, Meiothermus rosaceus* (99/94); *Thermomonas hydrothermalis* (98/95)
Sakarıılıca	50-65	6.65	*Thermomonas hydrothermalis* (98/90); *Bacteroidetes* spp.

TABLE XXIII: SELECTED CULTURES AND RESULTS FOR DOWNSTREAM GENETIC ASSAYS.

Sample Site	Growth Conditions	Carbon/ Energy Sources[a,b,c]	Cell density[d] (Avg. cells/ml)	DNA extraction successful?	Genes Detected	Sequence(s) Obtained?
Dokurcun	25°C; pH 8.3 aerobic	YP	> 10^8	Yes	16S rRNA narG, nirK, norB	16S rRNA; narG; norB
Yanartaş	50°C; pH 8.3 aerobic	YP	> 10^8	Yes	16S rRNA	Yes
		YP+$FeCl_3$	~10^7-10^8	Yes	16S rRNA	Yes
	50°C; pH 9.5 aerobic	YP+NR	~10^7-10^8	Yes	16S rRNA, norB, narG	16S rRNA only
		NR	~2*10^4	Yes	16S rRNA, nirS, narG	Yes
		SR	~10^6	Yes	16S rRNA	No
	50°C; pH 10.4 aerobic	YP	~10^5-10^6	No	N/A	N/A
		NR	~10^2-10^3			
		OA	~10^3-10^4			
Koza	60°C; pH 8.63 aerobic	YP	~10^5-10^8	Yes	16SrRNA	Yes
		OA	~10^5-10^6	No	N/A	N/A
		$FeCl_3$	~10^5-10^6	No	N/A	N/A
Sakarıılıca	50°C; pH 6.65; aerobic	YP	ND	Yes – 2010 only	16SrRNA	Yes
Kuzuluk	70-80°C; pH 6.7; aerobic; C-source:	YP	~10^5-10^6	No	N/A	N/A

[a]YP = Yeast extract-peptone media.

[b]NR = Nitrate reduction media.

[c]SR = Sulfate reduction media.

[d]ND = Not determined.

4.4.2 **Nitrogen-cycling Functional Genes**

The presence of several nitrogen-cycling genes was detected in DNA extracted from cultures from Dokurcun (DK) and Yanartaş (YT). Due to greater success in extracting amplifiable DNA from these cultures, the number of PCR-based assays performed was greater for these two sites. Cultures from the higher temperature site's [Kuzuluk (80°C), Koza (60°C), Sakarıılıca (50°C)],

cultures grew to much lower cell densities, and DNA extractions did not yield sufficient amplifiable DNA for downstream assays, so results for these samples are not shown. Table XXIV, below, indicates which nitrogen-cycling gene fragments were successfully amplified from environmental samples and detected via gel electrophoresis. In some cases, gene fragments suspected to belong to the target gene were detected in gel electrophoresis at the appropriate length, but cloning of the amplified fragments was not successful so no sequences were obtained. These cases are noted where appropriate.

TABLE XXIV: ASSAYS FOR NITROGEN-CYLCING FUNCTIONAL GENES IN CULTURES.

Site	Growth Conditions		Presence of Nitrogen-Cycling Functional Genes[a,b,c]						
	Temp. (°C)	pH	*nifH*	*narG*	*nirS*	*nirK*	*norB*	*nosZ*	*amoA_Bac*
Dokurcun	20-30	8.2-8.3	ND	P	P*	P*	P	ND	ND
Yanartaş	40-50	9.5-10.5	ND	P	P	P*	P*	ND	ND

[a] P = Gene is present and sequence was obtained.

[b] P* = likely gene presence based on gel electrophoresis, but no sequence obtained.

[c] ND = gene not detected in sample.

For cloned functional genes that were successfully sequenced, not all shared high identity with known functional gene sequences, likely due to inadequate sequencing of functional genes from organisms inhabiting 'extreme' environments. However, several genes from Yanartaş and Dokurcun did relate to sequenced functional genes, though, interestingly, they were not the same organisms with high sequence similarity in terms of 16SrDNA (shown in Table XXII), possible reflecting sharing of genetic sequences for widely-distributed functional genes among distinct species. The maximum percent sequence similarity and query coverage of shared sequences are shown in Table XXV, below. Accession numbers in GenBank are also provided.

TABLE XXV: NEAREST RELATIVES TO SEQUENCED FUNCTIONAL GENES.

Site	Growth Conditions	Gene	Nearest Relative	Max. % Similarity	Query Coverage (%)	Accession Number
Yanartaş	NO_3^- Reduction (no YP) pH 9.5 50°C	*nirS*	Halomonas sp. C8 NirS (nirS) gene, partial cds	84	75	GQ384048.1
		narG	Uncultured bacterium clone F42 dissimilatory membrane-bound nitrate reductase (narG) gene, partial cds	71	84	AY453356.1
Dokurcun	YP Media pH 8.22 25°C	*norB*	Alcaligenes xylosoxidans subsp. xylosoxidans partial norB gene for nitric oxide reductase	93	80	AJ507331.1
		narG	Unidentified bacterium clone NCSE22 putative dissimilatory membrane-bound nitrate reductase (narG) gene, partial cds	80	81	AY552358.1

CITED LITERATURE:

Cardace, D. & Hoehler, T. M. (2009a) Serpentinizing fluids craft microbial habitat. *Northeastern Naturalist* **16**(5): 272-284.

Meyer-Dombard, D. R., Shock, E. L., & Amend, J. P. (2012) Effects of trace element concentrations on culturing thermophiles. *Extremophiles* **16**:317-331.

Sleep, N. H., A. Meibom, Th. Fridriksson, R. G. Coleman, & D. K. Bird. (2004) H_2-rich fluids from serpentinization: Geochemical and biotic implications. *PNAS* **101**(35):12818-12823.

Stevenson, B. S., Eichorst, S. A., Wertz, J. T., Schmidt, T. M., & Breznak, J. A. (2004) New Strategies for Cultivation and Detection of Previously Uncultured Microbes. *Applied and Environmental Microbiology* **70**(8):4748–4755.

Stewart, E. J. (2012) Growing Unculturable Bacteria. *J. of Bacteriology*. **194**: 4151-4160.

Zengler, K., Toledo, G., Rappe, M., Elkins, J., Mathur, E. J., Short, J. M., & Keller, M. (2002) Cultivating the uncultured. *Proc. Natl. Acad. Sci. USA* **99:**15681–15686.

5. **DISCUSSION**

5.1 **Geochemical Characterization of Study Sites**

Geochemical profiles using on-site measurements and post-field analyses were produced for each of the spring sites visited during the 2010 and 2012 field surveys (described in Chapter 2). Spring fluids are grouped into three types: 1) meteoric water weathering serpentine rock (Dokurcun cool seep); 2) meteoric-derived hydrothermal waters with deeper circulation, dominated by Mg-HCO_3 (Sakarıılıca and Kuzuluk hot springs); and 3) Ca-OH dominated spring waters with some alkalinity from serpentine-derived waters mixing with hydrothermal fluids (Koza). Yanartaş –an example of the surficial weathering of ultramafic minerals from serpentinization-derived fluids and gases sourced at depth –provides geochemical reference with which to compare these systems to serpentinization-related processes. I will first discuss the geochemical regimes present at the sites surveyed, and will relate observations of growth in culture and the presence of functional genes to predictions of favorable metabolic options

5.1.1 **Chemical Regimes Among Hot and Cool Springs in Northwest Turkey**

The hottest spring, and likely the most deeply-sourced at ~190 m – Kuzuluk - has the highest dissolved solutes for most analytes (e.g. DOC and DIC; salts and trace elements) with some exceptions (Koza had the highest S^{-2} at ~60 µg/L) (Fig. 4). Kuzuluk thermal waters are hosted by Miocene volcanic rocks and elevated concentrations of trace elements (e.g. As, Ba, Rb, Sr, Zn) are likely related to weathering of these mineral assemblages (refer to Tables XXXII-XXXIII, Appendix B, for complete trace element chemistry at each site). High levels of cations (e.g. NH_4^+, Fe^{2+}, Ca^{2+}, Mg^{2+}) are typical of vapor-dominated hydrothermal systems (Meyer-Dombard et al., 2005), indicating significant water-rock alteration and little gas production at depth.

Ca:Mg ratio is plotted against aqueous silica to assess the relative inputs of serpentinization-derived (circled in blue) and hydrothermal waters (circled in red) in Fig. 5. Dissolved SiO_2 reflects weathering of parent rock; higher Ca:Mg ratios are typically associated with

serpentinization, though as in Fig. 5, a wide range of Ca:Mg ratios has been observed in alkaline systems associated with active serpentinization and weathering of serpentine minerals (Blank et al., 2008; Cardace & Hoehler, 2009; also refer to data plotted in Fig. 5 from cited literature). The relatively low Ca:Mg ratio in Kuzuluk spring fluids does not suggest active serpentinization at depth, though the value is comparable with alkaline springs observed by Barnes et al. (1978) in New Calcedonia (La Coulée Spring, pH ~10.7; which had a lower Ca:Mg ratio (1.83) than alkaline springs in the Semali Ophiolite in Oman (Ca:Mg ratio of 600) due to a higher input of Mg^{2+} relative to Ca^{2+}).

Spring fluids at Koza plot more closely to serpentine-hosted alkaline systems in terms of Ca:Mg, though Mg^{2+} concentrations in fluids are near zero at Koza, elevating the Ca:Mg ratio. The high Ca^{2+} found in Koza fluids suggest a different reservoir of fluid at depth, increased fluid-rock interaction with ultramafics in the reservoir, or modest input from serpentinized fluids at depth. Dissolved SiO_2 tends to be higher in these systems than other alkaline, serpentine-hosted seeps (e.g. John Day Spring, OR; Barnes et al. 1967) due to higher fluid temperatures and weathering of the parent rock.

A plot of sulfate vs. chloride concentrations (Fig. 6) illustrates the relative influences of silicate weathering (increasing Cl^- concentrations) and vapor-fluid interactions (increasing SO_4^{2-} concentrations). Water-rock dominated systems are circled in blue on Fig. 6; water-vapor dominated systems are circled in red on Fig. 6. Kuzuluk thermal spring, with the hottest temperatures, also has the greatest degree of water:rock interactions, with $[Cl^-] > [SO_4^{2-}]$ levels (798.8 vs 135.58 ppm respectively). Compared with several hot springs in Yellowstone, Kuzuluk fluids plot very close to those issuing from Sylvan Springs [78.7°C, pH 5.8; Shock et al., 2010]. At Koza, the opposite is true, with $[Cl^-] < [SO_4^{2-}]$ (9.684 vs 689.4 ppm, respectively), indicating this system is vapor-dominated, with significant sulfide oxidation to sulfate at depth. However, the elevated Ca:Mg ratios at Koza - comparable to known serpentinizing systems, also plotted - suggest

possible interaction of hydrothermal fluids with serpentinization-derived inputs at greater depth. From these data alone, it is not possible to determine whether the elevated Ca:Mg ratio and dissolved SiO_2 at Koza, coupled with low Cl^- levels (typical of serpentinizing systems) are a product of: 1) hydrothermal fluids weathering ultramafics or 2) dilution of serpentinization-derived fluids at depth with hydrothermal fluids. Either case would represent a novel type of hydrothermal system, the fluids being a product of two distinct rock alteration processes. Thus, Koza represents the only hydrothermal site surveyed that may be influenced by serpentinization at depth.

Fluids from Sakarıılıca reflect deep circulation of meteoric waters weathering silicate minerals, resulting in a hydrothermal system enriched in dissolved silica, but with a fairly low Ca:Mg ratio. Ion chromatography data for Ca^{2+} and Mg^{2+} concentrations was not obtained for this site and Ca:Mg ratios are inferred from total Ca and Mg content in the fluids as measured by ICP-MS. This system is similar to Koza, but the lower pH (pH ~6.65 versus pH 8.63 at Koza) suggests a greater proportion of felsic to mafic minerals in the reservoir rock.

Dokurcun – the cool seep observed trickling through exposed serpentine in northwest Turkey – is primarily of meteoric waters, with low dissolved mineral contents relative to hydrothermal fluids. The slightly alkaline pH (~8.22) is a reflection of minimal water-rock interactions with serpentine minerals. Data for dissolved silica, Ca^{2+} and Mg^{2+} are not available for fluids sampled in 2010, though based on the low trace element levels in Dokurcun snow (sampled in 2012), it is likely that all of these constituents are on the lower end of all sites sampled. As such, this site represents a meteoric endmember to the hydrothermal springs. Its chemistry is influenced by weathering of ultramafic minerals, but at much lower temperatures.

The water types identified among the hot springs in NW Turkey are consistent with previous geochemical studies on thermal waters along the North Anatolian Fault Zone (NAFZ). Süer et al., 2008 performed a comprehensive, multiyear monitoring study (2002-2004) on the geochemistry of springs along the NAFZ and observed that the majority of thermal waters were Na-

HCO_3 dominated systems. The carbonate is a product of dissolution of reservoir rocks (primarily Mesozoic limestones) while ion-exchange with overlying sediments in thermal reservoirs contributes significant Na^+, especially at Kuzuluk (see Fig. 4 for distribution of biologically-relevant ions at the sites). Only hot springs near Bolu and Mudurnu, a town near Koza, were Ca-HCO_3 dominated systems (Süer et al., 2008), corroborating this broad assessment of the primary water types observed in the area.

Sanliyuksel & Baba (2011) noted a significant sulfate component present in some hot springs in northwest Turkey, and have classified hotter waters as Na-SO_4 type versus Ca-HCO_3 type for cooler water counterparts. Close inspection of the spatial distribution of sulfate in hot springs reveals a very high spatial variability in SO_4^{2-} concentrations, likely due to different reservoir lithologies among the hot springs. Koza has a significant sulfate concentration, although its slightly elevated pH (~8.63) and high Ca:Mg ratio are not typical of sulfidic hot springs, possibly indicating mixing of hydrothermal fluids with fluids weathering ultramafic assemblages at depth.

FIGURE 4: DISTRIBUTION OF RELEVANT IONS IN SPRING FLUIDS SAMPLED IN 2012 SURVEY.

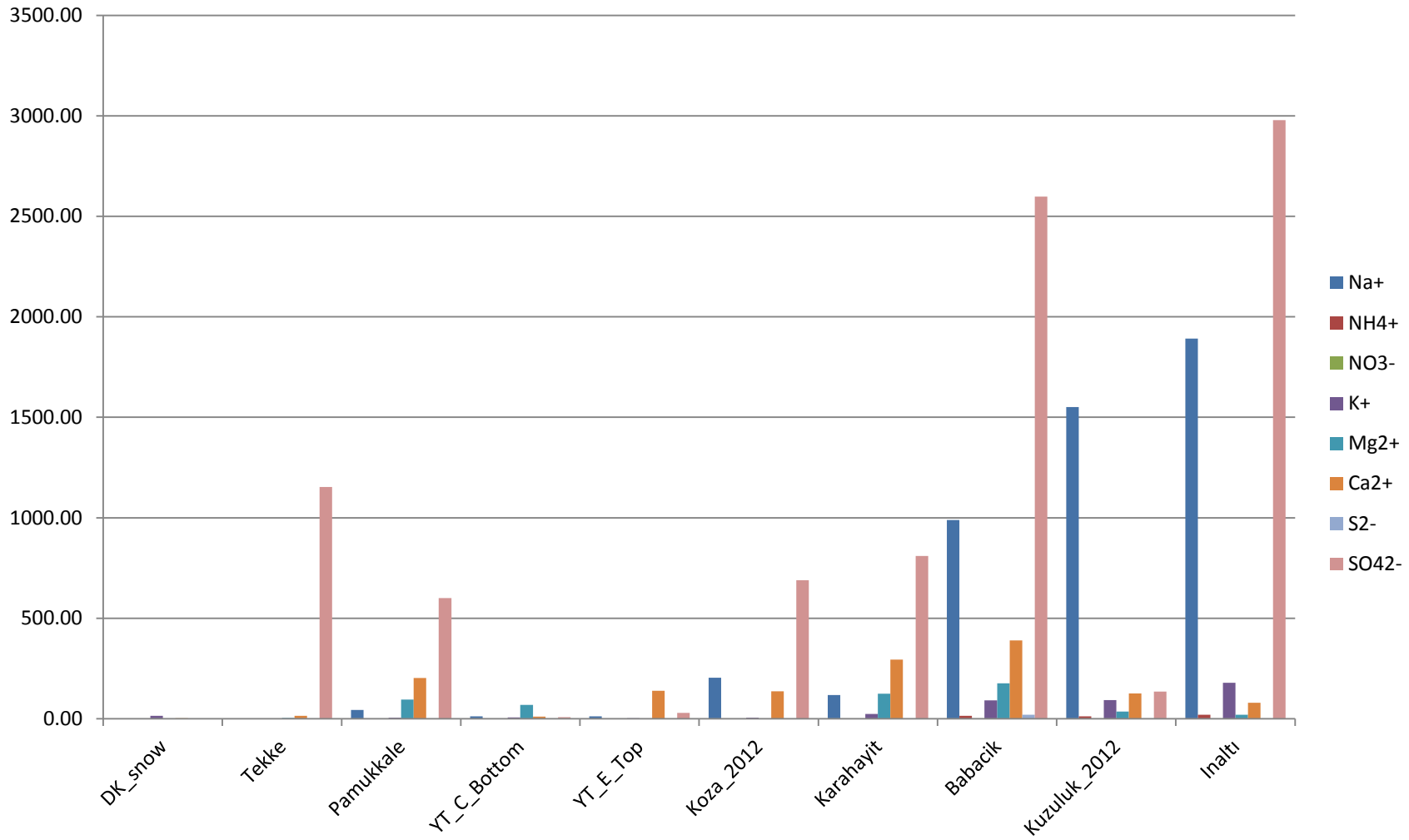

FIGURE 5: CA:MG RATIOS VERSUS DISSOLVED SiO_2 OF SAMPLED SPRINGS IN 2012 AND PUBLISHED DATA FROM ALKALINE SPRINGS ASSOCIATED WITH SERPENTINIZATION.

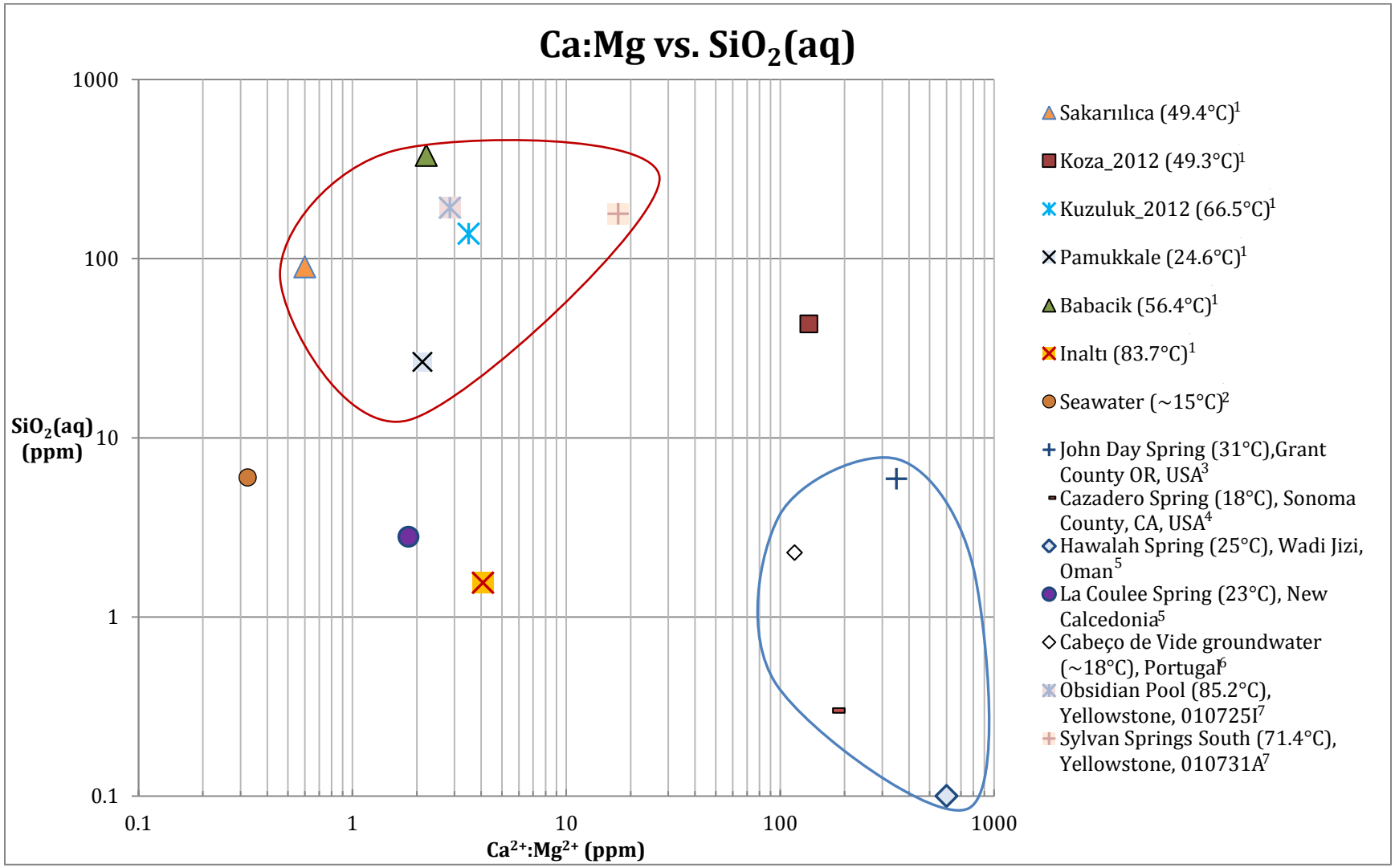

[1]This study;[2]Lodders & Fegley (1998); [3]Barnes et al. (1967);[4]Barnes et al. (1972);[5]Barnes et al. (1978);[6]Tiago et al. (2004);[7]Shock et al. (2010)

FIGURE 6: PLOT OF SULFATE VS. CHLORIDE FOR SAMPLED SPRINGS AND PUBLISHED VALUES FOR SERPENTINIZING AND HYDROTHERMAL SYSTEMS.

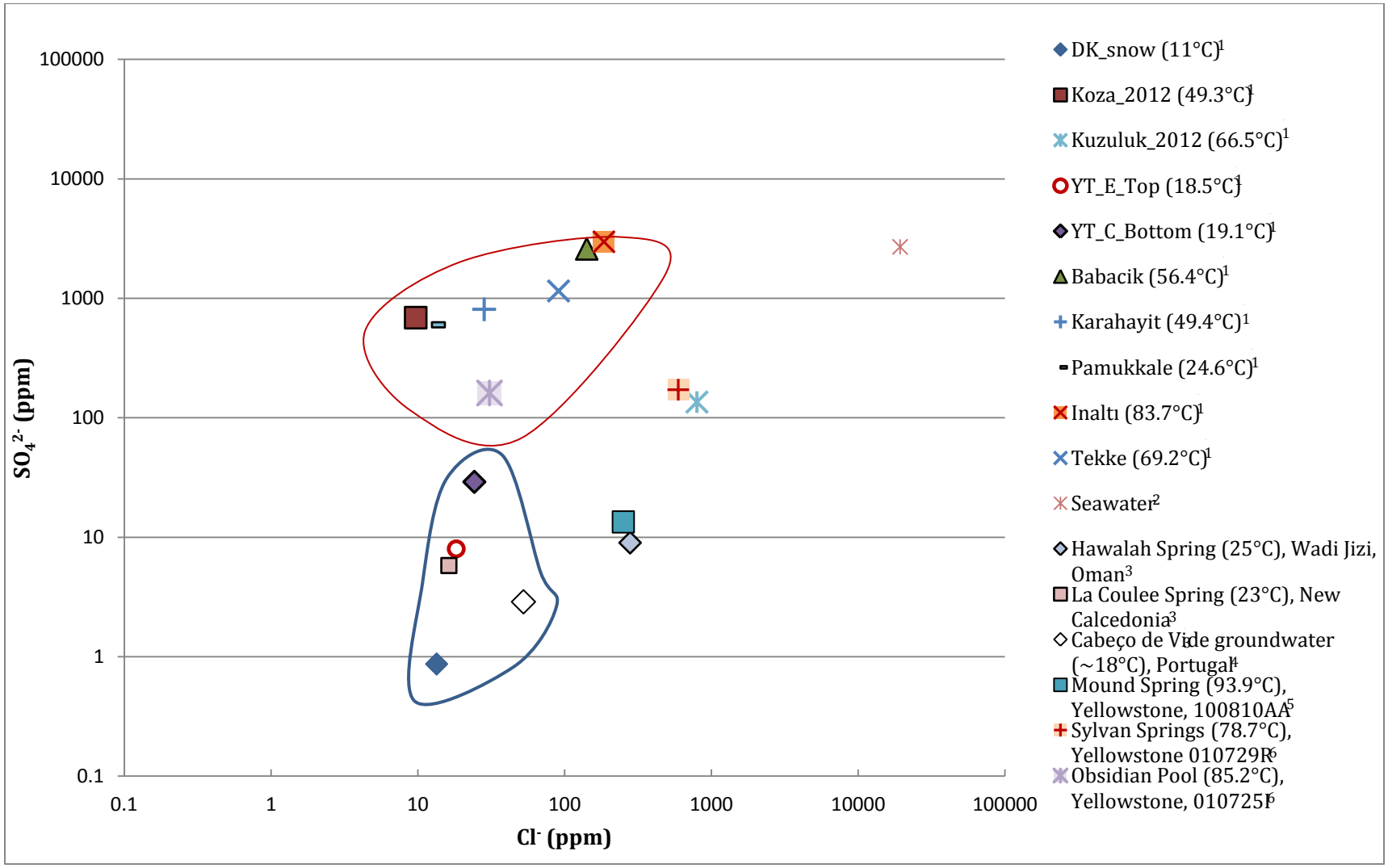

[1]This study;[2]Lodders & Fegley (1998); [3]Barnes et al. (1978);[4]Tiago et al. (2004);[5]Loiacono et al. (2012); [6]Shock et al. (2010)

5.1.2 ^{18}O and ^{2}H Isotopes in Spring Fluids

Comparison of $\delta^{18}O$ and δD values of springs sampled in 2010 (Kuzuluk, Koza, Sakarıılıca, and Dokurcun) with the global meteoric and Mediterranean meteoric water lines (GMWL and MMWL, respectively; refer to Fig. 7) indicates that these springs are likely recharged by meteoric waters, but undergo varying degrees of water-rock interaction at depth due to differing residence times of the spring fluids. Values for Dokurcun and Sakarıılıca lie very close to the GMWL, indicating a meteoric origin for these waters and minimal water-rock interaction; whereas at Koza there is slight enrichment in ^{18}O relative to the GMWL, though it is consistent with the MMWL. Kuzuluk waters, with the highest temperature (~75°C), are expected to undergo the most intense water-rock weathering at depth, and thus should be enriched in the heavy isotopes. Instead, we see the opposite: Kuzuluk waters are depleted in ^{18}O and deuterium with respect to the GMWL, indicating the recharge areas for this system is sourced at a substantially higher altitude than cooler springs nearby. The slight positive shift in 18O may also be attributed to isotopic exchange with the reservoir rocks during hydrothermal alteration of the subsurface lithology.

Depleted values of heavy isotopes in hotter waters were also observed in springs along the North Anatolian Fault Zone by Süer et al. (2008), who monitored geochemical and isotopic variations in spring fluids over a three year period (2002-2004), as well as by Karakus & Simsek (2008). However, Süer et al. noted that in order to adequately infer the reason for depleted isotopic values in some hot springs, measurements on the altitudes of recharge sites for cooler springs must be obtained. Given the highly fractured and seismically active subsurface, alterations in belowground mixing regimes are also a factor, and can result in dramatic shifts in isotopic composition of spring fluids if hydrogeologic flow is rerouted or a formerly sequestered source of organic material is introduced to the system through faulting and fracturing of underlying sedimentary units (Süer et al., 2008).

FIGURE 7: $\delta^{18}O$ VS. δD IN FLUID SAMPLES COLLECTED DURING THE 2010 SURVEY.

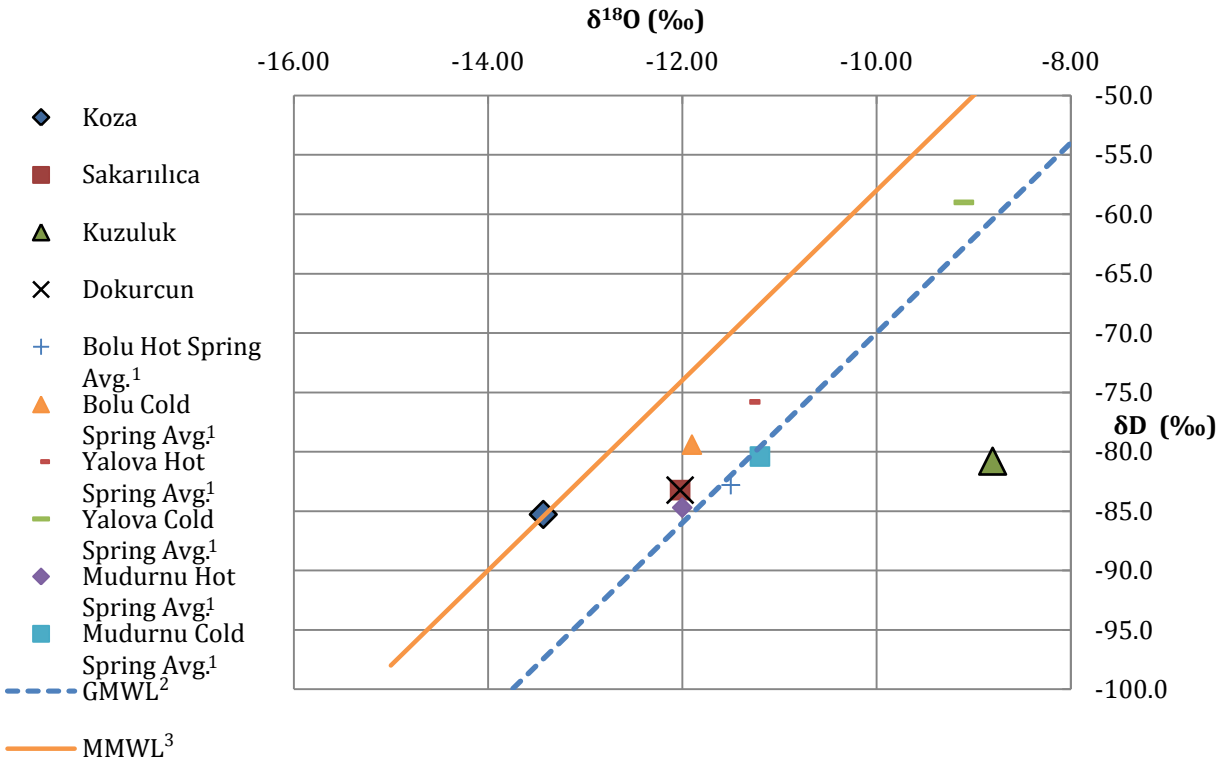

[1]Suer et al. (2008)

[2]GMWL = Global Meteoric Water Line; Craig (1961)

[3]MMWL = Mediterranean Meteoric Water Line; Gat et al. (1996)

5.1.3 Geochemistry at Yanartaş

Fluid chemistry from the source, near an actively burning methane vent (Site E) is compared with chemistry at the bottom of the outflow channel (Site C). All major cations and anions increase down the outflow channel (from E to C) except for NH_4^+ and Ca^{2+}. The decrease in Ca^{2+} in the fluid is likely due to the precipitation of Ca^{2+} in the fluid upon interaction with CO_2-laden air, as evidenced by extensive $CaCO_3$ precipitation in the lower portion of the biofilm channel. The

presence of NH_4^+ may be related to exogenous organic inputs. Figs. 8 and 9, below, illustrate changes in nitrogen content (total weight percent and $\delta^{15}N$ of solids) down the outflow channel.

A slight increase in $\delta^{15}N$ and concomitant increase in total N suggests that biological uptake of nitrogen may be relying on increasingly enriched dissolved fixed nitrogen in the fluid along the channel length, leading to the incorporation of heavier N into the solid phase (which included substantial portions of biofilm intermingled with sediment precipitates, mostly carbonate). Increased total N in solids with distance from the source (Fig. 8), may also require recycling of nitrogen sources within the biofilms.

The $\delta^{15}N$ values are slightly higher than what would be expected if N_2 fixation were occurring (~0 ‰, Jahnke et al., 1999), implicating instead that there is sufficient bioavailable nitrogen (as nitrate) to support the ephemeral biofilm community from exogenous organic inputs, and that this N is 'recycled' by members of the biofilm community downstream, causing a slight enrichment in $\delta^{15}N$ as microbes preferentially utilize $^{14}NO_3^-$ from the pool of intracellular nitrate sequestered within the biofilm community (Havig et al., 2011). Initially, microorganisms will preferentially utilize $^{14}NO_3^-$, resulting in enrichment of the remaining available nitrate in ^{15}N. Microbes downstream will be forced to uptake the heavier $^{15}NO_3^-$ remaining, so that nitrate passively lost by cells (i.e. after death phase) will be enriched in the heavier isotope (Havig et al., 2011), producing the observed enrichment in $\delta^{15}N$ down the outflow channel (Loiacono et al., 2012). Similar trends have been described in nitrate-limited systems under both natural (De Brabandere et al., 2007) and experimental settings (Waser et al., 1998; Needoba et al., 2004). These observations are further substantiated by the enrichment cultures in nitrate reduction growth media and the results of genetic surveys for nitrogen-cycling functional genes, further discussed in Sections 5.4.

FIGURE 8: TOTAL WEIGHT PERCENT NITROGEN OF SOLIDS AT YANARTAŞ VS DISTANCE FROM SOURCE VENT (M).

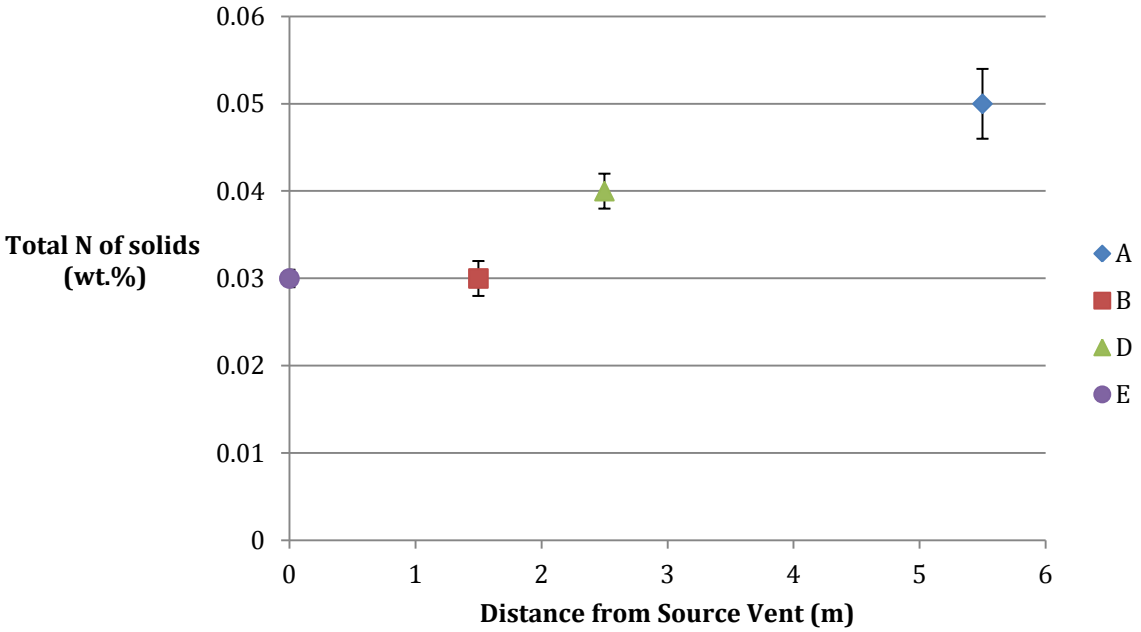

FIGURE 9: $\delta^{15}N$ (‰) VS AIR IN YANARTAŞ SOLID PHASE SAMPLES VS DISTANCE FROM SOURCE VENT (M).

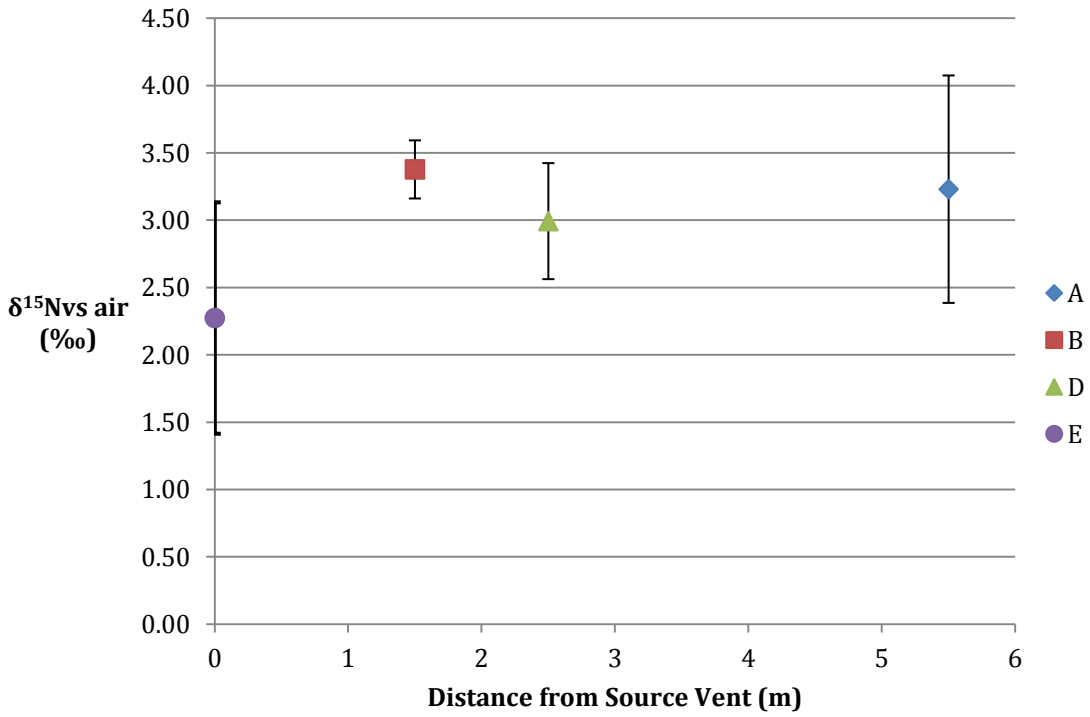

5.1.4 **Relation Between Site Geochemistry and Calculated Gibbs Free Energies**

Predictions for exergonic metabolic pathways were calculated for 4 out of the 5 study sites allowing comparison between observed metabolic capabilities in culture versus anticipated metabolic versatility based on thermodynamic favorability. Calculations were not made for Yanartaş due to lack of prior data on fluid chemistry at the site. Upper and lower estimates for reduced gas production in terrestrial seeps fed by serpentinization-derived fluids were used to calculate maximum and minimum values of ΔG_r for potential metabolic pathways, encompassing a range of possible concentrations for $H_{2(g)}$ [1-10 nM]and $CH_{4(g)}$ [1-500 μM] in these systems (Cardace & Hoehler, 2009). Shown in Fig. 10 are values of Gibbs free energies of reaction (in kJ, normalized per mole of electrons transferred) based on the lower estimates for both gases.

Although several metabolic options are exergonic at each site (Fig. 10), the ability to culture and isolate community members from sampled spring fluids varied widely. While some of these differences are likely related to the differences in site geochemistry, external factors, e.g. cultivation biases (Stewart, 2012; Stevenson et al., 2004; Zengler et al. 2002), also play a role in what can be cultivated in the laboratory. The potential impacts of cultivation biases are discussed in Section 5.3.2.

Gas chromatography (GC) analyses revealed that $H_{2(g)}$ concentrations were very low for all spring sites analyzed (Table XXVI), suggesting that serpentinization-derived fluid inputs are likely lower than anticipated in the NAFZ area springs. Rapid diffusion of light gases such as $H_{2(g)}$ could explain these data; the subsurface may be better equipped to trap H_2 in the pore spaces of geologic units, for example. Alternatively, microbial consumption of H_2 or other reduced gases at the oxic interface could proceed rapidly, maintaining low dissolved gas concentrations in the spring fluids sampled at the surface. As illustrated by data in Table XXVI, which compares measured gas concentrations at our sample sites with other known serpentine-associated systems, a wide range of H_2 and CH_4 concentrations have been observed. Several factors, including microbial

consumption of reduced gases and rapid oxidation at the surface, contribute to the loss of H_2 and CH_4 from such systems

FIGURE 10: VALUES OF GIBBS FREE ENERGIES FOR CHEMOTROPHIC METABOLIC OPTIONS BASED ON LOWER ESTIMATES OF H_2 AND CH_4 IN TERRESTRIAL SERPENTINIZING SPRINGS.

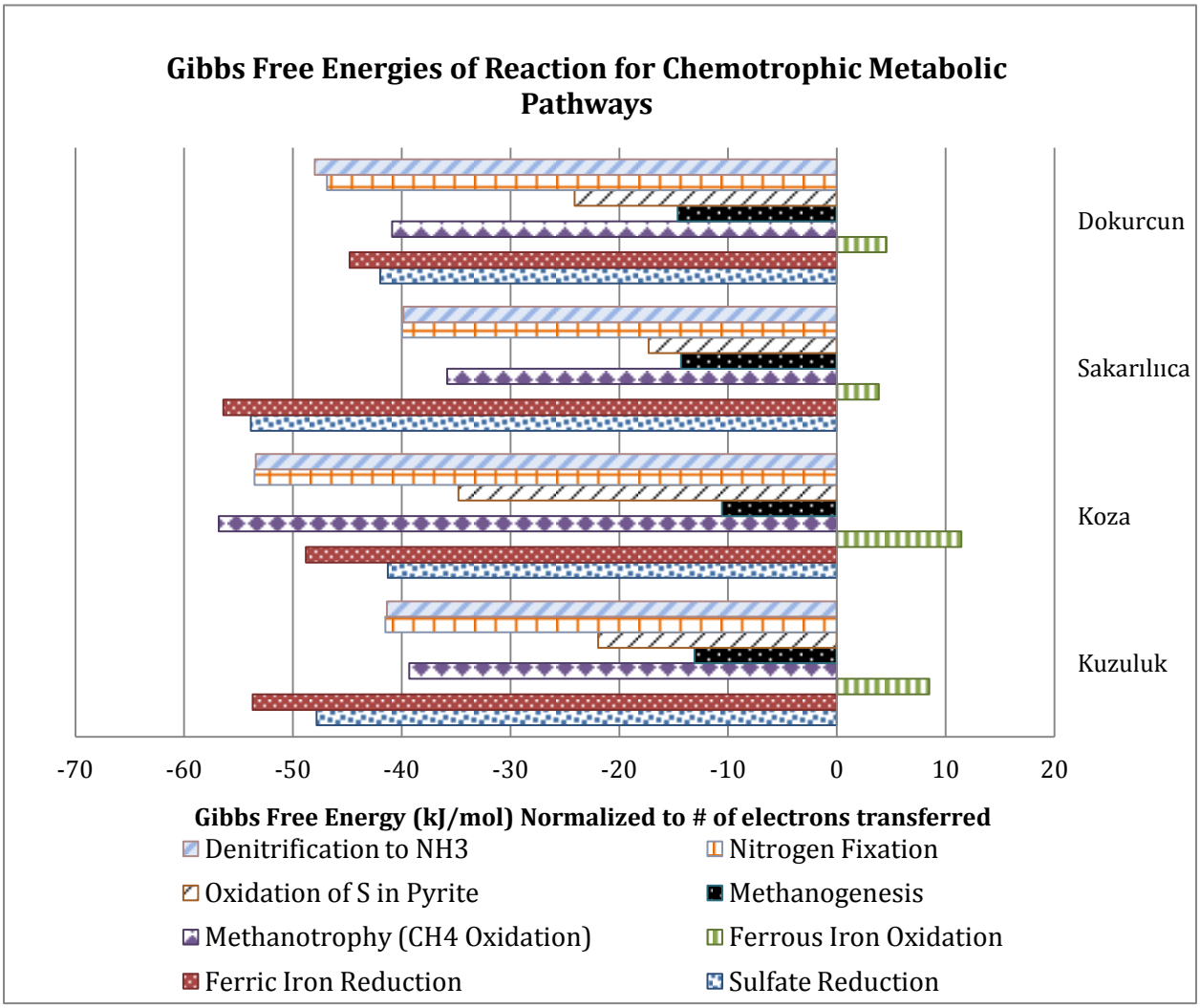

Though active serpentinization is unlikely, these data reveal that $H_{2(g)}$ concentrations at Koza and Kuzuluk are still within the ranges initially used to calculate Gibbs free energies of reaction for metabolic options investigated (1-10 nM H_2), albeit nearing the lower limit

for estimated $CH_{4(g)}$ levels (1-500 μM CH_4) in terrestrial serpentinizing systems. As such, the initial predictions of thermodynamic favorability are still valid for exergonic reactions with potentially more energy available if gas concentrations are enriched in subsurface pore spaces or secondary fractures.

TABLE XXVI: AVERAGE CONCENTRATIONS OF DISSOLVED GASES IN SAMPLED SPRING FLUIDS AT KOZA AND KUZULUK AND PUBLISHED VALUES FOR SERPENTINE-HOSTED AND SUBSURFACE SYSTEMS.

Site	Location	Host Rock Lithology	$H_{2(g)}$	$CO_{2(g)}$	$CH_{4(g)}$	D.O.	References
Koza	NW Turkey	Amphibolite	bdl[a]	86.94 μM	6.095 μM	84.4 μM	This study
Kuzuluk	NW Turkey	Miocene volcanics; near amphibolites	bdl	6604.0 μM	1.267 μM	21.9 μM	This study
Coast Range Ophiolites	N. California	Ophiolite	0.03 – 3 μM	NR	1-800 μM	NR	D. Cardace, pers. Comm..
Lost City Hydrothermal Field	Seafloor, near MAR[c]	Basalt	1,000-15,000 μM	NR	1000-2000 μM	NR	Kelley et al., 2005
Lidy Hot Springs , Idaho, USA	Terrestrial subsurface, 200 m depth	Basalt	0.013 ± 0.002 μM	NR	125 μM	NR	Chapelle et al., 2002
Leka Ophiolite Complex, Norway	Groundwater (0.6-1.3 m depth in borehole)	Serpentines, brucites, olivines	0.585 μM	NR	Peak detected	385 μM	Okland et al. (2012)

[a]Bdl = below detection limit

[b]NR = Not reported

[c]MAR = Mid-Atlantic Ridge.

5.2 **Observed Metabolism in Enrichment Cultures**

Mixed cultures and isolates obtained from hot spring fluid were generally heterotrophic aerobes. This trend appears fairly common among attempts to culture hot spring organisms from the region (e.g. Gul-Guven et al. 2008; Cihan et al. 2011; Adiguzel et al., 2011) and elsewhere (Meyer-Dombard et al., 2012). It is likely that these efforts have not captured the actual biodiversity present in these systems due to inherent cultivation bias (Stewart, 2012), further discussed in Section 5.3.2. Unrepresented members in culture may be dependent on symbiotic interactions with other microorganism in the natural environment that were removed during serial dilutions aimed at targeting the dominant members in the community. The possibility that other metabolic options not observed in this study are utilized *in situ* cannot be discounted.

5.2.1 **Hydrothermal Sites**

Initial cultures from 2010 were serially diluted in order to isolate the dominant members from each system; 16SrRNA phylogeny indicated relatives to other known hot spring microorganisms, allowing inference of metabolic capacities based on those utilized by taxonomic relatives. In 2012, enrichment cultures were not diluted; instead, enrichment cultures were kept in mixed culture to preserve the natural community diversity, and as such, metabolic diversity of the original samples. The results of these efforts are described in Chapter 4, in Tables XVI-XX.

Fluids sampled during the 2010 survey from each hydrothermal site (Kuzuluk, Koza, Sakarıılıca) yielded cultures able to use a variety of organic substrates (Yeast extract and peptone [YP], organic acids [OA], sugars) though growth was significantly enhanced when grown on complex organic compounds (e.g. YP) versus simple sugars or organic acids. This trend was commonly observed in thermophilic cultures especially, with heterotrophy apparently dominant over chemosynthetic metabolism.

Generally, growth in media other than YP was much slower and reached far lower cell densities. Growth in sugars media at temperatures above 55°C was also prohibited due to

carmelization of the sugars (preventing fermentation or oxidation by resident microorganisms). Anaerobic growth in all media types occurred extremely slowly, and it was difficult to determine if cell numbers were actually increasing over time. As a result, much of the successful cultures were aerobic, and may better represent microbial diversity at the surface, where hydrothermal fluids interact with an oxic atmosphere, rather than the deep biosphere, which is presumed to be nearly anoxic.

Growth was observed in nitrate, sulfate, and Fe(III) reduction media in all hydrothermal samples (though with varying degrees of success; cultures from Koza were viable for the longest, though growth eventually dissipated over time), supporting a correlation between thermodynamically-favored metabolic pathways and observed metabolism. In these three media types, growth appeared to be limited by availability of organic carbon in the system: the addition of organic substrates significantly enhanced growth in all cases. The low DOC in hot spring fluids (1.7 ppm at Koza; 3.6 ppm at Kuzuluk; 5.81 ppm at Sakarıılıca) also suggests that organic carbon may be the limiting nutrient for native microorganisms *in situ*, indicating that the media employed for these tests accurately mimicked environmental conditions. The same could be true for the other system under study, all of which had fairly low DOC (refer to Ch. 4, Table IX for DOC and DIC data).

Enrichment cultures from hydrothermal systems generally displayed smaller temperature ranges (10-15 degrees C) of growth than those from sites with highly variable conditions (i.e. Dokurcun (DK) and Yanartaş (YT), both of which are exposed to seasonal variations in temperature, moisture, and in the case of Yanartas, high amounts of ambient CH_4 gas). This growth pattern thus reflects environmental conditions: fluids sampled at hydrothermal springs are deeply sourced and likely have fairly stable temperatures and fluid chemistries, so resident microorganisms do not adapt to a wide range of conditions. Surface seeps undergo both seasonal and diurnal variations in environmental conditions that resident microorganisms must tolerate in order to survive.

Sakarıılıca was only sampled in the 2010 survey and, like many thermophilic locations, cultures did not fare well in isolation (Meyer-Dombard et al., 2012). Culture growth in serial dilutions (presumed isolates in latter dilution series) began to diminish after a few months of cultivation in the laboratory. Several measures were taken to improve growth: incubation time was increased; trace element solution was re-made and diluted; vitamins were added to the growth media to stimulate growth; larger transfer volumes were used, etc (Stevenson et al., 2004; Stewart, 2012; Meyer-Dombard et al., 2012). These efforts extended the viable lifetime of most enrichment cultures, though growth dissipated with time in all high-temperature cultures. However, as noted in Section 5.3.2, many microorganisms have proven recalcitrant to cultivation, and is a primary reason that the majority of microbial diversity do not have cultured representatives (Hugenholtz et al., 1998; Stewart, 2012). Amplifiable DNA was obtained from one culture grown under aerobic conditions with yeast extract and peptone at 50°C and pH 6.67; its phylogeny based on 16SrRNA gene sequences is discussed in Section 5.4.

Similar obstacles arose when culturing from Kuzuluk fluids. Though aerobic enrichment cultures grown in 2010 from Kuzuluk fluids grew to visual turbidity, cultures from 2012 exhibited consistently lower cell densities, and DNA extraction attempts failed numerous times. No functional or 16SrRNA gene assays were performed due to lack of amplifiable DNA from Kuzuluk cultures. From cultivation experiments it is apparent that aerobic heterotrophs exist in all subsurface hydrothermal environments sampled, with lower temperature sites generally exhibiting more metabolic versatility in enrichment cultures, likely reflective of the more variable conditions prevailing in near-surface environments versus the deep subsurface.

5.2.2 **Dokurcun Cool Seep**

The lowest temperature site surveyed – Dokurcun (DK) – represents a primarily meteoric water weathering a fresh exposure of serpentine, slightly raising the pH to ~8.2-8.3. Its shallow and ephemeral nature likely promote the growth of hearty, fast-growing cultures that are capable

of remaining in a state of slowed metabolic processes (or producing endospores that can be revived) until a source of organic carbon is available. Despite long-term storage, fresh transfers of Dokucun enrichments into sterile media would grow after several weeks without additional organic carbon or oxygen whereas other, higher-temperature strains all lost viability as time passed.

Dokurcun cultures grew very rapidly when given complex organic substrates (Yeast-Peptone) and an aerobic headspace. Serial dilutions yielded an isolate of unknown origin that survived well in culture, almost always yielding viable cultures even after months in storage at 4°C. The cells were motile, rod-shaped, and grew to high cell densities (visibly turbid) within a few hours (~6-8h). Limited growth was observed when provided media targeting reduction of nitrate, sulfate and iron (III), but it did not yield cultures as dense as with a nutrient-rich media.

Raising either the pH or NaCl concentration in media tended to decrease cell densities in DK cultures, though growth did occur in up to 20 g/L NaCl in growth media. As such, these microorganisms likely reflect opportunistic species that exist in surface environments and are not likely to survive well in subsurface aquifers nearby, where hydrothermal alteration of volcanic and ultramafic minerals produced fluids rich in salts and certain metals .

5.2.3 **Yanartaş Gas Seep**

Mixed cultures from Yanartaş were dominated by fast-growing, motile, aerobic, filamentous bacteria with rod-shaped morphologies. They were observed growing in up to pH 10.4 media, though growth was significantly stunted with increased pH; cells appeared shrunken and moved more slowly and erratically than at lower pH. Optimal growth appeared to occur at lower pH 8-9.5. DNA from cultures representing all pH conditions employed is represented among the results; functional nitrogen-cycling genes (*narG*, *norB*, *nirS*) were detected in pH 9.5 and pH 8.3 growth media. The pH 10.4 growth media did have limited growth of cells, but DNA did not amplify well, likely due to the use of a carbonate buffer to maintain high pH in the media inhibiting DNA

extraction. Despite multiple extraction attempts, no amplifiable DNA was obtained from cultures grown in carbonate-buffered pH 10.4 media.

A time series image of growth taken over four hours (Fig. 11) demonstrates how quickly cultures from Yanartaş grew into a biofilm community. Starting out as relatively short, motile rods at t = 0 hours, visible increases in cell numbers and size occur within 1-2 hours. By hour 3, cells begin to form filamentous chains of cells, linking together from end to end. At hour four, the filaments become wider as cells line up in filaments adjacent to one another, forming an interconnected 'web' of cellular filaments. This rapid growth pattern was observed in all cultures given organic carbon, and supports the idea that the community is ephemeral, akin to the fluid seep on which it depends (which was not observed previously and dried up within a few hours under our observation during sampling). The production of endospores by its nearest taxonomic relative (*Bacillus licheniformis*, 98% sequence similarity) also suggests these microorganisms are capable of surviving harsh conditions for extended periods of time until more favorable conditions arise, at which point growth can proceed rapidly.

FIGURE 11: TIME SERIES OF CULTURES FROM YANARTAŞ OVER A FOUR HOUR PERIOD.

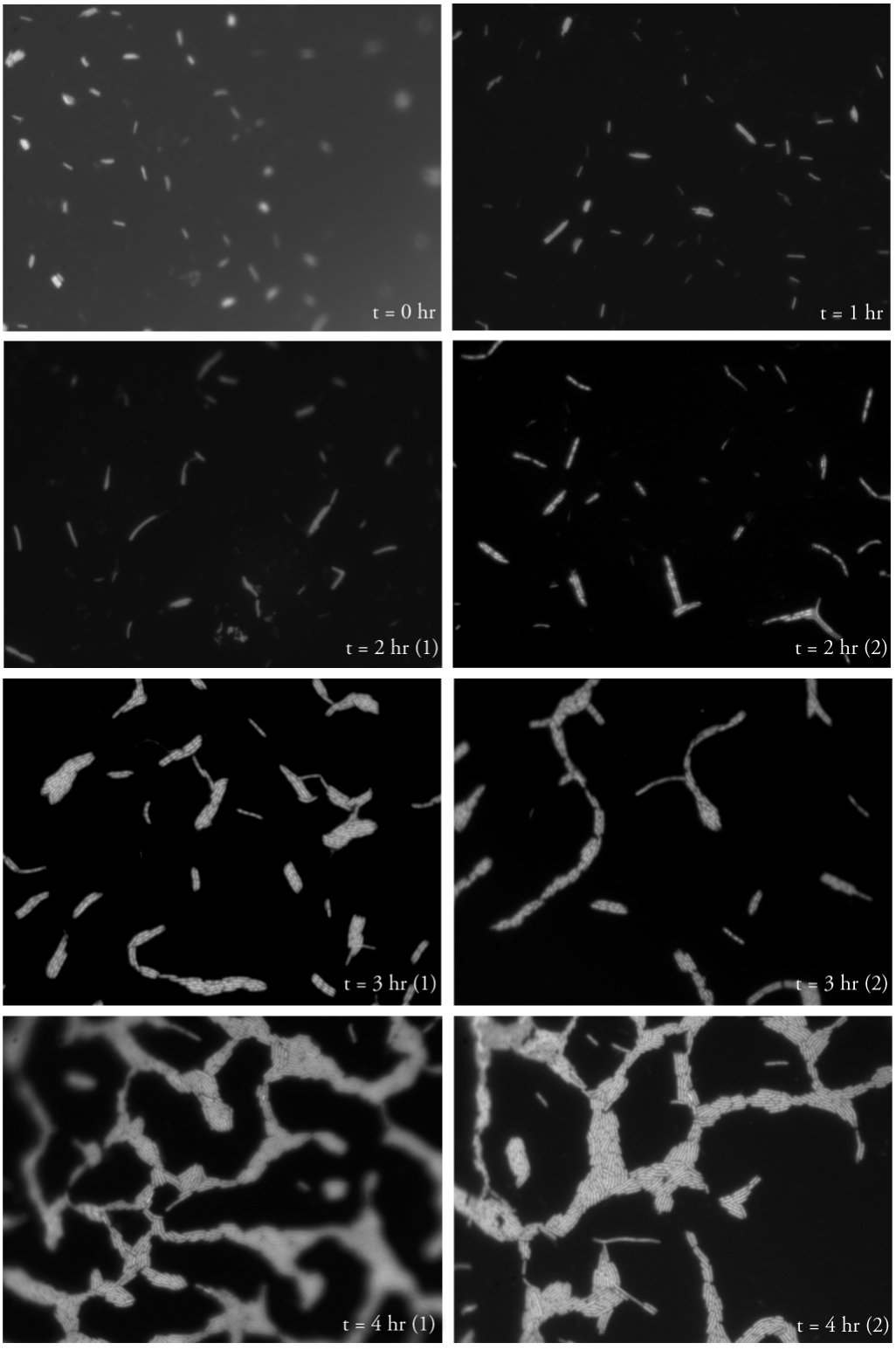

5.3 **Thermodynamic Predictions vs. Cultivable Microorganisms**

As illustrated in Fig. 10, all of the plotted chemotrophic metabolic pathways (CH_4 oxidation and methanogenesis; sulfate reduction; denitrification to NH_3; N_2 fixation; Fe(III) reduction) except for Fe(II) oxidation, are exergonic (have negative values of ΔG_r) over the range of hydrogen and methane concentrations experienced in terrestrial serpentinizing systems. As such it was predicted that culturable members would display a range of metabolic options as well. Prior observations of active nitrogen-cycling in hydrothermal and subsurface systems (e.g. Mehta & Baross, 2006; Hedlund et al., 2011; Loiacono et al., 2012) in addition to negative ΔG_r values for these systems suggests both denitrifying and N_2-fixing microorganisms are present. However, nitrogen fixation was not observed in culture nor were any genes diagnostic of nitrogen fixation (*nifH*) detected in DNA extracted from enrichment cultures. This may indicate that there is not an abundant need for organic nitrogen in these systems (which would prompt microorganisms to fix $N_{2(g)}$). These data are consistent with isotopic and geochemical data on total N in solid biomass along the outflow channel, which appear to reflect the recycling of nitrate within the biofilm community downstream, resulting in enriched $\delta^{15}N$ values and increasing total N in solids. As such, not all exergonic pathways were utilized by enrichment cultures, indicating that other factors (i.e. environmental levels of essential nutrients, carbon, or nitrogen and microbial energetics) influence metabolic processes besides thermodynamic favorability.

5.3.1 **Correlation Between Observed and Predicted Metabolic Options**

All of the observed metabolic options utilized by cultured microorganisms were predicted to be exergonic in these systems. However, it was not possible to demonstrate the use of certain exergonic chemosynthetic metabolic options (e.g. methanogenesis, Fe(III) reduction) due to recalcitrant growth in artificial media. It may be that the genetic potential to utilize chemoautotrophy exists within these habitats, but the microbial population has evolved to favor heterotrophy given available organic carbon and energy sources. Alternatively, facultative

chemoautotrophs with the capacity to utilize autotrophic metabolisms may be present but have sufficient organic carbon and/or energy to overcome any need for chemosynthetic energy production. This could explain the predominance of heterotrophs in cultured samples collected from the NAFZ in 2010. Known cultivation biases may be partly responsible for the preferential isolation of heterotrophs and several methods were employed to circumvent these biases (e.g. serial dilution, natural geochemical parameters in media, longer incubation times, careful selection of electron donors and acceptors) (Stewart, 2012; Meyer-Dombard et al., 2012).

Nitrate reduction appeared to be the most widely used alternate metabolic option, with growth observed at all sites (except Sakarıılıca due to loss of culture viability). For this metabolic option, the predictions appear to be well correlated with observed metabolism and genetic capacity. Diagnostic genes for nitrate and nitrite reduction (*narG* and *nirS*/*nirK*, respectively) were detected in cultures from Yanartaş given media targeting nitrate reduction, as well as those given yeast extract and peptone, indicating this process is fairly well-conserved over generations. However, despite thermodynamic favorability for nitrate reduction at all sites, the degree of growth among the sites was highly variable, with lower-temperature cultures (Yanartas and Dokurcun) growing much more readily on nitrate than hydrothermal enrichment cultures.

5.3.2 **Effects of Cultivation Bias**

The 'unculturability' of many microorganisms, especially those inhabiting 'extreme' environments has been well documented, with some workers estimating that up to 95% of all microorganisms have not been isolated in culture (Hugenholtz et al., 1998; Rappe & Giovannoni, 2003; Pace, 2009; Stewart, 2012). Studies have demonstrated that key growth factors available in the natural environment – often secreted by other microorganism living in symbiotic consortia - are lacking in traditional growth media (Stewart, 2012). As such, certain isolates can only be grown in the presence of another microorganism (e.g. Kim et al., 2011), or in a simulated environment that closely approximates natural conditions (e.g. Kaeberlein et al., 2002).

Clearly, this presents challenges in addressing the fundamental question of whether thermodynamic favorability and microbial metabolism *in situ* are reliably consistent with each other. However, the extent to which we can relate thermodynamics and metabolic pathways utilized can still be assessed; for example, there might exist a minimum threshold of energy released per mole of reactant that must be reached before inferences on metabolic potential can be made with any certainty. Below such a threshold, predictions based on thermodynamics may or may not be accurate, and with greater study it may be possible to assign probabilities to such predictions based on the calculated energy yield (e.g. a reaction yielding 20 kJ/mol could have a 60% probability of utilization in the environment whereas a reaction yielding half that would have a lower probability of utilization). At this point, the assignment of probabilities for utilization of different pathways is mere conjecture, but the value of quantifiable metrics governing habitability is great and this approach may hold promise. Future missions searching for evidence of life in extraterrestrial systems could be greatly aided if realistic probabilities could be assigned to utilization of various metabolic options, even if the correlation between thermodynamic favorability and observed metabolisms is not 100%. However, a robust dataset regarding favorable metabolisms with respect to those actually utilized must be produced in order for this model to hold weight in a variety of geochemical habitats, given the number of variables affecting microbial energetics *in situ*. For now, it may only serve as a coarse measure of the energetic potential provided by a given system.

5.4 **Correlation Between Genetic Capacity and Metabolic Potential**

Physiological and metabolic properties of the enrichment cultures is compared with those of the nearest taxonomic relatives, based on 16SrRNA phylogeny. Though minor physiological differences are known to exist among bacterial phyla, and even within some species (with different strains exhibiting slight differences in metabolic capacity), general metabolic schemes can still be attributed to certain groups of bacteria. Without direct observation however, the use of certain

metabolic processes cannot be determined conclusively based on 16S taxonomy alone. Furthermore, none of the hydrothermal cultures shared 100% sequence similarity to any known organisms indicating the possible cultivation of a novel strain of bacteria, maybe possessing metabolic properties not observed in this study. This also could be attributed to the relatively low diversity of sequenced representatives from hydrothermal environments in GenBank.

Functional genes diagnostic of nitrogen-cycling were chosen for polymerase chain reaction (PCR) based genetic assays, as active nitrogen cycling has been observed in hydrothermal settings in prior work (Loiacono et al., 2012; Mehta & Baross, 2006). The gene for nitrogen fixation –*nifH* – was expected to be present among the enrichment cultures based on the relatively low amounts of organic N in the system (i.e.in Yanartaş solid samples). However, *nifH* was not detected in any of the samples, indicating that not all processes thought to be occurring in these systems can be observed in cultured representatives.

5.4.1 **16SrRNA Taxonomy of Mixed Cultures and Isolates from Hydrothermal Springs**

Nearest taxonomic relatives to Koza enrichment cultures included thermophiles related to *Meiothermus ruber* and its close relative, *M. rosaceus*, and strains related to *Thermomonas hydrothermalis*. Members of the genus *Meiothermus* appear widely distributed in hydrothermal systems and have been found in hot springs throughout the world (Tindall et al., 2010; Nobre et al., 1996). *M. ruber* (formerly *Thermus ruber*) was first described by Loginova et al. (1984) and has subsequently been cultivated from several terrestrial hot springs (e.g. Munster et al., 1986; Sharp & Williams, 1988). *M. ruber* are obligate thermophiles, with optimal growth temperatures from 50 to 65°C and an optimal pH of ~ 8 (growth conditions analogous to those used in this study) (Tindall et al., 2010). *Meiothermus* spp. are gram-negative, aerobic and most strains are chemoorganotrophic utilizing O_2 as a terminal electron acceptor, though several species can use nitrate instead, consistent with observed growth in both aerobic yeast-peptone and nitrate reduction media by Koza cultures.

M. rosaceus, which shares over 99% sequence similarity with *M. ruber*, is a thermophilic isolate obtained from a hot spring in China (Tengchong hot springs, Yunnan province) by Chen et al. (2002). They reported that growth of *M. rosaceus* did not occur hotter than 70°C or cooler than 40°C, with an optimal temperature of ~55°C, within 5°C of the temperature at Koza. The optimal pH range for *M. rosaceus* (~pH 8) was close to the measured pH at Koza (pH 8.63) and several physiological properties observed in pure culture were also observed in enrichment cultures from Koza: neither could utilize certain sugars (sucrose, maltose); cells required yeast extract for growth; no motility was observed; colonies produced were yellow-pigmented (only observed in initial enrichment cultures that grew to visible turbidity) supporting the taxonomic relationship between *M. rosaceus* isolated by Chen et al. (2002) and aerobic enrichment cultures in heterotrophic (yeast extract and peptone) media from Koza fluids. Though Chen et al. (2002) notes that M. rosaceus did not reduce nitrate, several related strains (i.e. *M. silvanus*, DSM9946 and *M. chliarophilus*, DSM9947) were capable of nitrate reduction, indicating that Koza cultures capable of surviving in nitrate-reduction media are likely more closely related to either of these strains.

T. hydrothermalis – a gamma-proteobacteria first isolated from a hot spring (48°C, pH 8.6) in Central Portugal by Alves et al. (2003) – was a close relative to heterotrophic enrichment cultures from both Koza and Sakarıılıca, indicating that relatives of this species might be ubiquitous in the subsurface. Another alternative is that similar species are preferentially enriched during cultivation, though the presence of these microorganisms in all cultures, as well as in hot springs in other geographic areas, indicates they are fairly widespread. Metagenomic data could shed light on the abundance of these organisms based on identifying dominant community members (i.e. whether they are widespread in low numbers or in abundance), though that effort is beyond the scope of this study.

The optimal growth temperature for *T. hydrothermalis* is consistent with the average fluid temperature at Sakarıılıca (~50°C) and Koza (~50-60°C); additionally, the observed preference for

organic substrates and aerobic conditions in Sakarıılıca and Koza cultures is substantiated by the physiological classification of *T. hydrothermalis* as a strict, aerobic organotroph (Alves et al., 2003). This classification of the dominant community members at these sites likely explains the low yields in media targeting chemoautotrophy. Other similarities between Sakarıılıca and Koza enrichment cultures and *T. hydrothermalis* strains cultured by Alves et al. (2003) include: non-motility; growth between pH 6.5-8.5 and temperatures between 30-60°C (optimal at 50°C); nitrate reduction; short rod-shaped morphologies, and assimilation of several simple carbon compounds (i.e. D-glucose, D-maltose, acetate, pyruvate).

At Sakarıılıca, heterotrophic isolates were obtained via serial dilution from fluids sampled in the 2010 survey only, and dominant members had nearest taxonomic relatives to *Thermomonas hydrothermalis* (described in the preceding paragraphs) and *Bacteroidetes* spp. Member of the phylum Bacteroidetes have been detected in a wide variety of habitats, including ophiolite-hosted springs of pH ~8.7 (e.g. Del Puerto ophiolite, Blank et al. 2008) and alkaline (pH 11.4) groundwater in Portugal (Tiago et al., 2006). This phylum includes a wide variety of bacteria that are found in a number of environments including the human intestinal tract, though without high similarity to a member of this phylum it is difficult to determine the nature of this taxonomic relative. Generally, Bacteroidetes are anaerobic, gram-negative bacteria, indicating that anaerobes may be present in co-culture with Sakarıılıca enrichment cultures. If so, they may only exist in symbiosis with other microorganisms, as efforts to isolate anaerobes did not yield growth in the laboratory.

5.4.2 **16SrRNA Taxonomy of Isolates from Dokurcun Cool Seep**

Phylogeny from 2010 cultures indicated a taxonomic relationship to an unspecified member of the phylum *Pseudomonas*. Over time and many transfers into fresh media, DNA from DK cultures was extracted and sequenced a second time, revealing a taxonomic relationship to an opportunistic fish and mammal pathogen, *Aeromonas salmonicida* subsp. (Reith et al., 2008). However, some

important differences are observed from the type strain *A. salmonicida* and Dokurcun cultures. Most strains of *A. salmonicida* are non-motile, whereas motility was observed in all Dokurcun cultures. The yellow pigmentation of Dokurcun colonies is not consistent with the light-brown colonies developed by *A. salmonicida*. These facts, coupled with the fact that the sample was taken from a terrestrial system rather than an aquatic one where *A. salmonicida* are typically found, suggests that Dokurcun might be a distinct but related species. Whether this microbe was always present in the cultures in unclear, though aseptic technique and systemic quality controls during cultivation greatly reduce the introduction of foreign cells. Regardless, this culture demonstrated growth in nitrate reduction media and possessed the appropriate genes for the first two steps of denitrification (*narG* and *nirS/K*). Thus, both genetic and metabolic observations support thermodynamic predictions indicating nitrate reduction as a viable metabolic option in this system.

5.4.3 **Yanartaş Gas Seep**

Nearest taxonomic relatives for mixed cultures (after several transfers however, so likely representative of the most dominant member of the community) was a strain of *Bacillus licheniformis* . This species is commonly found in the soil environment and is known to produce endospores that can survive harsh environmental conditions (i.e. below an actively burning methane vent in sediments ~60°C) (Rey et al., 2004). It is motile, gram-positive and aerobic, though strains of this species have been known to be facultative anaerobes, which may explain its tolerance to such high levels of reducing gases in the atmosphere, as large amounts of CH_4 are emitted as diffuse seepage throughout the outcrop at Yanartaş (Hosgörmez et al., 2008; Etiope et al., 2011). Some *B. licheniformis* strains are known to be capable of denitrification as well – consistent with my observations of positive growth in nitrate reduction media and genetic assays. Based on the presence of functional nitrate and nitrite reductase genes, it is likely that Yanartaş cultures falls among these strains. *B. licheniformis* secretes a number of industrially and environmentally important enzymes that may facilitate nutrient cycling in the natural

environment. Its tendency to produce endospores allows it to remain dormant for periods of time, growing quickly when favorable conditions arise. This species is also alkaliphilic - as anticipated given the high pH of Yanartaş fluids (pH 9.5 to nearly pH 12 at the source vent) - with an optimal pH of 9 or above (Rey et al., 2004). Its optimal growth temperature (~50°C) is within 10°C of the highest measured temperatures within sediments near the source vent (~60°C), indicating that the site is favorable for slightly thermophilic, alkaliphiles related to *B. licheniformis*.

5.4.4 **Functional Gene Diversity vs. Observed Culture Function**

Observed growth in nitrate reduction media was substantiated by the presence of functional genes for nitrate (*narG*) and nitrite reduction (*nirS/nirK*) in enrichment cultures from Dokurcun (25°C, pH 8.3) and Yanartaş (50°C, pH 9.5). Both cultures demonstrated growth on nitrate and possession of the gene encoding for nitrate reductase (*narG*), illustrating a connection between genetic capacity, metabolic potential, and thermodynamic predictions. The presence of these genes is indicative of the first two steps of denitrification (nitrate and nitrite reduction) occurring in these systems, or, the capacity to use nitrate as an alternative electron acceptor (i.e. instead of O_2). The latter possibility may relate to the generally low O_2 availability in the subsurface: the ability to utilize nitrate could be an adaption developed by these organisms during periods of low oxygen.

The low sequence similarities observed in these samples with known functional gene sequences (refer to Ch. 4, Table XXV) is intriguing and could indicate either a unique gene sequence adopted by Yanartaş cultures or may simply reflect a need for deeper sequencing of nitrogen-cycling genes in 'extreme' environments analogous to those described in this study. Nearest taxonomic relatives based on *nirS* and *narG* phylogeny were not consistent with 16SrRNA taxonomic relatives, indicating phylogenetic differences between 16SrRNA sequences and functional gene sequences. Several sequences for functional nitrogen-cycling genes belonged to an uncultured bacterium, again reflecting the need for more cultivation-based studies.

The presence of active denitrification at Yanartaş is intriguing given recent studies highlighting the abundance of both nitrifying and denitrifying bacteria and archaea in geothermal, subsurface environments (e.g. the US Great Basin, Dodsworth et al., 2011; Hedlund et al., 2011) and the significance of nitrate as an alternate terminal electron acceptor for anaerobic respiration. It is unclear whether Yanartaş cultures are using NO_3^- for active denitrification or for dissimilatory nitrate reduction to ammonium, though based on increases in $\delta^{15}N$ and NH_4^+ along the outflow channel and the absence of *norB* and *nosZ* genes (which encode for enzymes responsible for the reduction of NO and N_2O, respectively), the latter process is more likely. Given the ability to utilize NO_3^-as an alternate terminal electron acceptor (as observed in many thermophilic bacteria and Archaea, Dodsworth et al., 2011), these organisms may be facultative anaerobes, capable of switching to NO_3^-- instead of O_2 as an oxidant in periods of low O_2-availability, which are likely given the abundance of reduced gases discharging nearby.

The connection between functional gene diversity and observed culture function was less obvious at other sites, where genetic capacity could not be directly tied to metabolic function in terms of possessing specific nitrogen-cycling genes. Taxonomic relationships do provide insight onto metabolism however. Nearest relatives for many thermophilic cultures utilized a variety of organic carbon sources, with several of them being strict organotrophs (e.g. *Thermomonas hydrothermalis*, *Meiothermus ruber*). Still, no taxonomic relatives had 100% sequence similarity with known organisms, so small differences in metabolic capacity from the nearest relative compared with enrichment cultures cannot be discounted, as minor divergence in metabolic potential (with no apparent genetic distinctions responsible) have been observed in cultured strains of the same clade [e.g. Alves et al. 2003 noted differences in single carbon assimilation by *T. hydrothermalis* strains and its close relative (97.4% sequence similarity), *Thermomonas haemolytica*]. As such, only observed metabolic options can provide concrete evidence of metabolic

utilization by a species, though genetic data is generally much easier to obtain, especially given recent technological advances in sequencing and analysis of genetic data (Pace, 2009).

Further, the percent sequence similarity for functional genes sequenced in this study in these samples compared with known sequences was fairly low (<90%). This may indicate a novel gene in these cultures or may simply reflect the need for deeper sequencing of functional genes utilized in extreme environments. More genomic studies in hydrothermal and subsurface environments would likely enhance the utility of BLAST searches by providing more relevant taxonomic relatives and functional genes in GenBank (the database against which sample sequences are compared).

5.5 **Summary**

Several ophiolite and non-ophiolite-hosted springs in western Turkey along a spectrum of hydrothermal and meteoric inputs were compared to assess relationships between environmental parameters, thermodynamics, and microbial metabolism. Cultivation of native microorganisms in fluids from different spring systems with distinct geochemistry lead to the isolation of several strains, each with optimal growth conditions reflective of environmental conditions. Hydrothermal isolates had taxonomic relationships with microorganisms known to inhabit hot spring environments (e.g. *Thermomonas hydrothermalis*); denitrifying bacteria found at Yanartaş are related to *Bacillus licheniformis*, several strains of which are known to perform denitrification and grow optimally at the temperature and pH conditions found at Yanartaş (50°C, pH 9 and above). The ubiquity of microorganisms found at surface seeps at Dokurcun and Yanartaş, coupled with the meteoric origins for the majority of thermal waters in springs along the North Anatolian Fault Zone, suggests that colonization of the subsurface – or transport through a subsurface hydrologic network to other surface upwellings – may be possible by these soil biota given their capability to produce endospores that can withstand high temperatures and environmental extremes for long periods of time (Rey et al., 2004).

Genetic properties were correlated with denitrification processes in both Dokurcun and Yanartaş enrichment cultures, indicating that these exergonic processes predicted to occur in serpentinizing and hydrothermal systems can be observed in culture and verified by PCR-based assays. At Yanartaş, we see a consistent pattern in terms of nitrogen cycling in both geochemical measurements (^{15}N isotopes and total weight percent nitrogen increase along the outflow channel, suggesting recycling of organic ^{15}N within the biofilm), observed culture function (growth in nitrate reduction media) and genetic capacity (the presence of genes for nitrate and nitrite reduction and absence of genes for N_2 fixation). It is clear that environmental conditions govern energy availability, and, in turn, affect microbial metabolism.

5.6 **Future Directions**

Further characterization of the metagenome in these systems may shed light on the total microbial diversity in these systems, and how microbial ecology varies in springs hosted by different geologic units, but related hydrogeologically via faulting or secondary fractures. This would elucidate geospatial trends in microbial diversity and help to answer whether related species dominate multiple spring systems (e.g. Koza and Sakarıılıca isolates shared high taxonomic affiliation with *T. hydrothermalis*) simply because they are more abundant and capable, or if this is a reflection of cultivation bias (i.e. differences in small-scale diversity are not apparent due to the elimination of less abundant species in culture). Exploring the presence of functional genes (that are not necessarily utilized *in vitro*) in the metagenome would also help address whether the primary driver of utilized metabolic pathways is thermodynamic favorability or microbial energetics.

The archaeal diversity in these systems, which was not investigated in this study, may also play an important role in subsurface ecology and merits further study. This is especially true for further investigation of nitrogen-cycling at Yanartaş, an alkaline surface seep associated with active serpentinization and methane generation at depth. Dodsworth et al. (2011) and colleagues have

recently highlighted the Archaeal role in ammonia oxidation (to nitrate) in subsurface geothermal systems. Further investigation of the source of ammonia and the abundance of Archaea at Yanartaş could provide new insight onto Archaeal role in these processes in serpentine-hosted and hydrothermal environments.

CITED LITERATURE:

Adiguzel, A., Ozkan, H., Baris, O., Inan, K., Gulluce, M., & Sahin, F. (2009) Identification and characterization of thermophilic bacteria isolated from hot springs in Turkey. *Journal of Microbiological Methods* **79**:321-328.

Alves, M. P., Rainey, F. A., Nobre, M. F., & da Costa, M. S. (2003) *Thermomonas hydrothermalis* sp. nov., a new slightly thermophilic γ-Proteobacterium isolated from a hot spring in Central Portugal. *System. Appl. Microbiol.* **26**:70-75.

Barnes, I., Lamarche, V. C., & Himmelberg, G. R. (1967) Geochemical evidence of present-day serpentinization. *Science* **56**:830-832.

Barnes, I., Rapp, J. B., & O'Neil, J. R. (1972) Metamorphic Assemblages and the Direction of Flow of Metamorphic Fluids in Four Instances of Serpentinization. *Contr. Mineral. and Petrol*. **35**:263—276.

Barnes, I. & O'Neil, J.R. (1978) Present-day serpentinization in New Calcedonia, Oman and Yugoslavia. *Geochimica et Cosmochimica Acta* **42**:144-145.

Cardace, D. & Hoehler, T. M. (2009a) Serpentinizing fluids craft microbial habitat. *Northeastern Naturalist* **16**(5): 272-284.

Chen, C. Lin, L., Peng, Q., Ben, K., & Zhou, Z. (2002) Meiothermus rosaceus sp nov isolated from Tengchong hot spring in Yunnan, China. F*EMS Microbiol Lett*. **216**(2):263-268.

Cihan, A. C., Ozcan, B., & Cokmus, C . Anoxybacillus salavatliensis sp. nov., an α-glucosidase producing, thermophilic bacterium isolated from Salavatli, Turkey. (2011) *J. Basic. Microbiol.* **51**(2):136-46.

Craig, H. (1961) Isotopic variations in meteoric waters. *Science* **133**:1702–1703.

De Brabandere, L., T. K. Frazer, and J. P. Montoya (2007), Stable nitrogen isotope ratios of macrophytes and associated periphyton along a nitrate gradient in two subtropical, spring-fed streams, Freshwater Biol., **52**:1564–1575.

Dodsworth, J. A., Hungate, B. A. & Hedlund, B. P. (2011) Ammonia oxidation, denitrification and dissimilatory nitrate reduction to ammonium in two US Great Basin hot springs with abundant ammonia-oxidizing archaea. *Environmental Microbiology* **13**(8):2371-2386.

Gat, J. R., Shemesh, A., Tziperman, E., Hecht, A., Georgopoulos, D., & Basturk, O. (1996) The stable isotope composition of waters of the Eastern Mediterranean Sea, *J. Geophys. Res.*, **101**:6441–6451.

Gul-Guven, R., Guven, K., Poli, A. & Nicolaus, B. (2008) *Anoxybacillus kamchatkensis* subsp. *asaccharedens* subsp. nov., a thermophilic bacterium isolated from a hot spring in Batman, *J. Gen. Appl. Microbiol.* **54**:327–334.

Havig, J. R., Raymond, J., Meyer-Dombard, D. R., Zolotova, N. & Everett L. Shock, E. L. (2011) Merging Isotopes and Community Genomics in a Siliceous Sinter-Depositing Hot Spring. *JGR Biogeosciences* **116**:G01005.

Hedlund, B. P., McDonald, A. I., Lam, J., Dodsworth, J. A., Brown, J. R. and Hungate, B. A. (2011), Potential role of *Thermus thermophilus* and *T. oshimai* in high rates of nitrous oxide (N_2O) production in ~80 °C hot springs in the US Great Basin. *Geobiology*, **9**: 471–480.

Hosgörmez, H., Etiope, G., & Yalcin, M. N. (2008) New evidence for a mixed inorganic and organic origin of the Olympic Chimaera fire (Turkey): a large onshore seepage of abiogenic gas. *Geofluids* **8**:263–273.

Hugenholtz, P., Goebel, B. M., & Pace, N. R. (1998) Impact of culture independent studies on the emerging phylogenetic view of bacterial diversity. *J. Bacteriol.* **180**:4765–4774.

Jahnke, L. L., Summons, R. E., Hope, J. M. & Des Marais, D. J. (1999) Carbon isotopic fractionation in lipids from methanotrophic bacteria II: The effects of physiology and environmental parameters on the biosynthesis and isotopic signatures of biomarkers. *Geochimica et Cosmochimica Acta* **63**(1): 79–93.

Kaeberlein, T., Lewis, K., Epstein, S. S. (2002) Isolating "uncultivable" microorganisms in pure culture in a simulated natural environment. *Science* **296**:1127–1129.
Kim, K., Kim J.J., Masui, R., Kuramitsu, S., Sung, M.H. (2011) A commensal symbiotic interrelationship for the growth of Symbiobacterium toebii with its partner bacterium, Geobacillus toebii. *BMC Res. Notes* **4**:437.
Lodders, K. & Fegley, B. (1998) The Planteray Scientist's Companion. Oxford University Press, Inc., New York, NY, USA. p. 371.
Loginova, L.G., Egorova, L. A., Golovacheva, R. S., & Seregina, L. M. (1984) *Thermus ruber* sp. nov., nom. rev. *Int. J. Syst. Bacteriol*. **34**:498-499.
Mehta, M. P. & Baross, J. A. (2006) Nitrogen Fixation at 92°C by a Hydrothermal Vent Archaeon *Science*: ***314***:1783-1786.
Meyer-Dombard, D.R., Shock, E.L., & Amend, J.P. (2005) Archaeal and bacterial communities in geochemically diverse hot springs of Yellowstone National Park, USA. *Geobiology* **3**:211–227.
Meyer-Dombard, D. R., Shock, E. L., & Amend, J. P. (2012) Effects of trace element concentrations on culturing thermophiles. *Extremophiles* **16**:317-331.
Munster, M.J., Munster, A. P., Woodrow, J. R., & Sharp, R. J. (1986) Isolation and preliminary taxonomic studies of *Thermus* strains isolated from Yellowstone National Park, USA. *J. Gen. Microbiol*. **132**:1677-1683.
Needoba, J. A., D. M. Sigman, and P. J. Harrison (2004) The mechanism of isotope fractionation during algal nitrate assimilation as illuminated by the 15N/14N of intracellular nitrate, *J. Phycol*., **40**:517–522.
Nobre, M.F., Trüper, H.G., Da Costa, M.S. (1996) Transfer of *Thermus ruber* (Loginova *et al.* 1984), *Thermus silvanus* (Tenreiro *et al.* 1995), and *Thermus chliarophilus* (Tenreiro *et al*. 1995) to *Meiothermus* gen. nov. as *Meiothermus ruber* comb. nov., *Meiothermus silvanus* comb. nov., and *Meiothermus chliarophilus* comb. nov., respectively, and emendation of the genus *Thermus*. *Int. J. Syst. Bacteriol.* **46**:604-606.
Okland, I.,Huang, S., Dahle, H., Thorseth, I.H., & Pedersen, R.B. (2012) Low temperature alteration of serpentinized ultramafic rock and implications for microbial life. *Chemical Geology* **318-319**:75-87.
Pace NR. 2009. Mapping the tree of life: progress and prospects. *Microbiol. Mol. Biol. Rev*. **73**:565–576.
Rappe, M. S., & Giovannoni, S. J. (2003) The uncultured microbial majority. *Annu. Rev. Microbiol*. **57:**369–394.
Rey M.W., Ramaiya P., Nelson B.A., Brody-Karpin S.D., Zaretsky E.J., Tang M., Lopez de Leon A., Xiang H., Gusti V., Clausen I.G., Olsen P.B., Rasmussen M.D., Andersen J.T., Jorgensen P.L., Larsen T.S., Sorokin A., Bolotin A., Lapidus A., Galleron N., Ehrlich S.D., Berka R.M. *Complete genome sequence of the industrial bacterium Bacillus licheniformis and comparisons with closely related Bacillus species.* Genome Biol. 2004;5(10):R77. Epub 2004 Sep 13.
Sharp, R. J., & Williams, R. A. D. (1988) Properties of *Thermus ruber* strains isolated from icelandic hot springs and DNA-DNA homology of *Thermus ruber* and *Thermus aquaticus. Appl. Environ. Microbiol*. **54**:2049-2053.
Stewart, E. J. (2012) Growing Unculturable Bacteria. *J. of Bacteriology*. **194**: 4151-4160.
Süer, S., Güleç, N., Mutlu, H., Hilton, D. R., Çifter, C., & Sayin, M. (2008) Geochemical Monitoring of Geothermal Waters (2002–2004) along the North Anatolian Fault Zone, Turkey: Spatial and Temporal Variations and Relationship to Seismic Activity. *Pure and Applied Geophysics* **165**:17–43.
Swingley, W., Meyer-Dombard, D. R., Shock, E. L., Alsop, E. B., Falenski, H. D., Havig, J. R., & Raymond, J. (2012) Coordinating Environmental Genomics and Geochemistry Reveals Metabolic Transitions in a Hot Spring Ecosystem. *PLoS ONE* **7**(6): e38108. doi:10.1371/journal.pone.0038108.
Tiago, I., Chung, A. P., and Veríssimo, A. (2004) Bacterial Diversity in a Nonsaline Alkaline Environment: Heterotrophic Aerobic Populations. *Applied and Environmental Microbiology* **70**(12): 7378–7387.
Tiago, I., Morais, P. V., da Costa, M. S., & Veríssimo, A. (2006) *Microcella alkaliphila* sp. Nov., a novel member of the family *Microbacteriacea* isolated from a non-saline alkaline groundwater, and emended description of the genus *Microcella*. *IJSEM* **56**(10):2313-2316.
Tindall, B.J., Sikorski, J., Lucas, S., Goltsman, E., Copeland, A., Glavina Del Rio, T., Nolan, M., Tice, H., Cheng, J.F., Han, C., et al. (2010) Complete genome sequence of *Meiothermus ruber* type strain (21^T). *Stand. Genomic Sci*. **3**:26-36.
Waser, N. A. D., P. J. Harrison, B. Nielson, S. E. Calvert, and D. H. Turpin (1998), Nitrogen isotope fractionation during the uptake and assimilation of nitrate, nitrite, ammonium, and urea by a marine diatom, *Limnol. Oceanogr*. **43**:215–224.

APPENDICES

APPENDIX A
ARTIFICIAL GROWTH MEDIA SOLUTION COMPONENTS

TABLE XXV: KOZA FLUID ARTIFICIAL MEDIA

Base Solution	mg/L	
KCl	324.3	
NaCl	20650.1	
$NaHCO_3$	233.5	*Final pH adjusted
Na_2SO4	86.07	to 8.63
$MgCl_2*6H_2O$	230	
$BaCl_2*2H_2O$	1.45	
$ZnSO_4*7H_2O$	31.87	
$SrCl_2*6H_2O$	95.96	
RbCl	130.57	

Trace Element Solution:	100x solution (use 10 ml/L) mg/L
$CoCl_2*6H_2O$	3.23
$CuSO_4*5H_2O$	16.00
$MnCl_2*4H_2O$	14.05
$Na_2MoO_4*2H_2O$	5
$NiCl_2*6H_2O$	5
$PbCrO_4$	0
$VOSO_4*3.5H_2O$	1.14
$CdSO_4*8/3H_2O$	2.51

N/P Solution	50x solution (use 10ml/L) mg/500ml
NH_4Cl	44.48
$NaNO_3$	25.02
K_2HPO_4	20.36

Fe-EDTA Solution	100x solution (use 2ml/L) mg/200ml
$FeSO_4*7H_2O$	37.72
Na_2-EDTA	37.73

$CaCl_2$ Solution	40x solution (use 5 ml/L) mg/200ml
$CaCl_2*2H_2O$	172.88

TABLE XXVII: SAKARIILICA FLUID ARTIFICIAL MEDIA

Base Solution (Final pH adjusted to 6.65)	
	mg/L
KCl	1244.9
NaCl	280
$NaHCO_3$	233.5
Na_2SO4	59.80
$MgCl_2*6H_2O$	1000.0
$MnCl_2*4H_2O$	3.06
$ZnSO_4*7H_2O$	11.2
$SrCl_2*6H_2O$	167.0
RbCl	6.0
$BaCl_2*2H_2O$	19.26

Trace Element Solution	100x solution (use 10 ml/L) mg/L
$CoCl_2*6H_2O$	7.67
$CuSO_4*5H_2O$	147.0
$Na_2MoO_4*2H_2O$	5.0
$NiCl_2*6H_2O$	5.0
$PbCrO_4$	0
$VOSO_4*3.5H_2O$	4.92
$CdSO_4*8/3H_2O$	1.83

N/P Solution	50x solution (use 10ml/L) mg/500ml
NH_4Cl	74.1
$NaNO_3$	20.6
K_2HPO_4	31.7

Fe-EDTA Solution	
	100x solution (use 2ml/L) mg/200ml
$FeSO_4*7H_2O$	892.8
Na_2-EDTA	892.8

$CaCl_2$ Solution	
	40x solution (use 5 ml/L) mg/200ml
$CaCl_2*2H_2O$	103.0

TABLE XXVIII: KUZULUK FLUID ARTIFICIAL MEDIA

Base Solution (Final pH adjusted to 6.67)	
	mg/L
KCl	2886.2
NaCl	10000.0
$NaHCO_3$	233.5
Na_2SO4	70.28
$MgCl_2*6H_2O$	6698.4
$MnCl_2*4H_2O$	4.95
$ZnSO_4*7H_2O$	4.98
$SrCl_2*6H_2O$	133.7
RbCl	12.46
$BaCl_2*2H_2O$	34.42

	100x solution (use 10 ml/L)
Trace Element Solution	mg/L
$CoCl_2*6H_2O$	3.63
$CuSO_4*5H_2O$	3.14
$Na_2MoO_4*2H_2O$	5.0
$NiCl_2*6H_2O$	115.4
$PbCrO_4$	0.0
$VOSO_4*3.5H_2O$	14.0
$CdSO_4*8/3H_2O$	1.83

N/P Solution	50x solution (use 10ml/L) mg/500ml
NH_4Cl	44.5
$NaNO_3$	102.8
K_2HPO_4	31.7

Fe-EDTA Solution	
	100x solution (use 2ml/L)
	mg/200ml
$FeSO_4*7H_2O$	733.5
Na_2-EDTA	733.5

$CaCl_2$ Solution	
	40x solution (use 5 ml/L)
	mg/200ml
$CaCl_2*2H_2O$	129.4

TABLE XXIX: DOKURCUN FLUID ARTIFICIAL MEDIA

Base Solution (Final pH adjusted to 8.22)	
	mg/L
KCl	40.0
NaCl	0
$NaHCO_3$	233.5
Na_2SO4	93.6
$MgCl_2*6H_2O$	1000.0
$ZnSO_4*7H_2O$	6.4
$SrCl_2*6H_2O$	12.9
	100x solution (use 10 ml/L)
Trace Element Solution	mg/L
$CoCl_2*6H_2O$	4.45
$CuSO_4*5H_2O$	22.0
$MnCl_2*4H_2O$	29.2
$Na_2MoO_4*2H_2O$	5.0
$NiCl_2*6H_2O$	88.3
$PbCrO_4$	3.3
$VOSO_4*3.5H_2O$	15.9
$CdSO_4*8/3H_2O$	2.3
RbCl	5.0
$BaCl_2*2H_2O$	72.7
N/P Solution	50x solution (use 10ml/L) mg/500ml
NH_4Cl	44.5
$NaNO_3$	102.8
K_2HPO_4	20.4
Fe-EDTA Solution	
	100x solution (use 2ml/L) mg/200ml
$FeSO_4*7H_2O$	157.3
Na_2-EDTA	157.3
$CaCl_2$ Solution	
	40x solution (use 5 ml/L) mg/200ml
$CaCl_2*2H_2O$	31.8

APPENDIX A (continued)

TABLE XXX: YANARTAŞ (SITE C) FLUID ARTIFICIAL MEDIA

Base Solution (Final pH adjusted to 9-10.5)	
	mg/L
KCl	12.5
NaCl	0
$NaHCO_3$	233.5
Na_2SO4	0
$MgCl_2*6H_2O$	575.0
	100x solution (use 10 ml/L)
Trace Element Solution	mg/L
$CoCl_2*6H_2O$	0.25
$MnCl_2*4H_2O$	1.3
$CuSO_4*5H_2O$	0.5
$Na_2MoO_4*2H_2O$	5.0
$NiCl_2*6H_2O$	5.0
$PbCrO_4$	0.0
$ZnSO_4*7H_2O$	4.1
$SrCl_2*6H_2O$	4.4
$VOSO_4*3.5H_2O$	0.6
$CdSO_4*8/3H_2O$	0.005
RbCl	0.1
$BaCl_2*2H_2O$	0.3
N/P Solution	50x solution (use 10ml/L) mg/500ml
NH_4Cl	0
$NaNO_3$	0
K_2HPO_4	20.4
Fe-EDTA Solution	
	100x solution (use 2ml/L) mg/200ml
$FeSO_4*7H_2O$	3.6
Na_2-EDTA	3.6
$CaCl_2$ Solution	
	40x solution (use 5 ml/L) mg/200ml
$CaCl_2*2H_2O$	0.4

APPENDIX B
SPRING FLUID CHEMISTRY: TRACE ELEMENT & CARBON ISOTOPE DATA

TABLE XXXI: ICP-MS TRACE ELEMENT DATA IN PPB, 2012 SURVEY.
Italicized values indicate the measurement is outside of the calibration range for that element.

	Kuzuluk	**Koza**	**DK-Snow**	**Yanartaş Site C**	**Yanartaş Site E**	**Pamukkale**	**Karahayit**	**Babacik**	**Tekke**	**Inaltı**
Li	2740	70	50	*24.3*	*23.6*	137	410	1630	2520	1260
Be	*0.63*	*0.008*	*0.006*	*0.007*	*0.004*	*0.202*	*0.34*	*0.34*	*0.06*	*0.09*
B	*23700*	1930	*18.6*	*13*	30	1040	1760	8400	*14000*	*14200*
Mg	*14400*	172	235	*77900*	297	*85000*	*105000*	*71200*	3900	4900
Al	5.4	21.3	7	21.8	10.8	*102*	107	11	162	12.7
P	*450*	*700*	15	*77*	5.9	*1340000*	*1280000*	*2000*	*1385000*	19
Ca	*79800*	*96000*	1360	*9700*	*170000*	*380000*	*320000*	*184000*	10400	*15800*
Ti	*0.13*	*0.038*	*0.12*	*0.38*	*0.05*	1.4	*1*	*0.21*	*2.1*	*0.13*
V	*0.16*	*0.112*	*0.49*	1.45	*0.244*	0.51	*0.14*	*0.09*	14.1	*0.09*
Cr	*0.07*	*0.028*	*0.27*	1.68	*0.075*	0.57	*0.72*	*0.32*	*0.7*	*0.16*
Mn	25.2	1.94	4	3.6	*0.06*	17.8	*34.3*	5.52	14.8	*0.19*
Fe	176	51	54	*59*	*1.5*	*44.9*	*400*	*44.2*	*59.5*	12.2
Co	*0.06*	*0.034*	*0.124*	0.56	*0.018*	*0.057*	2.3	*0.04*	*0.03*	*0.02*
Ni	5.9	1.55	0.72	14.7	*0.79*	9.86	*7.6*	*0.39*	*0.56*	*0.19*
Cu	*0.28*	*0.33*	*0.92*	1.16	*0.36*	0.725	*0.63*	*0.4*	*0.42*	*0.42*
Zn	38.4	29.2	23.5	9.4	2.93	17.8	25.7	16.5	*4.2*	5.6
As	*580*	41	*0.36*	0.61	*0.47*	1.18	7.1	137	*910*	*1250*
Rb	181	24.8	*0.44*	0.97	0.556	21	81	213	*371*	*372*
Sr	980	581	*4.6*	*14.1*	253	*5500*	*8540*	9400	1770	3360
Y	*0.19*	*0.022*	*0.012*	*0.034*	*0.005*	*0.187*	*0.148*	*0.19*	*0.06*	*0.08*
Zr	*0.15*	*0.062*	*0.018*	*0.066*	*0.015*	1.31	*0.44*	*0.25*	*0.65*	*0.49*
Nb	*0.04*	*0.012*	*0.01*	*0.017*	*0.007*	*0.039*	*0.044*	*0.05*	*0.07*	*0.05*
Mo	*0.13*	1.96	*0.098*	*0.459*	*0.13*	0.51	*0.72*	*0.16*	41	22.4
Cd	*0.07*	*0.01*	*0.058*	*0.022*	*0.025*	*0.009*	*0.04*	*0.04*	*0.16*	*0.13*
Sn	*0.12*	*0.13*	*0.12*	*0.404*	7.6	0.52	*0.104*	*0.15*	*0.16*	*0.09*
Sb	*1*	*0.15*	*0.104*	*0.119*	*0.04*	4.39	4.6	*0.05*	*625*	174.1
Cs	*300*	2.04	*0.336*	*0.194*	*0.13*	9.72	22.7	120.2	218.7	200.4
Ba	411	*15.7*	*1.3*	*1.6*	5.25	*49*	*51*	*23.6*	*23.2*	*20.8*
La	*0.04*	*0.006*	*0.012*	*0.023*	*0.002*	*0.04*	*0.032*	*0.02*	*0.07*	*0.02*
Ce	*0.06*	*0.012*	*0.02*	*0.048*	*0.004*	*0.058*	*0.076*	*0.05*	*0.11*	*0.01*
Sm	*0.02*	*0.002*	*0.002*	*0.006*	*0.001*	*0.008*	*0.008*	*0.01*	*0.01*	*0.01*
Eu	*0.07*	0.004	*0.002*	*0.002*	*0.001*	*0.008*	*0.012*	*0.01*	*0.03*	*0.01*
Ta	*0.06*	*0.018*	*0.01*	*0.008*	*0.005*	*0.087*	*0.088*	*0.07*	*0.13*	*0.13*
W	*4.6*	2.87	*0.046*	*0.05*	*0.081*	*0.04*	*0.06*	*0.84*	*2.51*	*3.3*
Tl	*0.05*	*0.052*	*0.018*	*0.007*	*0.001*	*0.024*	*0.056*	*0.01*	*0.02*	*0.01*
Pb	*0.24*	*0.384*	1.15	*0.116*	*0.038*	*0.42*	*0.24*	*0.08*	*0.89*	*0.11*
Th	*0.06*	*0.006*	*0.002*	*0.002*	*0*	*0.045*	*0.024*	*0.01*	*0.02*	*0.02*
U	*0.02*	*0.02*	*0.006*	*0.108*	*0.007*	1.393	*0.336*	*0.08*	12.7	*0.31*

APPENDIX B (continued)

TABLE XXXII: TRACE ELEMENT DATA IN PPB, 2010 SURVEY

	Field Blank	**Dokurcun SAMPLE 1**	**Dokurcun SAMPLE 2**	**Kuzuluk**	**Koza**	**Sakarılıca**
Li	0	1.74	1.02	991.04	9.36	197.44
Be	0	0	0	0.21	0	0.04
Na	19	844	1797.12	263512.5	82152.48	112504.48
Mg	0	37264	81470	8008	273.76	58560
K	5	205	355.31	15143.6	1705.22	6535.62
Ca	0	10844.8	20870	43376	58912	35120
V	0	0.42	0.23	0.37	0.13	0.13
Cr	2	17.46	42.74	1.28	0.38	0.14
Mn	0	0.81	0.73	13.73	0.39	8.49
Fe	5	25.84	18.07	120.53	14.28	146.72
Co	0	0.11	0.19	0.09	0.08	0.19
Ni	18	2.18	18.27	2.85	bdl	16.50
Cu	2	0.56	1.90	0.08	0.41	3.74
Zn	3	14.44	9.65	11.32	72.48	25.39
As	0	0.24	0.06	296.64	13.68	41.90
Se	0	0	0.59	0	0	1.11
Rb	0	0.36	0.21	88.03	9.23	42.77
Sr	0	42.35	85.19	439.36	315.36	547.84
Ag	0	0.15	0.03	0.13	0.10	0.12
Cd	0	0.10	0.07	0.08	0.11	0.08
Sb	0	0.06	0.06	0.56	0.13	0.57
Cs	0	0.10	0.05	142.61	1.05	76.80
Ba	0	4.09	4.16	193.53	8.14	108.27
La	0	0.25	0.02	0.15	0.11	0.05
Ce	0	0.43	0.05	0.26	0.18	0.10
Sm	0	0.04	0	0.02	0.01	0.03
Eu	0	0.01	0	0.03	0.01	0.01
Th	0	0	0	0	0	0.45
Pb	0	0.21	0.13	0.03	0.02	0.08
Th	0	0.38	0	0.43	0.31	0.24
U	0	0.02	0	0	0	0.13

TABLE XXXIII: DISSOLVED ORGANIC AND DISSOLVED INORGANIC CARBON CONTENT AND ^{13}C ISOTOPES IN SPRING FLUIDS, 2010 SURVEY

	DOC (ppm C)	DOC $\delta^{13}C$ VPDB (‰)	DIC (ppm C)	DIC $\delta^{13}C$ VPDB (‰)
Koza_2010	0.26	-61.37	0.98	-10.08
Sakarıılıca	5.81	2.38	*219.94*	*531.81*
Kuzuluk_2010	9.67	0.17	*211.02*	*421.33*
Dokurcun_2010	9.34	-15.73	88.83	-13.85

APPENDIX C
FIELD SITE PHOTOGRAPHS

FIGURE 12: SAMPLING FLUIDS AT KOZA HOT SPRING, 2010 SURVEY

FIGURE 13: WELL-HOUSE C ONSTRUCTED AT KOZA HOT SPRING, 2012 SURVEY

APPENDIX C (continued)

FIGURE 14: SAMPLING FLUIDS AT DOKURCUN COOL SEEP, 2010 SURVEY

A

B

FIGURE 15: WELL HOUSE SAMPLED FROM KUZULUK HOT SPRING, 2012 SURVEY

FIGURE 16: ACTIVELY BURNING METHANE SEEPS AT YANARTAŞ, 2012 SURVEY

A

B

VITA

NAME: Erin Nevriye Yargıçoğlu

EDUCATION: B.S., Earth and Environmental Sciences, Summa Cum Laude, University of Illinois at Chicago, Chicago, Illinois, 2010

M.S., Earth and Environmental Sciences, University of Illinois at Chicago, Chicago, Illinois, 2012

TEACHING EXPERIENCE: Fall 2012: Teaching Assistant, EAES 473 (Soils and the Environment)

Spring 2012: Teaching Assistant, EAES 101(Exploring Earth's Surface)

Fall 2011: Teaching Assistant, EAES 480 (Statistical Methods in the Earth Sciences)

Spring 2011: Teaching Assistant, EAES 101 (Global Environmental Change)

HONORS & AWARDS:

Spring 2012, Outstanding Teaching Assistant of the Year Award, 2011-2012

Fall 2011, Illinois Space Grant Consortium Graduate Fellowship

Spring 2010, NASA Astrobiology Institute Graduate Student Research Scholarship

PROFESSIONAL MEMBERSHIP:

Sustainable Remediation Forum, UIC Student Chapter, Vice President

ASCE Illinois Chapter, Student Member

American Geophysical Union, Student Member

Phi Beta Kappa Phi, Student Member

ABSTRACTS:

Yargicoglu, E.; J. Welch; G. Bourgon; K. Reddy. Green and Sustainable Remedy Selection and Design at Indian Ridge Marsh, Chicago, IL. SURF20 Meeting Presentation, July 2012.

Meyer-Dombard, D. R.; E. Yargicoglu; D. Cardace; Y. Gulecal; M Temel. 2012. Biogeochemical Cycling in Fault-Associated and Ophiolite-Hosted Springs. AbSciCon 2012, Atlanta, GA. Abstract # 4494.